IMPROVED SPANNING AND ROUTING RATIOS ON GEOMETRIC GRAPHS

DARRYL HILL

A thesis submitted to the Faculty of Graduate and Post Doctoral Affairs
in partial fulfillment of the requirements for the degree of

Doctor of Philosophy in Computer Science

Carleton University
Ottawa, Ontario, Canada, 2019

CONTENTS

PREFACE

This thesis is in "integrated article format" in which each chapter is based on published papers, conference proceedings, or papers awaiting publication.

- Chapter 2 considers competitive online local routing on the Delaunay triangulation. These results appeared in the proceedings of the European Symposium on Algorithms (ESA 18)[1].
- Chapter 3 considers competitive online local routing on the Θ_4-graph. These results appeared in the proceedings of the Symposium on Discrete Algorithms (SODA 19)[2].
- Chapter 4 improves the spanning ratio of the convex hull of points on a sphere. This was part of a result published in the Journal of Computational Geometry (JoCG) [3].
- Chapter 5 improves the spanning ratio of the Θ_5-graph. It is awaiting publication.

BIBLIOGRAPHY

[1] Nicolas Bonichon, Prosenjit Bose, Jean-Lou De Carufel, Vincent Despré, Darryl Hill, and Michiel Smid. Improved Routing on the Delaunay Triangulation. In Yossi Azar, Hannah Bast, and Grzegorz Herman, editors, *26th Annual European Symposium on Algorithms (ESA 2018)*, volume 112 of *Leibniz International Proceedings in Informatics (LIPIcs)*, pages 22:1–22:13, Dagstuhl, Germany, 2018. Schloss Dagstuhl–Leibniz-Zentrum fuer Informatik.

[2] Prosenjit Bose, Jean-Lou De Carufel, Darryl Hill, and Michiel H. M. Smid. On the spanning and routing ratio of theta-four. In Timothy M. Chan, editor, *Proceedings of the Thirtieth Annual ACM-SIAM Symposium on Discrete Algorithms, SODA 2019, San Diego, California, USA, January 6-9, 2019*, pages 2361–2370. SIAM, 2019.

[3] Michiel H. M. Smid, Prosenjit Bose, Paz Carmi, Mirela Damian, Jean-Lou De Carufel, Darryl Hill, Anil Maheshwari, and Yuyang Liu. On the stretch factor of convex polyhedra whose vertices are (almost) on a sphere. *JoCG*, 7(1):444–472, 2016.

1 INTRODUCTION

1.1 NAVIGATION ON GEOMETRIC GRAPHS

Graph navigation is a field with many real world applications, from road networks to computer networks. In this thesis we consider *geometric* graphs, and examine properties of these graphs that are relevant to navigation. Formally, a Euclidean geometric graph $G = (P, E)$ is a set P of points embedded in the plane (otherwise known as *vertices*), and a set E of edges, where each edge is a pair of points $(u, v) \in E$, where $u, v \in P$, and the weight of an edge (u, v) is the Euclidean distance $|uv|$. When referring to navigation on G, we are particularly interested in the ability to find a short path between two arbitrary vertices of P consisting of the edges of E.

When we have complete knowledge of a graph G, it is straightforward to compute the shortest path between two vertices s and t. We can, for example, use Dijkstra's algorithm. However, depending on the construction of the graph, the shortest path may not be very short, in particular in relation to the Euclidean distance between s and t. If our graph is the complete graph, then the shortest path is always the shortest distance possible. But complete graphs are not always economical or practical. A *spanning graph* H of G is a graph $H = (P, E')$, where $E' \subseteq E$, and for every edge $e = (u, v)$ in E there is a path from u to v in H. H is a t-spanner of G if there is a constant $t \geq 1$ such that for any edge (u, v) in E the shortest path from u to v in H not longer than $t|uv|$. If we do not specify the graph that H is a subgraph of, then we assume that the spanning ratio t is with respect to the complete graph. The constant t is also referred to as the *stretch factor* of a graph. In part in this thesis we examine geometric graphs with a constant spanning ratio and analyze these graphs in order to improve the known bounds on their spanning ratio.

There are cases where complete knowledge of the graph is not a given. For example, when routing messages in a distributed system, unknown changes could have occurred since the last message was sent out. We say we are routing in the *online setting* if initially we do not have global knowledge of the graph. Making things even more challenging, bandwidth or other limitations may bound the allowable size of forwarded messages. If the size bound is a constant, then accumulating global information of the graph in a single message is not possible. An online routing algorithm is called *k-local routing* if, at each step, forwarding decisions are made using only knowledge of the current vertex location, the location of its k-hop neighbouring vertices, and a constant amount of additional information. If we do not specify k and instead refer only to local routing,

we are referring to 1-local routing. A *memoryless* routing algorithm uses only knowledge of the current vertex u, the k-hop neighbourhood $N_k(u)$ of u, and the destination vertex t. For a routing algorithm A and a given graph G from a class $\mathcal{G}$ of graphs, let $\mathcal{P}_G^A(s,t)$ be the path found by A from s to t. The routing ratio of a local online routing algorithm A on $\mathcal{G}$ is the minimum value c such that $|\mathcal{P}_G^A(s,t)| \leq c \cdot |st|$ for all $G \in \mathcal{G}$ and all pairs s and t in G. When c is a constant, such an algorithm is called *competitive* on the class $\mathcal{G}$. Note that the routing ratio on a class of graphs $\mathcal{G}$ is an upper bound on the spanning ratio of $\mathcal{G}$, since the routing ratio proves the existence of a bounded-length path.

In the next section we introduce the different classes of geometric graphs we analyze in this proposal. In the following section we go over some of the previous work related to these problems. The next three sections give some high level details of the results obtained thus far. The final section details the results we will pursue next.

1.2 CLASSES OF GEOMETRIC GRAPHS CONSIDERED

1.2.1 Θ_k-*Graphs and* Y_k-*Graphs*

Yao-k-graphs (Y_k-graphs) and Θ-graphs have nearly identical construction. The major difference is in the distance metric used to determine edges. We will first give the details of Θ_k-graph construction.

Let $k \geq 3$ be an integer and for each i with $0 \leq i < k$, let $\mathcal{R}_i$ be the ray emanating from the origin that makes a counter-clockwise angle of $2\pi i/k$ with the negative y-axis. For each i with $0 \leq i \leq k$, let C_i be the cone consisting of all points in the plane that are on or between the rays $\mathcal{R}_i$ and $\mathcal{R}_{i+1}$. The Θ_k-graph of a given set P of points is the directed graph that is obtained in the following way. The vertex set is the set P. Each vertex v has at most k outgoing edges: For each i with $0 \leq i < k$, let C_i^v be the cone obtained by translating C_i such that its apex is at v. If C_i^v contains at least one point of $P \setminus \{v\}$, then let w_i be such a point whose perpendicular projection onto the bisector of C_i^v is closest to v (where closest refers to the Euclidean distance). Then the Θ_k-graph contains the directed edge (v, w_i). See Figure 1.1a for an example with $k = 4$.

For Y_k-graphs, the cones surrounding each vertex have the same construction as the Θ_k-graph. But for each cone $C_i^v, 0 \leq i < k$, we let w_i be the point in C_i^v closest to v using the Euclidean distance metric. Then the Y_k-graph contains the edge (v, w_i). See Fig. 1.1b for an example with $k = 4$.

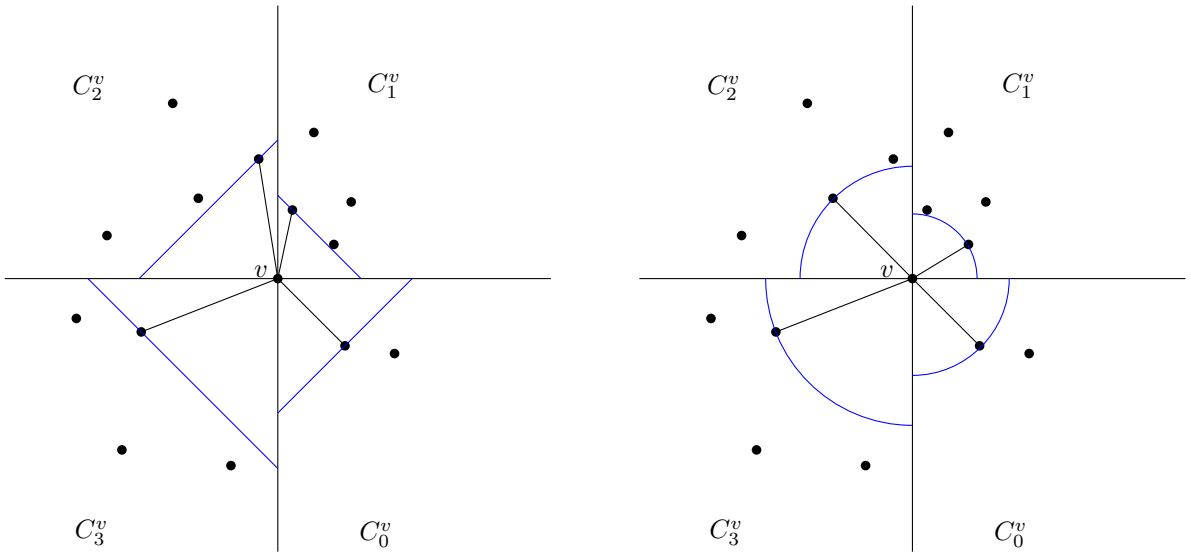

(a) How the Θ_4-graph selects edges.

(b) How the Y_4-graph selects edges.

Figure 1.1

1.2.2 *Delaunay Graphs*

The L_2-Delaunay graph is geometric graph constructed by identifying all triples of points (x, y, z) such that a circle with x, y, and z on the boundary does not contain any vertex in its interior. Such triples of points are said to be locally Delaunay. They are then connected by edges to form a triangle. Once all such triples are connected we have the Delaunay graph or Delaunay triangulation.

In general, a Delaunay graph can be constructed using any convex geometric shape to define a distance metric. To construct these Delaunay graphs, the convex shape is translated and scaled until its boundary intersects three vertices and contain no other vertices in the interior. This triple of vertices is then connected by edges to form a triangle. Repeating this process for all triples gives us a Delaunay graph of an arbitrary distance metric.

We can also generalize these constructions to 3 dimensions. In the L_2-Delaunay triangulation, we would therefore consider a sphere through 4 vertices, and if this sphere was empty of vertices in the interior, we would connect these vertices in a simplex (tetrahedron). This process can also be done with other convex shapes in 3 dimensions.

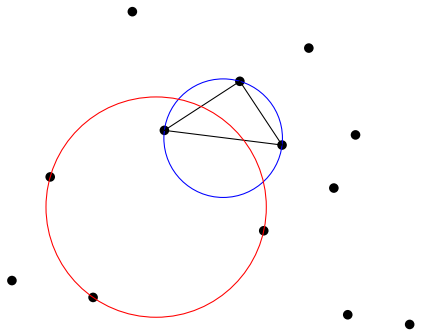

(a) How the L_2-Delaunay graph selects edges. Blue circle is through 3 points that are locally Delaunay. Red circle indicates 3 points that are not locally Delaunay.

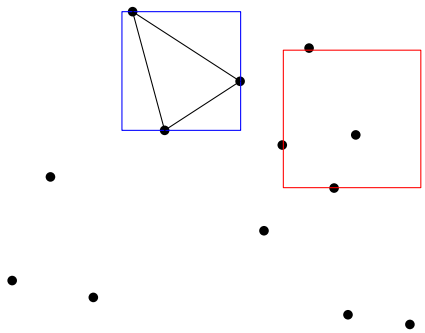

(b) How the L_∞-Delaunay graph selects edges. Blue square is through 3 points that are locally Delaunay. Red square indicates 3 points that are not locally Delaunay.

1.3 PREVIOUS WORK

Tables 1.1 and 1.2 give an overview of the relevant results. Geometric spanners were first introduced by Chew [15]. He examined the quality that Delaunay graphs have of providing "short" paths between vertices. He proved that between any pair of vertices there is a path in the graph at most $\sqrt{10}$ times the Euclidean distance. This was also the first local routing algorithm for Delaunay graphs, which Bonichon et al. [5] later generalized to the L_2-Delaunay graph.

Chew [16] showed that TD-Delaunay graphs, that is, Delaunay graphs where the convex shape defining the distance metric is an equilateral triangle, are 2-spanners. This graph was later shown to be identical to the half-θ_6-graph by Bonichon et. al[6].

The L_2-Delaunay graph was first proven a spanner by Dobkin et al.[19], who showed an upper bound on the spanning ratio of ≈ 5.08. This subsequently improved to 2.42 by Keil and Gutwin[22], and then to 1.998 by Xia[27]. Notably, this is the only known plane geometric graph with points not in convex position that has a spanning ratio of less than 2. In 3 dimensions, Bose et al.[25] showed that the convex hull of points on a sphere are a spanner with a spanning ratio of $3\pi(\pi/2+1)/2$ by exploiting properties related to the L_2-Delaunay triangulation in the plane.

Yao-graphs were introduced independently by Flinchbaugh and Jones[20] and Yao[29]. Yao showed that Y_8 is a supergraph of the minimum spanning tree. Althöfer[1] was the first to show their spanning properties, proving that for every spanning ratio $t > 1$, there exists a k such that Y_k is a t-spanner. Bose et al.[11] showed that for $k > 8$ and $\theta = 2\pi/k$, Y_k has a spanning ratio of at most $1/(\cos\theta - \sin\theta)$, which was later improved to $1/(1-2\sin(\theta/2))$ for $k > 6$ by Bose et. al[9]. Barba et al.[3] improved this to $1/(1-2\sin(3\theta/8))$ for any odd $k \geq 5$.

Table 1.1: Upper and lower bounds for the spanning ratio of Y_k- and Θ_k-graphs.

Yao	Lower Bound	Upper Bound
2,3	∞[23]	Not a spanner[23]
4	Open	≈ 54.62[18]
5	2.87[3]	$2+\sqrt{3} \approx 3.74$[3]
6	2[3]	5.8[3]
θ	Lower Bound	Upper Bound
2,3	∞[24]	Not a spanner[24]
4	7[2]	17 (this proposal)
5	≈ 3.798[14]	≈ 9.96[14]
6	2[6]	2[6]

Table 1.2: The spanning ratio of Delaunay graphs.

Metric	Lower Bound	Upper Bound
L_1, L_∞ (Square)	≈ 2.61[7]	≈ 2.61[7] (tight)
TD (Equilateral triangles)	2[16]	2[16]
L_2 (Circles)	1.5932[28]	1.998[27]
Rectangles	Open	Open

Θ-graphs were introduced by Keil and Gutwin[21, 22] and Clarkson[17] as an alternative to Yao-graphs since they were easier to compute. A spanning ratio of $1/(\cos\theta - \sin\theta)$ is proven in both articles. Ruppert and Seidel[26] improved this to $1/(1-2\sin(\theta/2))$.

Chew's[15] paper on the spanning ratio of the L_1-Delaunay triangulation is also a local routing algorithm on that same graph. Thus it simultaneously provides a bound on the routing ratio of the L_1-Delaunay triangulation of $\sqrt{10}$.

Bose and Morin[12] show that there are no 1-local memoryless routing algorithms that will work on any arbitrary graph. This implies that we must pair routing algorithms with particular classes of geometric graphs in order to route competitively. For example, in *greedy routing*, the message at vertex x moves to the neighbour y of x such that the distance $|yt|$ is minimized, i.e., the neighbour of x that is closest to t. In Figures 1.3a and 1.3b we see examples of graphs where greedy routing cycles between two and three vertices respectively. However, greedy routing will always find the destination on the L_2-Delaunay triangulation. They also give a competitive routing algorithm for the L_2-Delaunay triangulation. However, they show that there is no competitive online routing algorithm under the Euclidean distance metric in arbitrary triangulations.

Bose and Morin[13] provide a competitive local routing algorithm that works on triangulations that have the *diamond property*. This includes such graphs as the L_2-Delaunay triangulation, the greedy triangulation, and the minimum weight triangulation. A paper

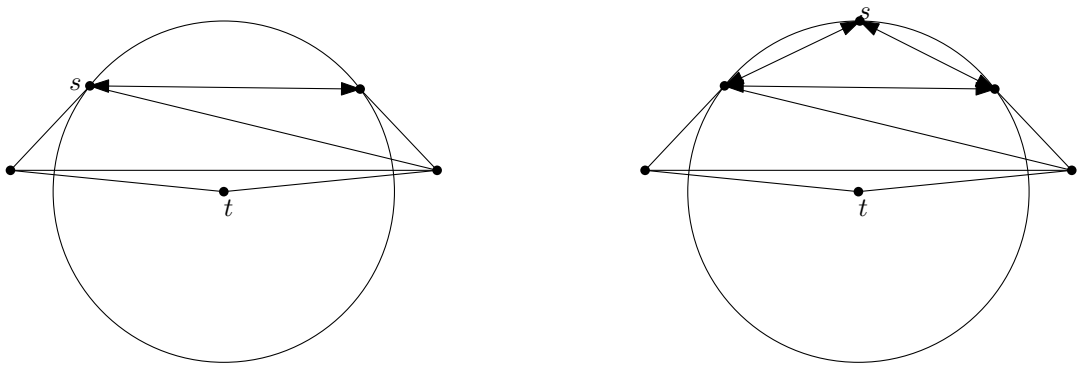

(a) Greedy routing cycling between two vertices.

(b) Greedy routing cycling between three vertices.

Figure 1.3

by Bonichon et. al[8] showed that we could route competitively on the L_2-Delaunay triangulation with a routing ratio of around 5.9, using a generalization of Chew's[15] algorithm. This was the best known routing ratio for L_2-Delaunay triangulations until a paper by Bonichon et. al [4] (outlined in this thesis) found a new algorithm with a routing ratio of 3.56, which is currently the best known. Bose et. al[10] show that the half-θ_6 graph, which is identical to the TD-Delaunay graph, has a routing ratio of $5/\sqrt{3}$, and this is shown to be tight. Since the spanning ratio of this graph is 2, local routing cannot guarantee finding the shortest path, and we see a separation between routing and spanning ratios in this graph.

For Y_k- and Θ_k-graphs, there is a simple routing algorithm called *cone-routing* that is competitive for $k \geq 7$. To route from a vertex s to a vertex t, let C_i^s be the cone of s that contains t. We forward the packet from s to its neighbour in C_i^s. Let $\theta = 2\pi/k$, then for $k \geq 7$ cone routing gives a routing ratio of $1/(1 - 2\sin(\theta/2))$. Cone routing also has the advantage of that each vertex needs only store the location of at most k neighbours, since we only forward packet's to the "closest" vertex in each cone. However, for $k < 7$, cone-routing does not necessarily give a competitive path.

BIBLIOGRAPHY

[1] Ingo Althöfer, Gautam Das, David Dobkin, Deborah Joseph, and José Soares. On sparse spanners of weighted graphs. *Discrete & Computational Geometry*, 9(1):81–100, Jan 1993.

[2] Luis Barba, Prosenjit Bose, Jean-Lou De Carufel, André van Renssen, and Sander Verdonschot. On the stretch factor of the theta-4 graph. In Frank Dehne, Roberto Solis-Oba, and Jörg-Rüdiger Sack, editors, *Algorithms and Data Structures - 13th International Symposium, WADS 2013, London, ON, Canada, August 12-14, 2013. Proceedings*, volume 8037 of *Lecture Notes in Computer Science*, pages 109–120. Springer, 2013.

[3] Luis Barba, Prosenjit Bose, Mirela Damian, Rolf Fagerberg, Wah Loon Keng, Joseph O'Rourke, André van Renssen, Perouz Taslakian, Sander Verdonschot, and Ge Xia. New and improved spanning ratios for yao graphs. In *Proceedings of the Thirtieth Annual Symposium on Computational Geometry*, SOCG'14, pages 30:30–30:39, New York, NY, USA, 2014. ACM.

[4] Nicolas Bonichon, Prosenjit Bose, Jean-Lou De Carufel, Vincent Despré, Darryl Hill, and Michiel Smid. Improved Routing on the Delaunay Triangulation. In Yossi Azar, Hannah Bast, and Grzegorz Herman, editors, *26th Annual European Symposium on Algorithms (ESA 2018)*, volume 112 of *Leibniz International Proceedings in Informatics (LIPIcs)*, pages 22:1–22:13, Dagstuhl, Germany, 2018. Schloss Dagstuhl–Leibniz-Zentrum fuer Informatik.

[5] Nicolas Bonichon, Prosenjit Bose, Jean-Lou De Carufel, Ljubomir Perković, and André van Renssen. Upper and lower bounds for online routing on delaunay triangulations. In Nikhil Bansal and Irene Finocchi, editors, *Algorithms - ESA 2015*, volume 9294 of *Lecture Notes in Computer Science*, pages 203–214. Springer Berlin Heidelberg, 2015.

[6] Nicolas Bonichon, Cyril Gavoille, Nicolas Hanusse, and David Ilcinkas. Connections between theta-graphs, delaunay triangulations, and orthogonal surfaces. In DimitriosM. Thilikos, editor, *Graph Theoretic Concepts in Computer Science*, volume 6410 of *Lecture Notes in Computer Science*, pages 266–278. Springer Berlin Heidelberg, 2010.

[7] Nicolas Bonichon, Cyril Gavoille, Nicolas Hanusse, and Ljubomir Perkovć. Tight stretch factors for L_1 and L_∞ delaunay triangulations. *Computational Geometry*, 48(3):237 – 250, 2015.

[8] Nicolas Bonichon, Cyril Gavoille, Nicolas Hanusse, and Ljubomir Perković. Plane spanners of maximum degree six. In Samson Abramsky, Cyril Gavoille, Claude Kirchner, Friedhelm Meyer auf der Heide, and PaulG. Spirakis, editors, *Automata, Languages and Programming*, volume 6198 of *Lecture Notes in Computer Science*, pages 19–30. Springer Berlin Heidelberg, 2010.

[9] Prosenjit Bose, Mirela Damian, Karim Douïeb, Joseph O'Rourke, Ben Seamone, Michiel Smid, and Stefanie Wuhrer. $\pi/2$-angle yao graphs are spanners. *International Journal of Computational Geometry and Applications*, 22(01):61–82, 2012.

[10] Prosenjit Bose, Rolf Fagerberg, André van Renssen, and Sander Verdonschot. Competitive routing in the half-theta-6-graph. In *Proceedings of the Twenty-third Annual ACM-SIAM Symposium on Discrete Algorithms*, SODA '12, pages 1319–1328. SIAM, 2012.

[11] Prosenjit Bose, Anil Maheshwari, Giri Narasimhan, Michiel H. M. Smid, and Norbert Zeh. Approximating geometric bottleneck shortest paths. *Computational Geometry - Theory and Applications*, 29(3):233–249, 2004.

[12] Prosenjit Bose and Pat Morin. Online routing in triangulations. In *Algorithms and Computation*, volume 1741 of *Lecture Notes in Computer Science*, pages 113–122. Springer Berlin Heidelberg, 1999.

[13] Prosenjit Bose and Pat Morin. Competitive online routing in geometric graphs. *Theor. Comput. Sci.*, 324(2-3):273–288, 2004.

[14] Prosenjit Bose, Pat Morin, André van Renssen, and Sander Verdonschot. The theta-5-graph is a spanner. *Computational Geometry - Theory and Applications*, 48(2):108–119, 2015.

[15] L. Paul Chew. There is a planar graph almost as good as the complete graph. In *Proceedings of the Second Annual Symposium on Computational Geometry*, SCG '86, pages 169–177, New York, NY, USA, 1986. ACM.

[16] L. Paul Chew. There are planar graphs almost as good as the complete graph. *Journal of Computer and System Sciences*, 39(2):205 – 219, 1989.

[17] K. Clarkson. Approximation algorithms for shortest path motion planning. In *Proceedings of the Nineteenth Annual ACM Symposium on Theory of Computing*, STOC '87, pages 56–65, New York, NY, USA, 1987. ACM.

[18] Mirela Damian and Naresh Nelavalli. Improved bounds on the stretch factor of y_4. *Computational Geometry - Theory and Applications*, 62:14–24, 2017.

[19] David P. Dobkin, Steven J. Friedman, and Kenneth J. Supowit. Delaunay graphs are almost as good as complete graphs. *Discrete & Computational Geometry*, 5(1):399–407, 1990.

[20] B. E. Flinchbaugh and L. K. Jones. Strong connectivity in directional nearest-neighbor graphs. *SIAM Journal on Algebraic Discrete Methods*, 2(4):461–463, 1981.

[21] J. Mark Keil. Approximating the complete euclidean graph. In Rolf G. Karlsson and Andrzej Lingas, editors, *SWAT 88, 1st Scandinavian Workshop on Algorithm Theory, Halmstad, Sweden, July 5-8, 1988, Proceedings*, volume 318 of *Lecture Notes in Computer Science*, pages 208–213. Springer, 1988.

[22] J. Mark Keil and Carl A. Gutwin. Classes of graphs which approximate the complete euclidean graph. *Discrete & Computational Geometry*, 7(1):13–28, 1992.

[23] Nawar M. El Molla. Yao spanners for wireless ad-hoc networks. Master's thesis, Villanova University, Pennsylvania, USA, 2009.

[24] Nawar M. El Molla. *Yao spanners for wireless ad-hoc networks*. PhD thesis, Villanova University, Pennsylvania, USA, 2009.

[25] Simon Pratt, Michiel Smid, and Prosenjit Bose. The convex hull of points on a sphere is a spanner. In *Proceedings of the Canadian Conference on Computational Geometry*, CCCG '14, 2014.

[26] Jim Ruppert and Raimund Seidel. Approximating the d-dimensional complete euclidean graph. In *Proceedings of the 3rd Canadian Conference on Computational Geometry*, CCCG 1991, 1991.

[27] Ge Xia. Improved upper bound on the stretch factor of Delaunay triangulations. In *Proceedings of the Twenty-seventh Annual Symposium on Computational Geometry*, SoCG '11, pages 264–273, New York, NY, USA, 2011. ACM.

[28] Ge Xia and Liang Zhang. Toward the tight bound of the stretch factor of Delaunay triangulations. In *Proceedings of the Canadian Conference on Computational Geometry*, CCCG '11, 2011.

[29] Andrew Chi-Chih Yao. On constructing minimum spanning trees in k-dimensional spaces and related problems. *SIAM Journal on Computing*, 11(4):721–736, 1982.

2

IMPROVED ROUTING ON THE DELAUNAY TRIANGULATION

ABSTRACT

A geometric graph $G = (P, E)$ is a set of points in the plane and edges between pairs of points, where the weight of an edge is equal to the Euclidean distance between its two endpoints. In local routing we find a path through G from a source vertex s to a destination vertex t, using only knowledge of the current vertex, its incident edges, and the locations of s and t. We present an algorithm for local routing on the Delaunay triangulation, and show that it finds a path between a source vertex s and a target vertex t that is not longer than $3.56|st|$, improving the previous bound of $5.9|st|$.

This chapter appeared in the proceedings of the European Symposium on Algorithms (ESA 2018) [7] and was presented there.

2.1 INTRODUCTION

A Euclidean geometric graph $G = (P, E)$ is a set P of points embedded in the plane, and a set E of edges, where each $e \in E$ is a pair of points (u, v) in P, and the weight of e is the Euclidean distance $|uv|$.

A *local routing algorithm* A is an algorithm that routes a packet through the geometric graph G from a source vertex s to a target vertex t using only knowledge of the locations of s and t, as well as the location of the current vertex and its adjacent vertices. Let $\mathcal{P}\langle s, t\rangle$ be the path found in G from s to t using A. The *routing ratio* of A for any two points s and t in the geometric graph G is the ratio of the length of $\mathcal{P}\langle s, t\rangle$ to the Euclidean distance from s to t. An algorithm A has a routing ratio c for a class of geometric graphs $\mathcal{G}$, if, for any two vertices s and t in $G \in \mathcal{G}$, $|\mathcal{P}\langle s, t\rangle| \leq c \cdot |st|$.

A graph $G = (P, E)$ is a c-spanner if for any pair of points u and v in P the shortest path in G not longer than $c|uv|$. The value c is referred to as the *stretch factor* or *spanning ratio* of G. The stretch factor of G is thus a lower bound on the routing ratio of G for any routing algorithm A, and the routing ratio is an upper bound on the spanning ratio of G. Geometric spanners are described in detail in the book by Narasimhan and Smid [13].

A notable geometric graph is the *Delaunay triangulation*. Given a set P of points in the plane, we construct the Delaunay triangulation of P as follows. For each triple (p, q, r)

of points in P, let C be the circle through p, q, and r. If there are no points of P in the interior of C, then we connect p, q, and r by edges to form a triangle. Though we did consider degenerate cases in the formation of these techniques and analysis, their inclusion ultimately adds nothing to the core anlysis. Thus in this paper we assume that P is in general position: no 3 points are colinear and no 4 points are cocircular. This allows us to focus on what is significant and new in our analysis, and avoid tedious specification of edge cases.

The Delaunay triangulation was first proven to be a spanner by Dobkin et al. [11], who showed an upper bound of 5.08 on the spanning ratio. This was subsequently improved to 2.42 by Keil and Gutwin [12], and then to 1.998 by Xia [14]. Xia and Zhang proved later that there exist Delaunay triangulations with spanning ratio greater than 1.59 [15].

Bose and Morin [6] explored some of the theoretical limitations of routing, and provided some of the first deterministic routing algorithms with constant routing ratio on the Delaunay triangulation. They denoted the spanning ratio found by Dobkin et al. [11] as $c_{dfs} \approx 5.08$. They showed that it is possible to locally route on the Delaunay triangulation with a routing ratio of $9 \cdot c_{dfs} \approx 45.749$. Bose et al. [4] further improved this bound to ≈ 15.479. Then, Bonichon et al. [2] showed that we can locally route on the Delaunay triangulation with a routing ratio of at most 5.9. In the same paper it was shown the routing ratio of any deterministic local algorithm is at least 1.70 for the Delaunay triangulation.

Table 2.1: Spanning and Routing Ratios of Delaunay Triangulations. Tight results are shown in bold.

Graph	Spanning Ratio	Routing Ratio
TD-Delaunay	**2** [9]	$\mathbf{5/\sqrt{3} \approx 2.89}$ [5]
L_1 and L_∞-Delaunay	$\mathbf{\sqrt{4+2\sqrt{2}} \approx 2.61}$ [3]	$\sqrt{10} \approx 3.16$ [8]
Hexagon-Delaunay	**2** [10]	
L_2-Delaunay	1.998 [14]	3.56 (this paper)

Efforts to evaluate spanning ratio and routing ratio have been made for Delaunay triangulations defined on other metrics. We can define these metrics by taking a convex shape and translating and scaling it until it intersects three vertices but contains no points of P in its interior. When we use a circle we obtain the L_2, or classical Delaunay triangulation. When the metric is not specified (as in the rest of this paper), then we are referring to the L_2-Delaunay triangulation. The L_1-Delaunay triangulation uses an axis aligned square, while the L_∞-Delaunay triangulation uses a square tipped at 45 degrees. By rotating the point set 45 degrees, it is easy to show the L_1 and L_∞ triangulations are equivalent. Bonichon et al. [3] showed that the L_1 and L_∞ Delaunay triangulations are $\sqrt{4+2\sqrt{2}} \approx 2.61$-spanners, and they showed that this bound was tight. On this

triangulation, Chew [8] proposed a routing algorithm with routing ratio $\sqrt{10}$. Moreover, the routing ratio of any deterministic local algorithm is at least 2.70 for this class of graph [1]. The TD-Delaunay triangulation is constructed using an equilateral triangle. Chew [9] showed that they are 2-spanners and Bose et al. [5] proposed a routing algorithm of routing ratio $\sqrt{5/3} \approx 2.89$ and they show that this ratio is the best possible. Recently Dennis, Perkovic and Duru [10] showed that the stretch factor of *Hexagon*-Delaunay triangulation is 2 and this is tight.

In this paper we present a local routing algorithm, called *MixedChordArc*, for the L_2-Delaunay triangulation, with a routing ratio of 3.56. This improves the current best routing ratio of 5.9 [1]. Table 2.1 shows our result in the context of spanning and routing ratios of other Delaunay triangulations.

In Section 2.2 we define a local algorithm that achieves this routing ratio. In Section 2.3 we prove the result for a special case, called *balanced configurations*. In Section 2.4 we extend the technique presented in Section 2.3 to prove the main result in the general case. In Section 2.5 we present our conclusions and our ideas for future directions for this line of research.

2.2 THE MIXEDCHORDARC ALGORITHM

Let P be a finite set of points in the plane, and let $DT(P)$ be the Delaunay triangulation of P. We want to route a packet between two vertices of P along edges of $DT(P)$ using only local knowledge and knowledge of our start and destination vertices.

Let s and t be the start and terminal vertices respectively, and assume, without loss of generality, that s and t are on the x-axis with s to the left of t. Consider two triangles T and T' that have non-empty intersections with st. We say that T is to the left of T', and T' is to the right of T, if a walk from s to t along st intersects T before T'.

Let C be a circle that intersects st. We denote by t_C the rightmost point of C on st. Let u and v be two points on C. We denote by $\mathcal{A}_C(u,v)$ the clockwise arc of C from u to v, and by $\mathcal{B}_C(u,v)$ the counter-clockwise arc of C from u to v. We denote the length of a geometric structure S by $|S|$.

Let $p \neq t$ be the vertex representing the current location of the packet. Let T be the rightmost triangle with p as a vertex that has a non-empty intersection with st. Let $a \neq p$ be the vertex of T that is above st, and let $b \neq p$ be the vertex of T that is below st. Let C be the circumcircle of T. We assume s to be above st, and we assume t to be on the opposite side of st from the current vertex. This ensures that when t is a neighbour of the current vertex, the algorithm will forward the packet directly to t.

Here is the algorithm MixedChordArc. First assume that $p = s$. If $|\mathcal{A}_C(s,t_C)| \leq |\mathcal{B}_C(s,t_C)|$, set $p = a$, otherwise set $p = b$. See Fig. 2.1a. If $p \neq s$, we repeat the following until $p = t$.

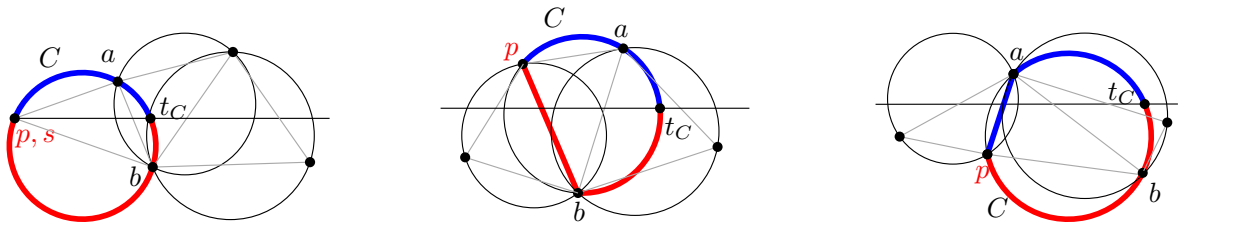

(a) From $p = s$, the blue arc is shorter than the red arc, so we forward to a.

(b) From p, the blue path is shorter than the red path, so we forward to a.

(c) From p, the blue path is shorter than the red path, so we forward to a.

Figure 2.1: Illustrating one step of the algorithm.

Algorithm MixedChordArc:

1. If p is above st:
   (a) If $|\mathcal{A}_C(p, t_C)| \leq |pb| + |\mathcal{B}_C(b, t_C)|$, set $p = a$
   (b) Else set $p = b$.
2. If p is below st:
   (a) If $|\mathcal{B}_C(p, t_C)| \leq |pa| + |\mathcal{A}_C(a, t_C)|$, set $p = b$
   (b) Else set $p = a$.

The possible choices are illustrated in Fig. 2.1. Let $\mathcal{P}\langle s, t\rangle = (s = p_0, p_1, ..., p_n = t)$ be the sequence of vertices produced by the algorithm. In this paper we prove the following theorem.

Theorem 2.2.1. *The MixedChordArc Algorithm finds a path $\mathcal{P}\langle s, t\rangle$ from s to t whose length $|\mathcal{P}\langle s, t\rangle|$ is not more than $\mu|st|$, where $\mu = \sqrt{\frac{2}{1-\sin(1)}} < 3.56$.*

We present a complete trace of the algorithm in Fig. 2.9a of Appendix 2.6. In the remaining figures of Appendix 2.6, we illustrate the proof of Theorem 2.2.1 on a complete example.

If the points are arranged in a specific way, the path produced by our algorithm is a *balanced configuration*. A balanced configuration is a construction that is effective in demonstrating our analysis technique, but would likely not be seen in practice, since the construction is very specific. It can be thought of as a worst case configuration. In Section 2.3 we define what a balanced configuration is, and analyze the length of $\mathcal{P}\langle s, t\rangle$ for this specific case. Then, in Section 2.4, we generalize the balanced configuration technique so that we can analyze the length of $\mathcal{P}\langle s, t\rangle$ in the general case.

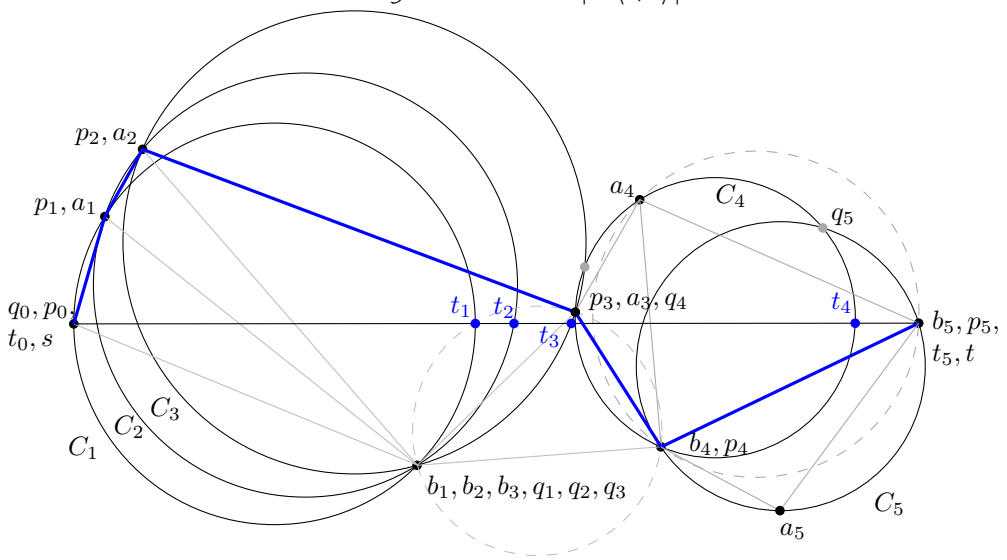

Figure 2.2: Sequence of circles in a balanced configuration and the path in blue. The dotted circles are circumcircles of triangles intersected by st but not in $\mathcal{T}$.

2.3 BOUNDING $|\mathcal{P}\langle s,t\rangle|$ IN A BALANCED CONFIGURATION

Let us consider a path $\mathcal{P}\langle s,t\rangle$ of vertices such that $p_0 = s, p_n = t$ and $p_{i-1}p_i$ is an edge of the rightmost triangle T_i of p_{i-1} that has a non-empty intersection with st. Let a_i and b_i be the other two vertices of T_i, where a_i is above st, and b_i is below st. Thus $p_i = a_i$ or $p_i = b_i$. Let $s = p_0 = a_0 = b_0$ and let $t = p_n = a_n = b_n$. Let C_i be the circumcircle of T_i, let r_i be its radius and let c_i be its center. Let C_0 be the circle centered at s with radius $r_0 = 0$. Let $\mathcal{T} = (T_1, T_2, ..., T_n)$, and let $\mathcal{C} = (C_0, C_1, ..., C_n)$ be the sequence of circles starting at C_0, followed by the circumcircles of $\mathcal{T}$. Note that the vertex of T_i that is on the opposite side of st to p_{i-1} may not be at the intersection of C_{i-1} and C_i. Thus we define a second intersection point of C_{i-1} and C_i as follows (p_{i-1} being one intersection point). If p_{i-1} is above st, then q_i is the lowest intersection of C_i and C_{i-1}. If p_{i-1} is below st, let q_i be the highest intersection of C_{i-1} and C_i. Observe that if T_i and T_{i-1} share an edge, then q_i is the vertex of T_i on the opposite side of st from p_{i-1}. See Fig. 2.2. To simplify the notation, we write t_i instead of t_{C_i}, and we write $\mathcal{A}_i(u,v)$ and $\mathcal{B}_i(u,v)$ instead of $\mathcal{A}_{C_i}(u,v)$ and $\mathcal{B}_{C_i}(u,v)$, respectively.

We say that a pair of consecutive circles C_{i-1} and C_i is *balanced* if $|\mathcal{A}_i(p_{i-1}, t_i)| = |p_{i-1}q_i| + |\mathcal{B}_i(q_i, t_i)|$ when p_{i-1} is above st, and if $|\mathcal{B}_i(p_{i-1}, t_i)| = |p_{i-1}q_i| + |\mathcal{A}_i(q_i, t_i)|$ when p_{i-1} is below st. A path $\mathcal{P}\langle s,t\rangle$ on a point set P is a *balanced configuration* when C_{i-1} and C_i are balanced for all $1 \leq i \leq n$.

2.3.1 *Analysis Technique*

To analyze the length of $\mathcal{P}\langle s,t\rangle$ we will analyze each individual step of the algorithm from p_{i-1} to p_i, and "charge" the length $|p_{i-1}p_i|$ to fixed lengths of st, and find an upper bound on the ratio of $|p_{i-1}p_i|$ to these fixed lengths. To do this in a smooth and accurate manner we introduce certain potentials, based on the circumcircles of the Delaunay triangles, that help this ratio from spiking. The balanced configuration represents a worst case and allows us to consider only one specific configuration.

Lemma 2.3.1. *Let C_{i-1} and C_i be arbitrary circles of $\mathcal{C}$, where $1 \leq i \leq n$. Then*

1. $|p_{i-1}b_i| + |\mathcal{B}_i(b_i,t_i)| \leq |p_{i-1}q_i| + |\mathcal{B}_i(q_i,t_i)|$ *when p_{i-1} is above st, and*
2. $|p_{i-1}a_i| + |\mathcal{A}_i(a_i,t_i)| \leq |p_{i-1}q_i| + |\mathcal{A}_i(q_i,t_i)|$ *when p_{i-1} is below st.*

Proof. By the triangle inequality we have $|p_{i-1}b_i| \leq |p_{i-1}q_i| + |\mathcal{B}_i(q_i,b_i)|$, from which 1 follows. Case 2 is symmetric. □

For the rest of this section, we assume that $\mathcal{P}\langle s,t\rangle$ is a balanced configuration. Consider the case when p_{i-1} is above st (the case when p_{i-1} is below st is symmetric). If $q_i = b_i$ then $|\mathcal{A}_i(p_{i-1},t_i)| = |p_{i-1}b_i| + |\mathcal{B}_i(b_i,t_i)|$, and the algorithm proceeds to a_i. If $q_i \neq b_i$, observe that $|p_{i-1}b_i| \leq |p_{i-1}q_i| + |\mathcal{B}_i(q_i,b_i)|$ by the triangle inequality (see circles C_4 and C_5 in Fig. 2.2). Thus we have $|p_{i-1}b_i| + |\mathcal{B}_i(b_i,t_i)| < |p_{i-1}q_i| + |\mathcal{B}_i(q_i,t_i)| = |\mathcal{A}_i(p_{i-1},t_i)|$, and the algorithm proceeds to b_i. Thus a balanced configuration allows for steps that cross st and steps that do not cross st. It also allows us to use $|\mathcal{A}_i(p_{i-1},t_i)|$ as an upper bound on $|p_{i-1}b_i| + |\mathcal{B}_i(b_i,t_i)|$ in the case where $p_{i-1}p_i$ crosses st.

Let $x(v)$ and $y(v)$ be the x and y-coordinates of a point v, respectively. Let s_i be a point on st such that $x(s_i) = x(t_i) - 2r_i$. We define the following potential function that we use to bound the length of $\mathcal{P}\langle s,t\rangle$.

Definition 2.3.2. *If p_{i-1} is above st, then*

$$\Phi(C_{i-1},C_i) = |\mathcal{A}_i(p_{i-1},t_i)| - |\mathcal{A}_{i-1}(p_{i-1}t_{i-1})| - \lambda|s_{i-1}s_i| - (\mu-\lambda)|t_{i-1}t_i|.$$

Otherwise, if p_{i-1} is below st, then

$$\Phi(C_{i-1},C_i) = |\mathcal{B}_i(p_{i-1},t_i)| - |\mathcal{B}_{i-1}(p_{i-1}t_{i-1})| - \lambda|s_{i-1}s_i| - (\mu-\lambda)|t_{i-1}t_i|,$$

where $\lambda = \left(\frac{1+\sin(1)}{\cos(1)} - \pi/2 - 1\right)/2 \approx 0.42$ (see (2.18) in Lemma 2.8.4, Appendix 2.8.2.3) and $\mu = \sqrt{\frac{2}{1-\sin(1)}} < 3.56$ (see (2.17) in Lemma 2.8.3, Appendix 2.8.2.3).

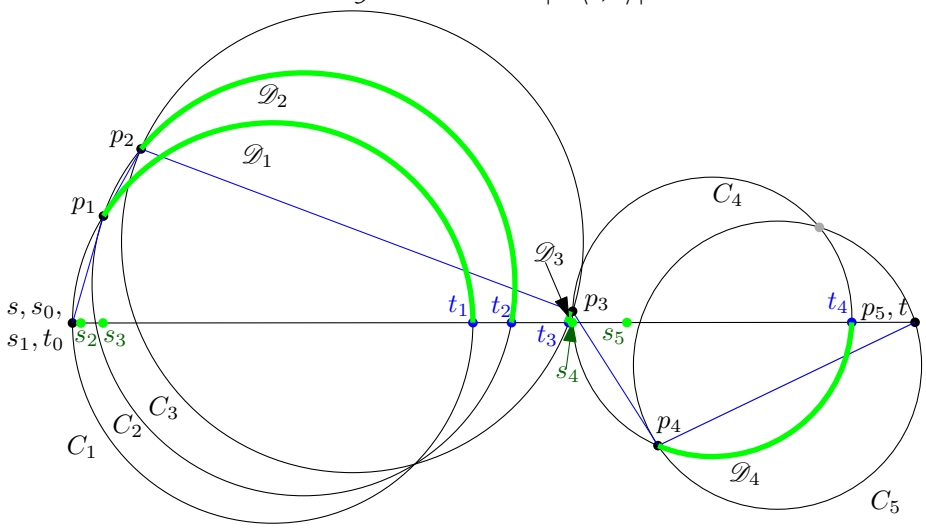

Figure 2.3: Potential functions of a balanced configuration.

See Fig. 2.2 and 2.3 for a complete example and an illustration of the potential functions. See Fig. 2.4 for an illustration of $\Phi(C_{i-1}, C_i)$. Three lemmas are used to prove Theorem 2.2.1 for balanced configurations. The proof of Lemma 2.3.3 is found in Section 2.3.3 while the proof of Lemma 2.3.4 is in Section 2.3.2.

Lemma 2.3.3. *Given a pair of balanced circles C_{i-1} and C_i,*

$$\Phi(C_{i-1}, C_i) \leq 0.$$

Lemma 2.3.4. *For any balanced configuration $\mathcal{P}\langle s,t\rangle$, $\sum_{i=1}^{n} |s_{i-1}s_i| \leq |st|$.*

Lemma 2.3.5. *For any $\mathcal{C}$, $\sum_{i=1}^{n} |t_{i-1}t_i| \leq |st|$.*

Proof. We have $t_0 = s$ and $t_n = t$. We claim that $x(t_{i-1}) < x(t_i)$ for all $1 \leq i \leq n$. If this is true, the lemma follows. We prove the claim by contradiction. Assume that $x(t_{i-1}) \geq x(t_i)$. If q_i is to the same side of st as p_{i-1}, then C_{i-1} must contain the vertex of T_i on the opposite side of st. If q_i is on the opposite side of st as p_{i-1}, then C_{i-1} contains the vertex of T_i on the same side of st as p_{i-1}. Both cases contradict the construction of a Delaunay triangulation. □

Lemma 2.3.6. *For $1 \leq i \leq n$, if p_{i-1} is above st, then*

1. *(a) $|\mathcal{A}_i(p_{i-1}, t_i)| > |p_{i-1}p_i| + |\mathcal{A}_i(p_i, t_i)|$ if p_i is above st, and*
   (b) $|\mathcal{A}_i(p_{i-1}, t_i)| > |p_{i-1}p_i| + |\mathcal{B}_i(p_i, t_i)|$ if p_i is below st

   otherwise p_{i-1} is below st and

2. *(a)* $|\mathcal{B}_i(p_{i-1},t_i)| > |p_{i-1}p_i| + |\mathcal{B}_i(p_i,t_i)|$ *if* p_i *is below* st*, and*

   (b) $|\mathcal{B}_i(p_{i-1},t_i)| > |p_{i-1}p_i| + |\mathcal{A}_i(p_i,t_i)|$ *if* p_i *is above* st*.*

Proof. Case 1a is because $|\mathcal{A}_i(p_{i-1},p_i)| > |p_{i-1}p_i|$, and Case 1b is because if p_i is below st, then the algorithm chose to cross st, which implies 1b. Case 2 is symmetric. □

Theorem 2.2.1 follows from Lemmas 2.3.3, 2.3.4, 2.3.5, and 2.3.6:

Proof. We first analyze the case when p_{i-1} is above st. Recall that in this case, $\Phi(C_{i-1},C_i)$ is defined as

$$\Phi(C_{i-1},C_i) = |\mathcal{A}_i(p_{i-1},t_i)| - |\mathcal{A}_{i-1}(p_{i-1}t_{i-1})| - \lambda|s_{i-1}s_i| - (\mu-\lambda)|t_{i-1}t_i|.$$

If p_i is above st (same side of st as p_{i-1}), then $|\mathcal{A}_i(p_{i-1},t_i)| > |p_{i-1}p_i| + |\mathcal{A}_i(p_i,t_i)|$ by Lemma 2.3.6. In this case, let $\mathscr{D}_i = \mathcal{A}_i(p_i,t_i)$. If p_i is below st, then $|\mathcal{A}_i(p_{i-1},t_i)| > |p_{i-1}p_i| + |\mathcal{B}_i(p_i,t_i)|$ by Lemma 2.3.6. In this case, let $\mathscr{D}_i = \mathcal{B}_i(p_i,t_i)$. In both cases we have $|\mathcal{A}_i(p_{i-1},t_i)| > |p_{i-1}p_i| + |\mathscr{D}_i|$.

Let $\Phi'(C_{i-1},C_i)$ be the function defined by

$$\Phi'(C_{i-1},C_i) = |p_{i-1}p_i| + |\mathscr{D}_i| - |\mathscr{D}_{i-1}| - \lambda|s_{i-1}s_i| - (\mu-\lambda)|t_{i-1}t_i|.$$

Observe that $\Phi'(C_{i-1},C_i) \le \Phi(C_{i-1},C_i)$. Lemma 2.3.3 tells us that $\Phi(C_{i-1},C_i) \le 0$, thus $\Phi'(C_{i-1},C_i) \le 0$. When p_{i-1} is below st, a symmetric proof again shows us that $\Phi'(C_{i-1},C_i) \le 0$. Recall that $p_0 = t_0 = s$, and $p_n = t_n = t$, which means $|\mathscr{D}_0| = |\mathscr{D}_n| = 0$. Therefore we have

$$\sum_{i=1}^{n} \Phi'(C_{i-1},C_i) \le 0$$

from which we get:

$$\sum_{i=1}^{n} (|p_{i-1}p_i| + |\mathscr{D}_i| - |\mathscr{D}_{i-1}|) \le \sum_{i=1}^{n} (\lambda|s_{i-1}s_i| + (\mu-\lambda)|t_{i-1}t_i|)$$

$$|\mathcal{P}\langle s,t\rangle| - |\mathscr{D}_0| + |\mathscr{D}_n| \le (\lambda+\mu-\lambda)|st| \tag{2.1}$$

$$|\mathcal{P}\langle s,t\rangle| \le \mu|st|.$$

The right hand side of (2.1) is due to Lemmas 2.3.4 and 2.3.5. □

Lemma 2.3.4 is discussed in the next section. Lemma 2.3.3 is discussed in Section 2.3.3.

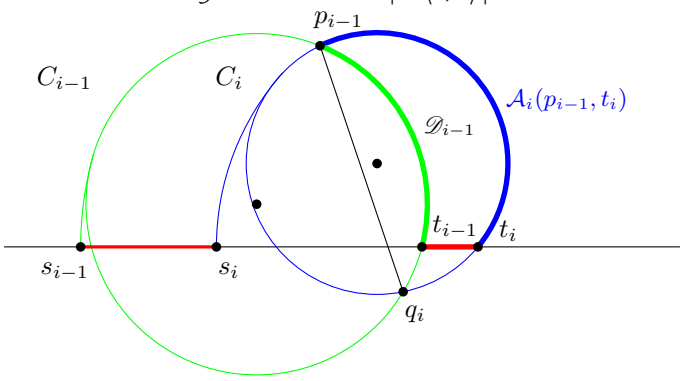

Figure 2.4: $\Phi(C_{i-1}, C_i)$.

2.3.2 *Proof of Lemma 2.3.4*

Lemma 2.3.4 uses the following supporting result:

Lemma 2.3.7. *Let C_{i-1} and C_i be balanced. Let s_{i-1} be the point on st where $x(s_{i-1}) = x(t_{i-1}) - 2r_{i-1}$ and let s_i be the point on st where $x(s_i) = x(t_i) - 2r_i$. Then $x(s_{i-1}) \leq x(s_i)$.*

Proof. See Fig. 2.5. Let u_{i-1} be the point on C_{i-1} that is diametrically opposed to t_{i-1} and let u_i be the point on C_i that is diametrically opposed to t_i. We will show the case when p_{i-1} is above st; the case when it is below st is symmetric. Since C_{i-1} and C_i are balanced, we have that $|\mathcal{A}_i(p_{i-1}, t_i)| = |p_{i-1}q_i| + |\mathcal{B}_i(q_i, t_i)|$ which implies that $|\mathcal{A}_i(p_{i-1}, t_i)| \leq \pi r_i$ and $|\mathcal{B}_i(q_i, t_i)| \leq \pi r_i$. Since $|\mathcal{A}_i(u_i, t_i)| = |\mathcal{B}_i(u_i, t_i)| = \pi r_i$, u_i is not on the open interval $\mathcal{A}_i(p_{i-1}, t_i)$ or $\mathcal{B}_i(q_i, t_i)$, which implies that either u_i is to the left of $p_{i-1}q_i$, or $u_i = p_{i-1} = q_i$, which implies that u_i is on or inside C_{i-1}.

Let O_i be the circle centered at t_i with radius $|t_iu_i| = 2r_i$. Thus O_i and C_i are tangent at u_i, and O_i intersects st at s_i. Let O_{i-1} be the circle centered at t_{i-1} with radius $2r_{i-1}$. Thus O_{i-1} and C_{i-1} are tangent at u_{i-1}, and O_{i-1} intersects st at s_{i-1}.

We prove the lemma by contradiction, thus assume that $x(s_i) < x(s_{i-1})$. In the proof of Lemma 2.3.5, we showed that $x(t_i) > x(t_{i-1})$. Therefore, it must be that O_{i-1} is in the interior of O_i, and thus they do not intersect. Since u_i is on or inside C_{i-1}, and O_i intersects u_i, O_i must intersect C_{i-1}. But C_{i-1} is contained in O_{i-1} except for the point u_{i-1}, and O_{i-1} is contained in O_i, and thus O_i cannot intersect C_{i-1}, which is a contradiction. See Fig. 2.5. □

We can now prove Lemma 2.3.4:

Proof of Lemma 2.3.4. Follows from Lemma 2.3.7 and the fact that $x(s_0) = x(s)$ and $x(s_n) < x(t)$. □

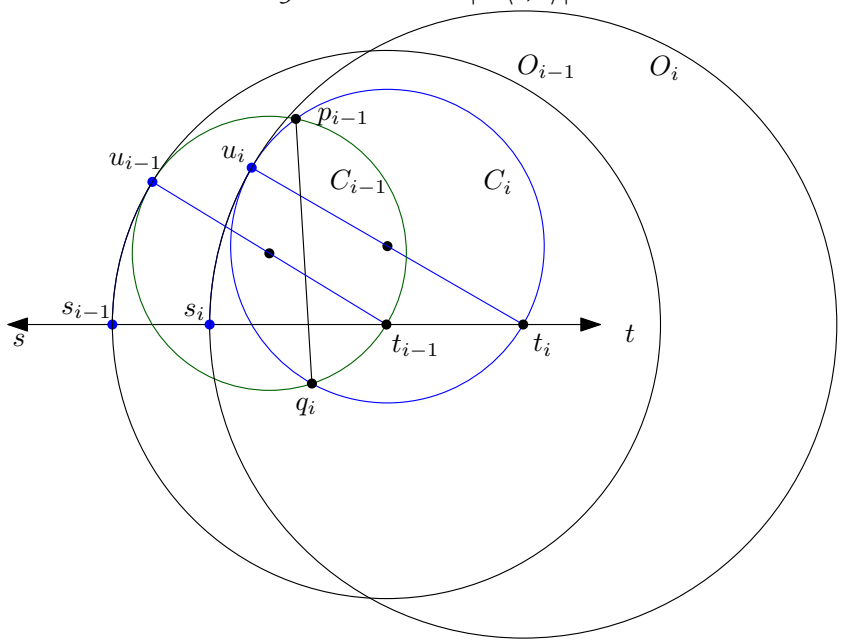

Figure 2.5: O_i must intersect O_{i-1} if C_{i-1} and C_i are path balanced, which implies that $x(s_{i-1}) \leq x(s_i)$.

2.3.3 *Proof of Lemma 2.3.3*

To show that $\Phi(C_{i-1}, C_i) \leq 0$ when C_{i-1} and C_i are balanced, we set up the following coordinate system. We show the proof for the case when p_{i-1} is above st; the case when p_{i-1} is below st is symmetric. Let c_{i-1} and c_i lie along the x-axis, and let p_{i-1} and q_i lie along the y-axis. See Fig. 2.6. Lemma 2.3.3 follows from the following two lemmas:

Lemma 2.3.8. *When C_{i-1} and C_i are balanced, if $y(t_{i-1}) \leq 0$, then $\Phi(C_{i-1}, C_i) \leq 0$.*

Lemma 2.3.9. *When C_{i-1} and C_i are balanced, if $y(t_{i-1}) > 0$, then $\Phi(C_{i-1}, C_i) \leq 0$.*

The main tool to prove these two lemmas is the following transformation, which is similar to a transformation used by Xia [14].

Transformation 2.3.10. *Fix p_{i-1} and q_i, and translate c_i to the left along the x-axis until $c_i = c_{i-1}$. Moreover keep C_{i-1} unchanged and maintain C_i as the circle with center c_i with p_{i-1} on its boundary.*

Observe that, after we have completed Transformation 2.3.10, we have $C_i = C_{i-1}$ and thus $\Phi(C_{i-1}, C_i) = 0$. If we can show that $\Phi(C_{i-1}, C_i)$ is increasing while $x(c_i)$ decreases, then it must be that $\Phi(C_{i-1}, C_i) \leq 0$ before Transformation 2.3.10. Thus we wish to find the change in $\Phi(C_{i-1}, C_i)$ with respect to the change in $x(c_i)$ during Transformation 2.3.10. Formally:

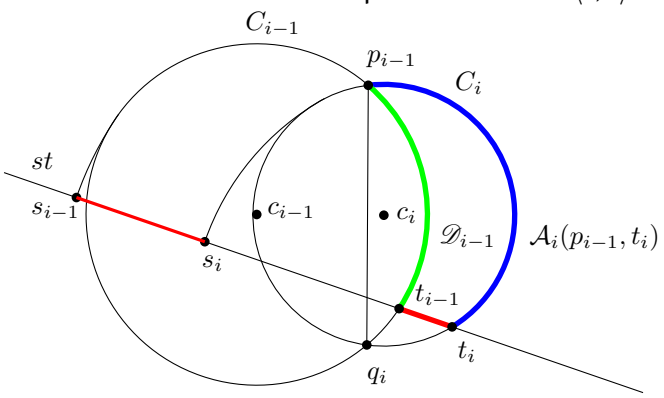

Figure 2.6: Coordinate system for analyzing $\Phi(C_{i-1}, C_i)$.

Lemma 2.3.11. *If* $\frac{d\Phi(C_{i-1},C_i)}{dx(c_i)} \leq 0$ *during Transformation 2.3.10, then* $\Phi(C_{i-1}, C_i) \leq 0$.

Proof. At the end of Transformation 2.3.10 we have that $\Phi(C_{i-1}, C_i) = 0$. If $\frac{d\Phi(C_{i-1},C_i)}{dx(c_i)} \leq 0$ then $\Phi(C_{i-1}, C_i)$ is not decreasing during Transformation 2.3.10, and thus $\Phi(C_{i-1}, C_i) \leq 0$ before Transformation 2.3.10. □

The analysis of this function is similar to Xia's approach[14]. Full details of this analysis and the proofs for Lemmas 2.3.8 and 2.3.9 can be found in Appendix 2.8.

2.4 BOUNDING $\mathcal{P}\langle s,t\rangle$ IN THE GENERAL CASE

In Section 2.3, we proved Theorem 2.2.1 for the case when the path produced by our algorithm results in a balanced configuration. In this section, we prove Theorem 2.2.1 for the general case. Given a sequence $\mathcal{C}$ of circles that intersect st, no series of transformations were found that could achieve a balanced configuration, while simultaneously providing a provable upper bound on the length of $|p_{i-1}, p_i|$. However, we were able to find *two* sequences of circles to substitute for $\mathcal{C}$. To represent each C_i in $\mathcal{C}$, we have a *potential circle* C_i^P and a *bounding circle* C_i^B. Like C_i, both C_i^P and C_i^B have t_i as their rightmost intersection with st. However, C_i intersects both p_i and p_{i-1}, while C_i^B is only required to intersect p_{i-1}, and C_i^P is only required to intersect p_i. If we look at a bounding circle C_i^B and the previous potential circle C_{i-1}^P, which intersect at p_{i-1}, they are balanced, and we can thus apply the function $\Phi(C_{i-1}^P, C_i^B)$ to relate the lengths of the arcs of these circles to $|st|$. Finally, when analyzed properly, they provide an upper bound on the length $|p_i p_{i-1}|$.

Formally, let C_0^P be the circle centered at $s = p_0$ with radius $r_0^P = 0$, and let C_n^P be the circle centered at t with radius $r_n^P = 0$. Assuming we have defined C_{i-1}^P, we will define C_i^B and C_i^P. If p_{i-1} is above st, let C_i^B be the circle through p_{i-1} and t_i for which $|\mathcal{A}_{C_i^B}(p_{i-1}, t_i)| = |p_{i-1}q_i'| + |\mathcal{B}_{C_i^B}(q_i', t_i)|$, where q_i' is the bottommost intersection

of C_{i-1}^P and C_i^B. If p_{i-1} is below st, let C_i^B be the circle through p_{i-1} and t_i for which $|\mathcal{B}_{C_i^B}(p_{i-1},t_i)| = |p_{i-1}q_i'| + |\mathcal{A}_{C_i^B}(q_i',t_i)|$, where q_i' is the topmost intersection of C_{i-1}^P and C_i^B. That is, C_{i-1}^P and C_i^B are balanced. Let r_i^B be the radius of C_i^B. The potential circle C_i^P is the circle through p_i, whose rightmost intersection with st is t_i, and whose radius is given by $r_i^P = \min\{r_i, r_i^B\}$ (with the exception of $r_n^P = 0$). Let s_i^P be the point on st with $x(s_i^P) = x(t_i) - 2r_i^P$, and let s_i^B be the point on st with $x(s_i^B) = x(t_i) - 2r_i^B$.

To simplify notation, for points u and v on C_i^P, instead of writing $\mathcal{A}_{C_i^P}(u,v)$ and $\mathcal{B}_{C_i^P}(u,v)$ to indicate clockwise and counter-clockwise arcs of C_i^P from u to v, respectively, we write $\mathcal{A}_i^P(u,v)$ and $\mathcal{B}_i^P(u,v)$. Likewise, for points u and v on C_i^B, instead of writing $\mathcal{A}_{C_i^B}(u,v)$ and $\mathcal{B}_{C_i^B}(u,v)$, we write $\mathcal{A}_i^B(u,v)$ and $\mathcal{B}_i^B(u,v)$.

See Figs. 2.7a and 2.7 for an example of the initial sequences $\mathcal{T}$ and $\mathcal{C}$ and the resulting bounding and potential arcs that we are interested in. See Appendix 2.6 for a series of diagrams walking through a complete example.

Since C_{i-1}^P and C_i^B are balanced, Φ can be extended to C_{i-1}^P and C_i^B, and thus we have

$$\Phi(C_{i-1}^P, C_i^B) = |\mathcal{A}_i^B(p_{i-1},t_i)| - |\mathcal{A}_{i-1}^P(p_{i-1},t_{i-1})| - \lambda|s_{i-1}^P s_i^B| - \mu|t_{i-1}t_i|$$

when p_{i-1} is above st and

$$\Phi(C_{i-1}^P, C_i^B) = |\mathcal{B}_i^B(p_{i-1},t_i)| - |\mathcal{B}_{i-1}^P(p_{i-1},t_{i-1})| - \lambda|s_{i-1}^P s_i^B| - \mu|t_{i-1}t_i|$$

when p_{i-1} is below st. Lemma 2.3.3 tells us that $\Phi(C_{i-1}^P, C_i^B) \le 0$. To prove Theorem 2.2.1 in the general case, it is sufficient to prove the following two lemmas. Lemma 2.4.1 is a generalization of Lemma 2.3.4, whereas Lemma 2.4.2 is a generalization of Lemma 2.3.6.

Lemma 2.4.1. $\sum_{i=1}^n |s_{i-1}^P s_i^B| \le |st|$.

Proof. Since C_{i-1}^P and C_i^B are balanced, Lemma 2.3.7 tells us that $x(s_{i-1}^P) \le x(s_i^B)$. We know that $x(s_i^P) = x(t_i) - 2r_i^P$ and $x(s_i^B) = x(t_i) - 2r_i^B$, thus the fact that $r_i^P = \min\{r_i, r_i^B\}$ implies that $x(s_i^B) \le x(s_i^P)$. Thus $|s_{i-1}^P s_i^B| \le |s_{i-1}^P s_i^P|$, and it is sufficient to show that $\sum_{i=1}^n |s_{i-1}^P s_i^P| \le |st|$. The fact that $x(s_{i-1}^P) \le x(s_i^B)$ implies that $x(s_{i-1}^P) \le x(s_i^P)$, and C_0^P is the circle centered at s with radius 0, and thus $s_0^P = s$. Since $x(s_n^P) \le x(t)$, this completes the proof. □

Due to space constraints, the following lemma will be proved in Appendix 2.7.

Lemma 2.4.2. *For $1 \le i \le n$, if p_{i-1} is above st, then*

1. (a) $|\mathcal{A}_i^B(p_{i-1},t_i)| \ge |p_{i-1}p_i| + |\mathcal{A}_i^P(p_i,t_i)|$ *if p_i is above st, and*
   (b) $|\mathcal{A}_i^B(p_{i-1},t_i)| \ge |p_{i-1}p_i| + |\mathcal{B}_i^P(p_i,t_i)|$ *if p_i is below st*

   otherwise p_{i-1} is below st and

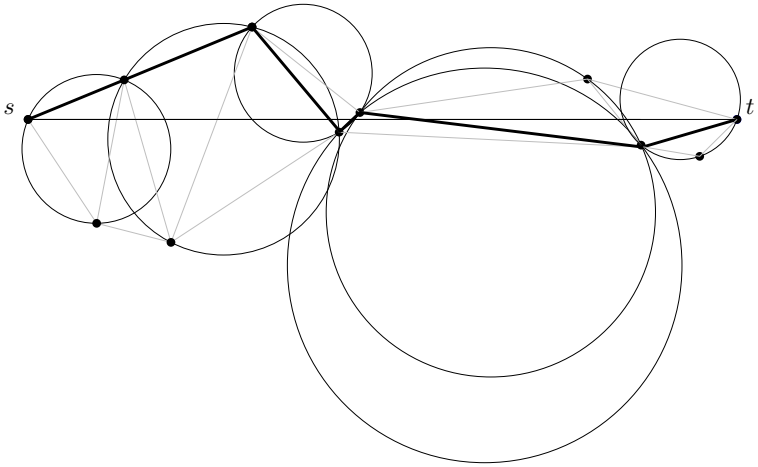

(a) The triangles and the respective circumcircles of a Delaunay triangulation intersected by st, as well as the path $\mathcal{P}\langle s,t\rangle$ found by the algorithm.

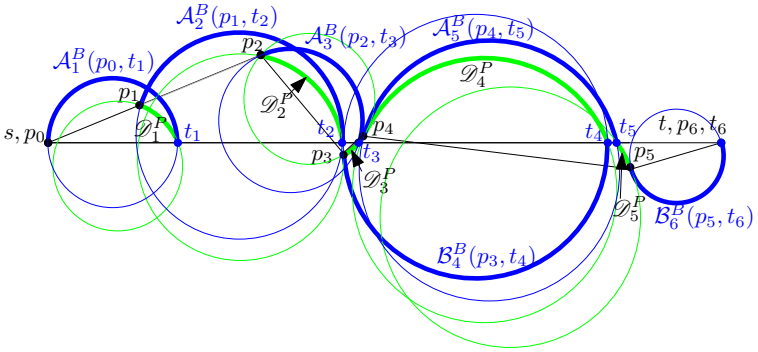

(b) The complete set of bounding arcs and potential arcs.

Figure 2.7: The construction of the potential circles and bounding circles in the general case.

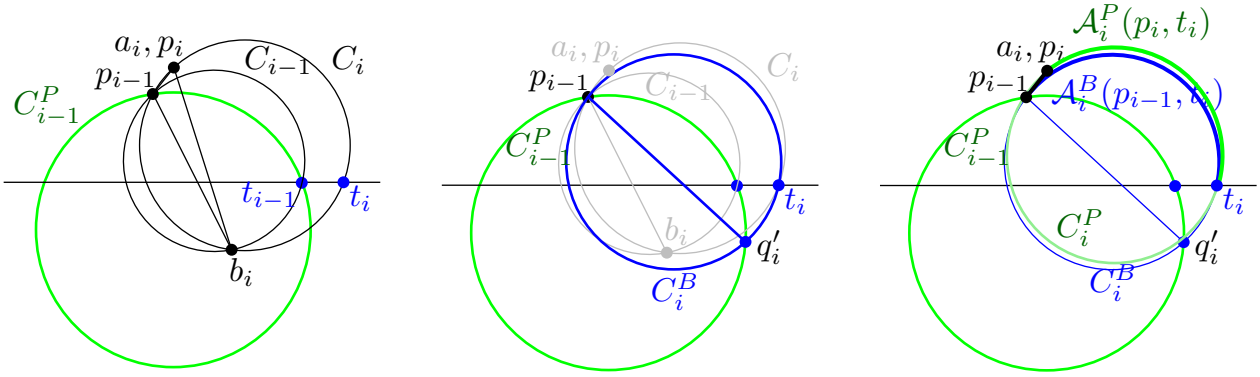

(a) C_{i-1}, C_i, and C^P_{i-1}. Notice that $r^P_{i-1} > r_{i-1}$.

(b) C^B_i and its intersection with C^P_{i-1}.

(c) $|\mathcal{A}^B_i(p_{i-1},t_i)| < |p_{i-1},p_i| + |\mathcal{A}^P_i(p_i,t_i)|$.

Figure 2.8: The reasoning behind $r^P_i = \min\{r_i, r^B_i\}$. In this diagram, $r^P_i > r_i$, and we show why it is detrimental to our analysis. Notice that $|\mathcal{A}^B_i(p_{i-1},t_i)| < |p_{i-1},p_i| + |\mathcal{A}^P_i(p_i,t_i)|$. Thus the arc $\mathcal{A}^B_i(p_{i-1},t_i)$ of the bounding circle is not long enough to pay for $|p_{i-1},p_i| + |\mathcal{A}^P_i(p_i,t_i)|$.

2. *(a)* $|\mathcal{B}^B_i(p_{i-1},t_i)| \geq |p_{i-1}p_i| + |\mathcal{B}^P_i(p_i,t_i)|$ *if* p_i *is below* st*, and*
   (b) $|\mathcal{B}^B_i(p_{i-1},t_i)| \geq |p_{i-1}p_i| + |\mathcal{A}^P_i(p_i,t_i)|$ *if* p_i *is above* st*.*

Theorem 2.2.1 follows from Lemmas 2.3.3, 2.3.5, 2.4.1, and 2.4.2.

Proof of Theorem 2.2.1. If p_i is above st, let $\mathscr{D}^P_i = \mathcal{A}^P_i(p_i,t_i)$. If p_i is below st, let $\mathscr{D}^P_i = \mathcal{B}^P_i(p_i,t_i)$. Let $\Phi'(C^P_{i-1}, C^B_i) = |p_{i-1}p_i| + |\mathscr{D}^P_i| - |\mathscr{D}^P_{i-1}| - \lambda|s^P_{i-1}s^B_i| - (\mu-\lambda)|t_{i-1}t_i|$. Lemmas 2.4.2 and 2.3.3 imply that $\Phi'(C^P_{i-1}, C^B_i) \leq \Phi(C^P_{i-1}, C^B_i) \leq 0$. Using $\Phi'(C^P_{i-1}, C^B_i)$ we get:

$$\sum_{i=1}^{n} \Phi'(C_{i-1}, C_i) \leq 0$$

$$\sum_{i=1}^{n} \left(|p_{i-1}p_i| + |\mathscr{D}^P_i| - |\mathscr{D}^P_{i-1}| \right) \leq \sum_{i=1}^{n} (\lambda|s^P_{i-1}s^B_i| + (\mu-\lambda)|t_{i-1}t_i|)$$

$$|\mathcal{P}\langle s,t\rangle| - |\mathscr{D}^P_0| + |\mathscr{D}^P_n| \leq (\lambda+\mu-\lambda)|st| \tag{2.2}$$

$$|\mathcal{P}\langle s,t\rangle| \leq \mu|st|.$$

Line (2.2) follows from Lemmas 2.3.5 and 2.4.1. □

We give some insight into the selection of r^P_i. Assume that p_{i-1} is above st (when p_{i-1} is below st the explanation is symmetric).

The purpose of $|\mathcal{A}^B_i(p_{i-1},t_i)|$ is to bound $|p_{i-1}p_i| + |\mathcal{A}^P_i(p_i,t_i)|$, as expressed in Lemma 2.8. This lemma is also the reason for selecting the radius of C^P_i as $r^P_i =$

$\min\{r_i, r_i^B\}$. It would be simpler to let $r_i^P = r_i^B$, since then we would have $s_i^P = s_i^B$. However, if we allow $r_i^P > r_i$, it can happen that the arc $|\mathcal{A}_{i+1}^B(p_i, t_{i+1})|$ on the next bounding circle is not large enough to cover $|p_i p_{i+1}| + |\mathcal{A}_{i+1}^P(p_{i+1}, t_{i+1})|$. See Fig. 2.8. Thus Lemma 2.4.2 would not hold. To account for this, we ensure that C_i^P has radius at most r_i.

2.5 CONCLUSION AND FUTURE WORK

Consider the algorithm presented in Section 2.2, along with two variations. To keep the algorithms simple, assume we are at a vertex p above st. Otherwise all assumptions are the same as in Section 2.2.

A) **BestChord:** If $|pa| + |\mathcal{A}_C(a, t_C)| \leq |pb| + |\mathcal{A}_C(b, t_C)|$ then $p = a$ else $p = b$.
B) **MixedChordArc:** If $|\mathcal{A}_C(p, t_C)| \leq |pb| + |\mathcal{A}_C(b, t_C)|$ then $p = a$ else $p = b$.
C) **MinArc:** If $|\mathcal{A}_C(p, t_C)| \leq \pi r$ then $p = a$ else $p = b$.

The algorithm presented in this paper is *MixedChordArc*. Following the techniques used in [1] we are able to show that the routing ratio of *MinArc* is between 3.14 and 3.96. Since the routing ratio of 3.56 of *MixedChordArc* is better, we do not present the details of *MinArc*.

We suspect that *BestChord* is an improvement on *MixedChordArc*. It seems plausible that we can modify the proofs presented in this paper to obtain the same upper bound for *BestChord* as for *MixedChordArc*, but for now that remains unverified. Whether or not *BestChord* is asymptotically superior to *MixedChordArc*, or whether they are asymptotically the same is still unknown.

Although we have improved the upper bound of the routing ratio on the L_2-Delaunay triangulation, it is not clear how tight our analysis is. The upper bound on the analysis is where our potential function is the weakest. A more clever potential function could lower the routing ratio using a comparable analysis. Or perhaps one of the algorithms above would respond to a completely different style of analysis.

Furthermore, the lower bound on *MixedChordArc* is still the same as the lower bound on routing on the L_2-Delaunay triangulation in general, which is approximately 1.70 [1]. So it seems there is still much room for improvement. The question remains, what other algorithms or analysis can we use to improve the routing ratio of the Delaunay triangulation? And given that the upper and lower bounds on the spanning ratio of the L_2-Delaunay triangulation are 1.998 [14] and 1.5932 [15] respectively, is there a separation of the spanning and routing ratios of the Delaunay triangulation?

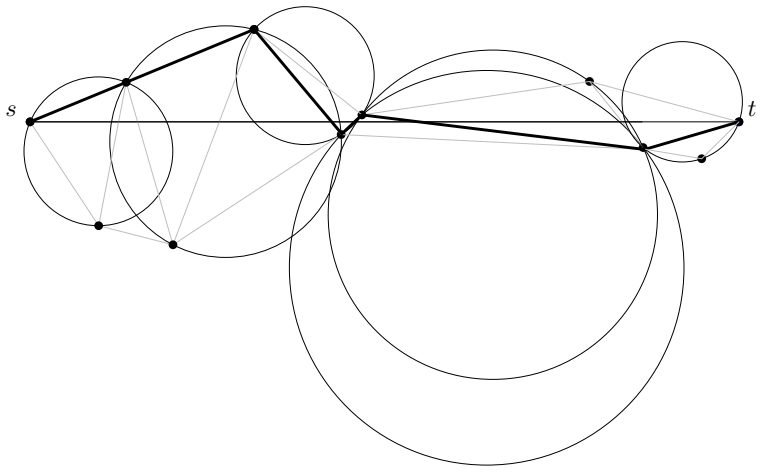

(a) $\mathcal{T}, \mathcal{C}$, and $\mathcal{P}\langle s, t\rangle$.

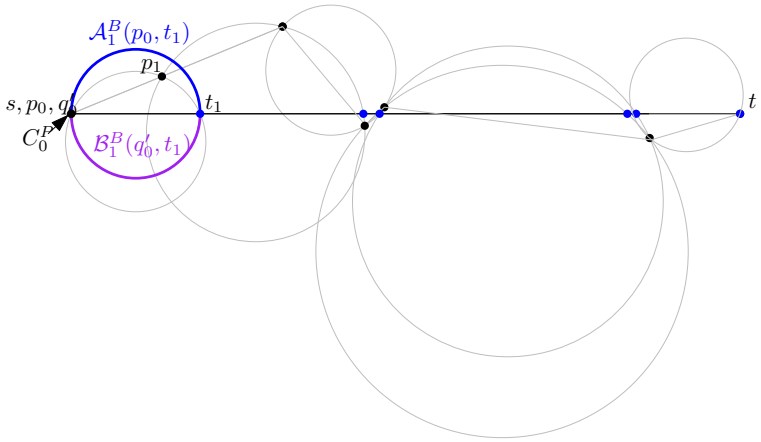

(b) C_0^P and C_1^B are balanced.

Figure 2.9: Initial configuration and construction of C_1^B given C_0^P.

2.6 A TRACE OF MIXEDCHORDARC AND AN ILLUSTRATION OF THE PROOF OF THEOREM 2.2.1

In these figures we illustrate the proof of Theorem 2.2.1.

Figure 2.9a illustrates the triangles and their respective circumcircles of the Delaunay triangulation intersected by st, as well as the path $\mathcal{P}\langle s, t\rangle$. In figure 2.9b, recall that C_0^P is the circle centered at s with radius $r_0^P = 0$. We see that C_1^B is the circle through t_i that is balanced with respect to C_0^P, i.e., $|\mathcal{A}_1^B(p_0, t_1)| = |\mathcal{B}_1^B(b_1' = p_0, t_1)| = \pi r_1^B$.

In Figure 2.10a we see C_1^P through p_1 and t_1 with radius $r_1^P = r_1^B < r_1$. In this example it is clear that $|\mathcal{A}_1^B(p_0, t_1)| \geq |p_0 p_1| + |\mathcal{A}_1^P(p_1, t_1)|$ since they are both convex and $\mathcal{A}_1^B(p_0, t_1)$ contains $p_0 p_1 + \mathcal{A}_1^P(p_1, t_1)$.

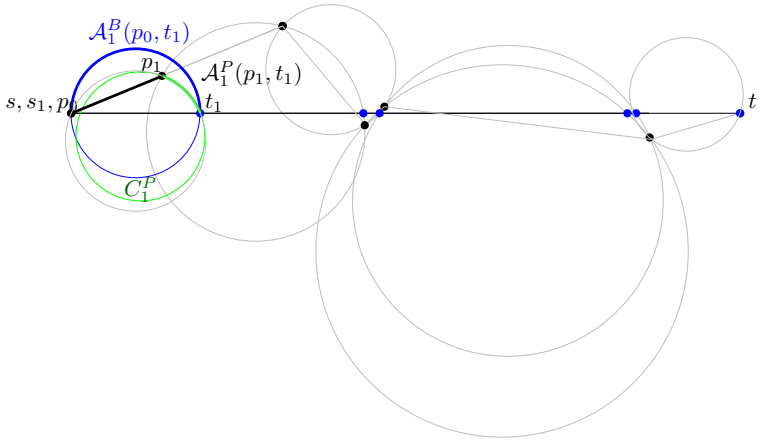

(a) C_1^P with radius $r_1^p = r_1^B$.

Figure 2.10

In Figure 2.11a, C_2^B is balanced with respect to C_1^P, that is, $|\mathcal{A}_2^B(p_1,t_2)| = |p_1q_2'| + |\mathcal{B}_2^B(q_2',t_2)|$. If Figure 2.11b we show the placement of C_2^P.

In Figure 2.11c, C_3^B is balanced with C_2^P, but note that this time $r_3^B > r_3$. Thus in Figure 2.12a, we note that $r_3^P = r_3 < r_3^B$, and therefore $C_3^P = C_3$.

In Figure 2.12b, C_4^B is balanced with C_3^P, with p_3 is under st, thus $|\mathcal{B}_4^B(p_3,t_4)| = |p_4q_4'| + |\mathcal{A}_4^B(q_4',t_4)|$. In Figure 2.12c, p_3p_4 and $\mathcal{A}_4^P(p_4,t_4)$ are not convex. Thus $|\mathcal{B}_4^B(p_3,t_4)| = |p_3q_4'| + |\mathcal{A}_4^B(q_4',t_4)| \geq |p_3p_4| + |\mathcal{A}_4^P(p_4,t_4)|$ is proven by other means. See Appendix 2.7.

In Figures 2.13a and 2.13b, the path of p_4q_5' and $\mathcal{B}_5^B(q_5',t_5)$ does not contain the path of p_4p_5 and $\mathcal{B}_5^P(p_5,t_5)$, thus we cannot use a simple proof to show $|\mathcal{A}_5^B(p_4,t_5)| = |p_4q_5'| + |\mathcal{B}_5^B(q_5',t_5)| \geq |p_4p_5| + |\mathcal{B}_5^P(p_5,t_5)|$. See Appendix 2.7.

In Figure 2.13c, note that $p_5 = q_6'$. Thus C_6^B being balanced with C_5^P implies that $|\mathcal{A}_6^B(p_5,t_6)| = |\mathcal{B}_6^B(p_5 = q_6',t_6)|$. Since $p_6 = t$, C_6^P is the circle centered at t with radius $r_6^P = 0$, and thus degenerate.

In Figure 2.14a, we see the arcs in $\Phi(C_{i-1}^P, C_i^B)$, for all $0 < i \leq 6$. For example, $\Phi(C_1^P, C_2^B) = |\mathcal{A}_2^B(p_1,t_2)| - \mathscr{D}_1^P - \lambda|s_1^Ps_2^B| - (\Phi - \lambda)|t_1t_2|$.

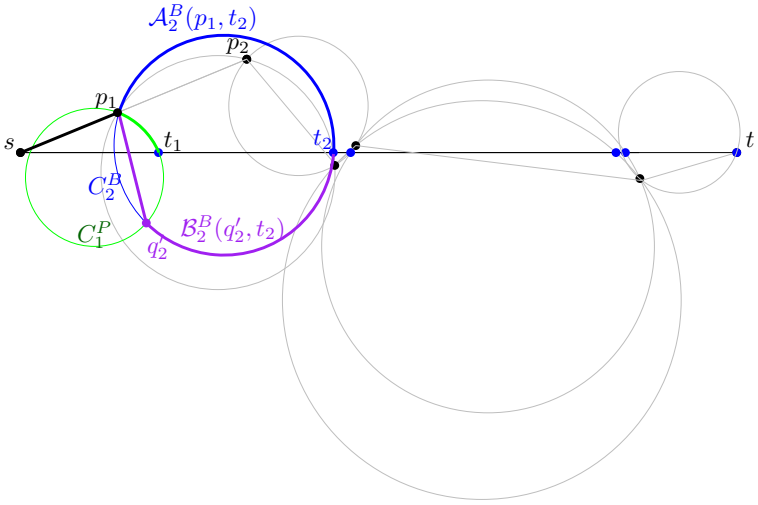

(a) C_2^B is balanced with C_1^P.

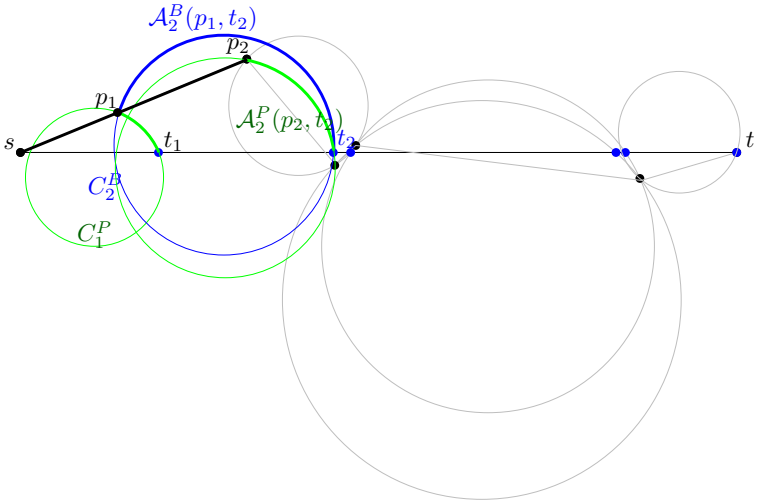

(b) C_2^P with radius $r_2^P = r_2^B$.

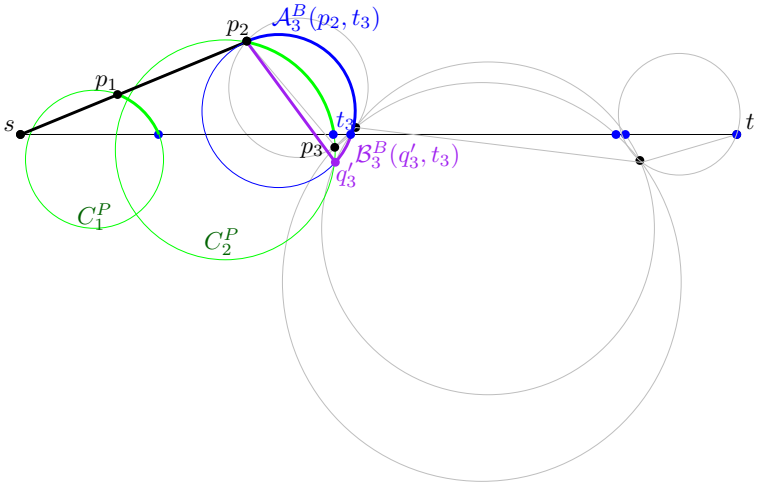

(c) C_3^B is balanced with C_2^P.

Figure 2.11

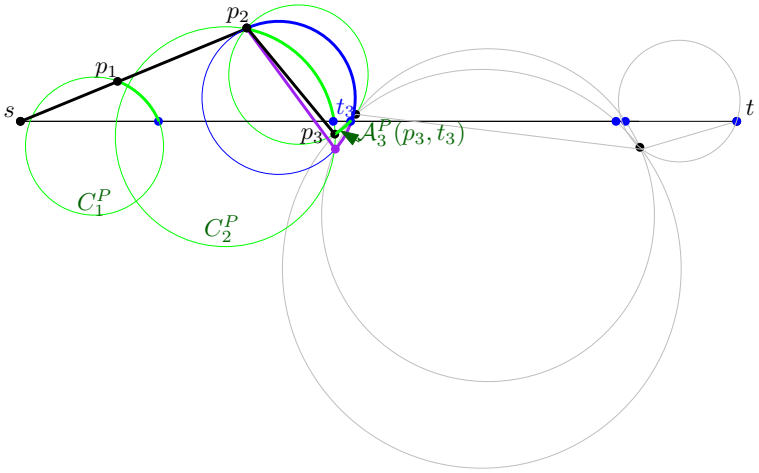

(a) Since $r_3 < r_3^B$, we set $r_3^P = r_3$, and thus $C_3^P = C_3$.

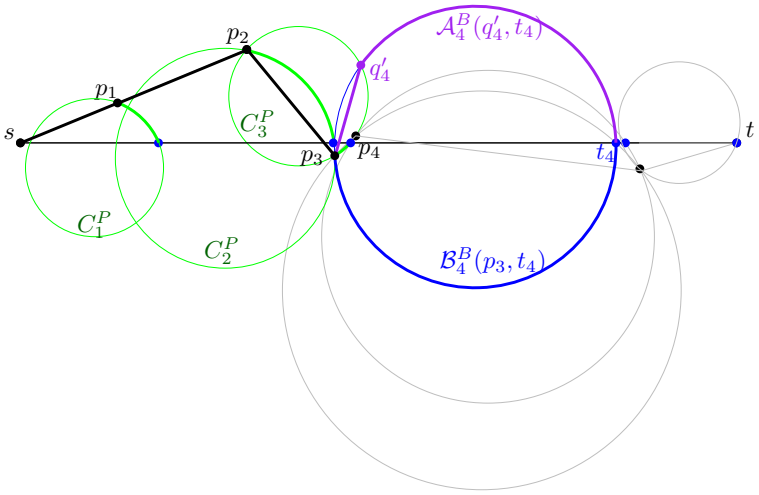

(b) C_4^B is balanced with C_3^P.

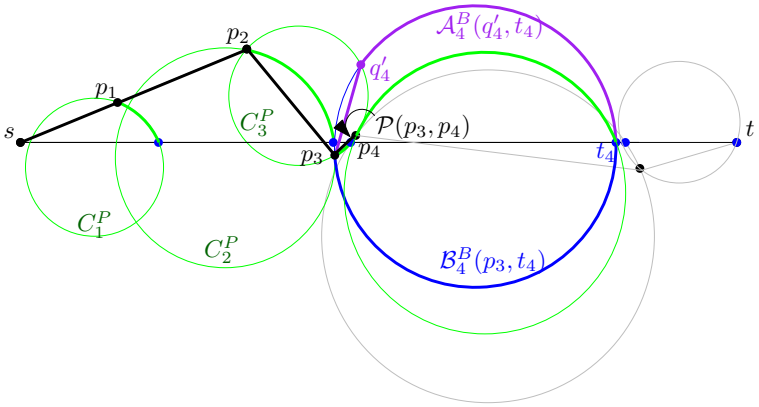

(c) C_4^P with radius $r_4^P = r_4^B$.

Figure 2.12

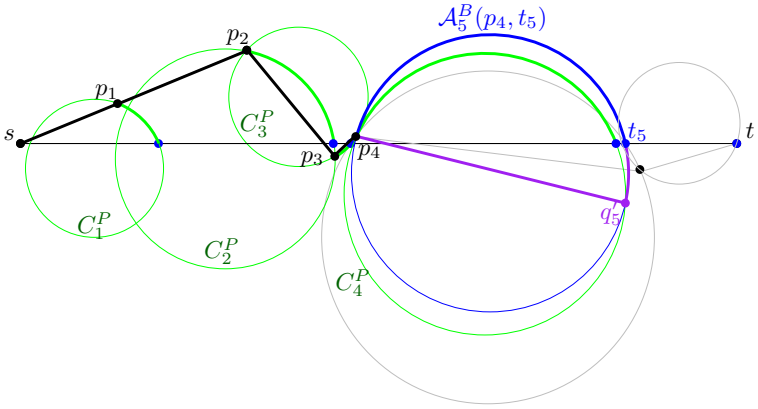

(a) C_5^B is balanced with C_4^P.

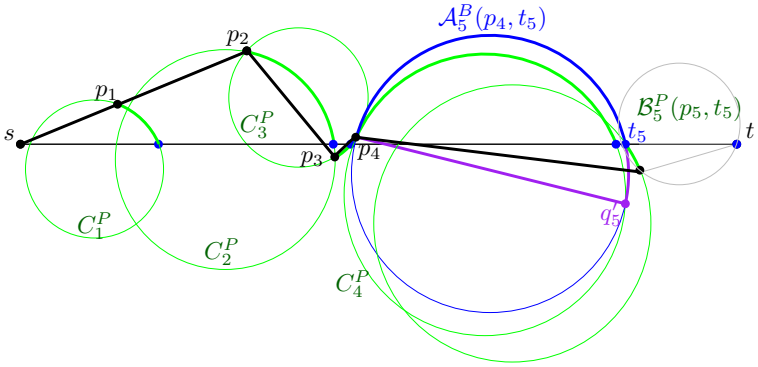

(b) C_5^P with radius $r_5^P = r_5^B$.

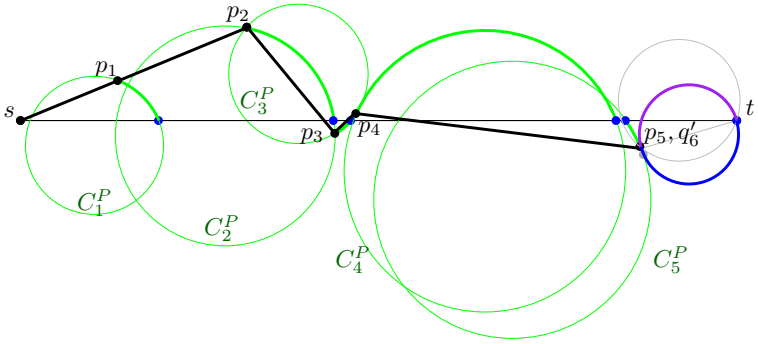

(c) C_6^B is balanced with C_5^P. Note that $q_6' = p_5$.

Figure 2.13

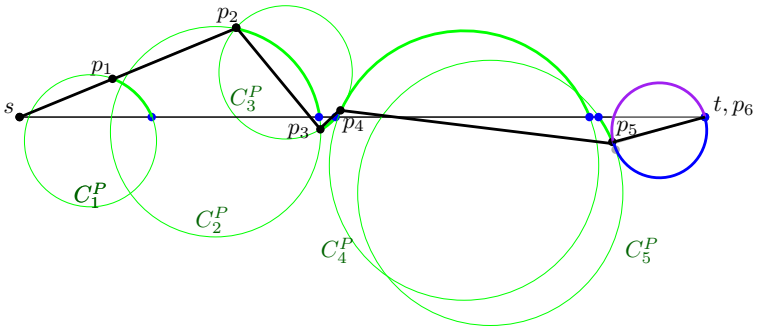

(a) C_6^P is centered at t with radius $r_6^P = 0$.

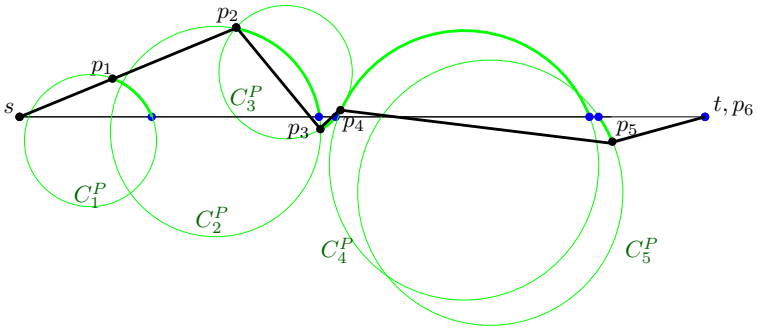

(b) $\mathcal{P}\langle s, t\rangle$ and all the potential circles.

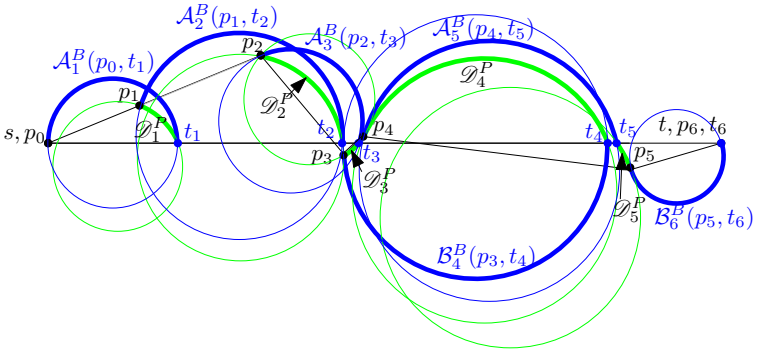

(c) The thick blue and green arcs are all the arcs considered when summing over $\Phi(C_{i-1}^P, C_i^B)$, for $1 \leq i \leq n$.

Figure 2.14

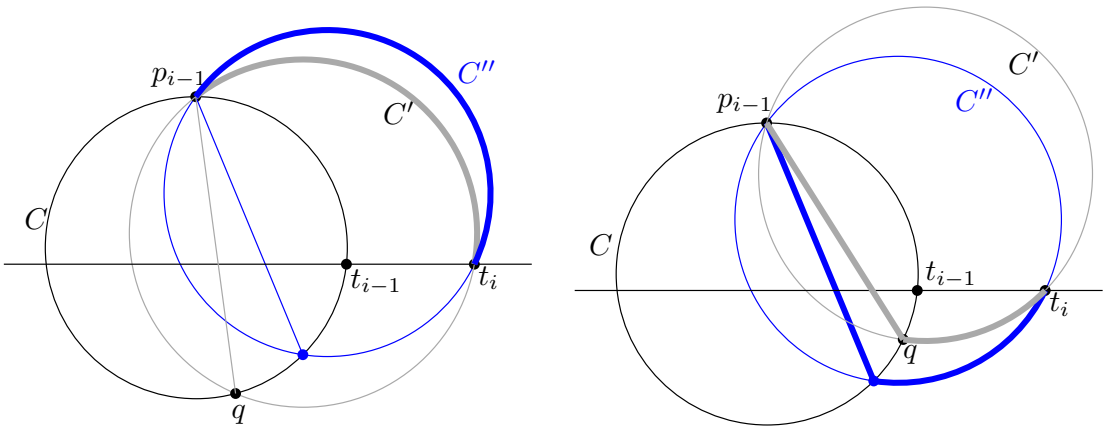

Figure 2.15: Lemma 2.7.1. $\mathcal{P}_{\mathcal{S}}(C_{i-1}, C_i)$ is longest when $C_i = C_i'$, that is C_{i-1} and C_i are balanced.

2.7 PROOF OF LEMMA 2.4.2

We will prove part 1 of Lemma 2.4.2; the proof of part 2 is symmetric. Thus we assume that p_{i-1} is above st. Let C be any circle with p_{i-1} and t_{i-1} on its boundary. Let C' be any circle with p_{i-1} and t_i on its boundary. Let q be the lowest intersection point of C and C'.

Of the following two paths from p_{i-1} to t_i, $|p_{i-1}q| + |\mathcal{B}_{C'}(q, t_i)|$ and $|\mathcal{A}_{C'}(p_{i-1}, t_i)|$, let $\mathcal{P}_{\mathcal{S}}(C, C')$ be the shorter and let $\mathcal{P}_{\mathcal{L}}(C, C')$ be the longer. If the paths have equal length label both paths $\mathcal{P}_{\mathcal{S}}(C, C')$.

Lemma 2.7.1. *Let C be a fixed circle with p_{i-1} and t_{i-1} on its boundary. Of all circles C' with p_{i-1} and t_i on its boundary, $|\mathcal{P}_{\mathcal{S}}(C, C')|$ is maximized when C and C' are balanced.*

Proof. Note that $\mathcal{P}_{\mathcal{S}}(C, C')$ and $\mathcal{P}_{\mathcal{L}}(C, C')$ are both convex. We prove the lemma by contradiction. Let C' be the circle through p_{i-1} and t_i such that C and C' are balanced. Let C'' be a circle through p_{i-1} and t_i such that $|\mathcal{P}_{\mathcal{S}}(C, C'')| > |\mathcal{P}_{\mathcal{S}}(C, C')|$. Since C' and C'' intersect in p_{i-1} and t_i, the part of C' on one side of $p_{i-1}t_i$ is contained in C'', and the part of C' to the other side of $p_{i-1}t_i$ contains C''. Consider the path $\mathcal{P}_{\mathcal{S}}(C, C')$ to the side of $p_{i-1}t_i$ where C' contains C''. Observe that $\mathcal{P}_{\mathcal{S}}(C, C')$ is convex and either contains $\mathcal{P}_{\mathcal{S}}(C, C'')$ or $\mathcal{P}_{\mathcal{L}}(C, C'')$. In either case, $|\mathcal{P}_{\mathcal{S}}(C, C')| > |\mathcal{P}_{\mathcal{S}}(C, C'')|$, a contradiction. See Fig. 2.15. □

Recall that in this section, p_{i-1} is assumed to be above st. Therefore q_i denotes the lowest intersection point of C_{i-1} and C_i. Let $\widehat{q}_i$ be the lowest intersection point of C_{i-1}^P and C_i. Then we have the following lemma.

Lemma 2.7.2. $|p_{i-1}q_i| + |\mathcal{B}_i(q_i, t_i)| \leq |p_{i-1}\widehat{q}_i| + |\mathcal{B}_i(\widehat{q}_i, t_i)|$.

Proof. Let l_i be the leftmost intersection of C_i with st. We know q_i is on the opposite side of st as p_{i-1}. If $\widehat{q}_i$ is on the same side of st as p_{i-1}, then it must be on the arc $\mathcal{B}_i(p_{i-1}, l_i)$ (by construction), thus q_i is on $\mathcal{B}_i(\widehat{q}_i, t_i)$, and the lemma is true by the triangle inequality.

Assume that $\widehat{q}_i$ is below st. If $r^P_{i-1} = r_{i-1}$, then $C^P_{i-1} = C_{i-1}$ and $\widehat{q}_i = q_i$, from which the inequality becomes trivial. Assume that $r^P_{i-1} = \min\{r_{i-1}, r^B_{i-1}\} = r^B_{i-1} < r_{i-1}$.

Since C^P_{i-1} and C_{i-1} intersect p_{i-1} and t_{i-1}, and since $r^P_{i-1} < r_{i-1}$, the convex hull of $\mathcal{A}^P_{i-1}(p_{i-1}, t_{i-1})$ contains the convex hull of $\mathcal{A}_{i-1}(p_{i-1}, t_{i-1})$. That means that the part of C^P_{i-1} to the left of $p_{i-1}t_{i-1}$ is contained in C_{i-1}. Therefore q_i is on $\mathcal{B}_i(\widehat{q}_i, t_i)$, and thus $|p_{i-1}q_i| < |p_{i-1}\widehat{q}_i| + |\mathcal{B}_i(\widehat{q}_i, q_i)|$ by the triangle inequality, which implies the lemma. □

Lemma 2.7.3. $|p_{i-1}p_i| + |\mathscr{D}_i| \leq |\mathcal{P}_{\mathcal{S}}(C_{i-1}, C_i)| \leq |\mathcal{P}_{\mathcal{S}}(C^P_{i-1}, C_i)| \leq |\mathcal{A}^B_i(p_{i-1}, t_i)|$.

Proof. For the first inequality, we consider two cases: Either p_i is above st, or p_i is below st. If p_i is above st, then the path does not cross st, therefore $|p_{i-1}p_i| + |\mathscr{D}_i| = |p_{i-1}p_i| + |\mathcal{A}_i(p_i, t_i)| < |\mathcal{A}_i(p_{i-1}, t_i)| = |\mathcal{P}_{\mathcal{S}}(C_{i-1}, C_i)|$ by the triangle inequality. If p_i is below st, then the path does cross st, therefore $|p_{i-1}p_i| + |\mathscr{D}_i| = |p_{i-1}p_i| + |\mathcal{B}_i(p_i, t_i)| \leq \min\{|\mathcal{A}_i(p_{i-1}, t_i)|, |p_{i-1}q_i| + |\mathcal{B}_i(q_i, t_i)|\} = |\mathcal{P}_{\mathcal{S}}(C_{i-1}, C_i)|$ by the triangle inequality.

By Lemma 2.7.2, we have

$$\begin{aligned} |\mathcal{P}_{\mathcal{S}}(C_{i-1}, C_i)| &= \min\{|\mathcal{A}_i(p_{i-1}, t_i)|, |p_{i-1}q_i| + |\mathcal{B}_i(q_i, t_i)|\} \\ &\leq \min\{|\mathcal{A}_i(p_{i-1}, t_i)|, |p_{i-1}\widehat{q}_i| + |\mathcal{B}_i(\widehat{q}_i, t_i)|\} \\ &= |\mathcal{P}_{\mathcal{S}}(C^P_{i-1}, C_i)|. \end{aligned}$$

For the last inequality, $|\mathcal{P}_{\mathcal{S}}(C^P_{i-1}, C_i)|$ is equal to the smallest of $|p_{i-1}\widehat{q}_i| + |\mathcal{B}_i(\widehat{q}_i, t_i)|$ and $|\mathcal{A}_i(p_{i-1}, t_i)|$. Therefore, $|\mathcal{P}_{\mathcal{S}}(C^P_{i-1}, C_i)| \leq |\mathcal{P}_{\mathcal{S}}(C^P_{i-1}, C^B_i)| = |\mathcal{A}^B_i(p_{i-1}, t_i)|$ by Lemma 2.7.1, since C^P_{i-1} and C^B_i are balanced. This proves the lemma. □

Proof of Lemma 2.4.2. Assume that p_{i-1} is above st. We have to prove that

$$|\mathcal{A}^B_i(p_{i-1}, t_i)| \geq |p_{i-1}p_i| + |\mathscr{D}^P_i|. \tag{2.3}$$

If $r^P_i = r_i < r^B_i$, then $C^P_i = C_i$, and the right-hand side of (2.3) is equal to $|p_{i-1}p_i| + |\mathscr{D}_i|$. Lemma 2.4.2 then follows from Lemma 2.7.3. Otherwise $r^P_i = \min\{r_i, r^B_i\} = r^B_i < r_i$. We consider two cases:

1. $|\mathcal{A}_i(p_{i-1}, t_i)| < \pi r_i$ and
2. $|\mathcal{A}_i(p_{i-1}, t_i)| > \pi r_i$.

Note that if $|\mathcal{A}_i(p_{i-1}, t_i)| = \pi r_i$, then r_i is the smallest radius of any circle through p_{i-1} and t_i, and thus $r^B_i \geq r_i$. Thus these two cases cover all possibilities.

Observation 2.7.4. *We have the following two inequalities*

$$|p_{i-1}t_i| > |p_it_i| \text{ and} \tag{2.4}$$
$$|\mathcal{A}_i(p_{i-1}, t_i)| \geq |p_{i-1}p_i| + |\mathscr{D}_i|. \tag{2.5}$$

Given a circle C and two points u and v on C, let $\Gamma_C(u, v)$ be the shorter of the two arcs $\mathcal{A}_C(u, v)$ and $\mathcal{B}_C(u, v)$. For a given radius r, let

$$\mathcal{Z}(r) = |\Gamma_C(p_{i-1}, t_i)| - |p_{i-1}p_i| - |\Gamma_{C'}(p_i, t_i)|,$$

where C (respectively C') is any circle with radius r, and with p_{i-1} (respectively p_i) and t_i on its boundary[1]. Since $r_i^P = r_i^B$, we need to show that $\mathcal{Z}(r_i^P) \geq 0$.

Let us consider Case 1. Observe that in $\mathcal{Z}(r_i)$, $C = C' = C_i$ since p_{i-1}, p_i, and t_i all belong to C_i. Therefore, by (2.5) and the definition of $\mathscr{D}_i$, we have $\mathcal{Z}(r_i) \geq 0$. Thus, if we can prove that $\mathcal{Z}(r)$ never decreases as r goes from r_i down to $r_i^P = r_i^B$, we are done. Hence, we want to show that $\frac{d\mathcal{Z}(r)}{dr} \leq 0$. In other words, we want to show

$$\frac{d|\Gamma_C(p_{i-1}, t_i)|}{dr} \leq \frac{d|\Gamma_{C'}(p_i, t_i)|}{dr}. \tag{2.6}$$

Let α be the angle at the center of C subtended by $\Gamma_C(p_{i-1}, t_i)$, and let β be the angle at the center of C' subtended by $\Gamma_{C'}(p_i, t_i)$. By (2.4) we have $\alpha > \beta$. Note that $|\Gamma_C(p_{i-1}, t_i)| = \alpha r$, and $|\Gamma_{C'}(p_i, t_i)| = \beta r$. Since they are both linear in r, if we prove

$$\frac{d\alpha}{dr} \leq \frac{d\beta}{dr}, \tag{2.7}$$

we have proven (2.6). We have $\sin(\alpha/2) = \frac{|p_{i-1}t_i|}{2r}$, thus $\alpha = 2\arcsin\left(\frac{|p_{i-1}t_i|}{2r}\right)$. Therefore

$$\frac{d\alpha}{dr} = -\frac{|p_{i-1}t_i|}{2\sqrt{1 - \left(\frac{|p_{i-1}t_i|}{2r}\right)^2}} \underset{by (2.4)}{\leq} -\frac{|p_it_i|}{2\sqrt{1 - \left(\frac{|p_it_i|}{2r}\right)^2}} = \frac{d\beta}{dr},$$

which proves Case 1.

Let us consider Case 2. Since $|\mathcal{A}_i(p_{i-1}, t_i)| > \pi r_i$, it must be that $|p_{i-1}b_i| + |\mathcal{B}_i(b_i, t_i)| < |\mathcal{A}_i(p_{i-1}, t_i)|$, and the algorithm crossed st at p_{i-1} (and thus $p_i = b_i$). Note that $\pi r_i > |\mathcal{B}_i(p_{i-1}, t_i)| > |p_{i-1}b_i| + |\mathcal{B}_i(b_i, t_i)| = |p_{i-1}p_i| + |\mathscr{D}_i|$. Thus $|\mathcal{B}_i(p_{i-1}, t_i)| - |p_{i-1}p_i| - |\mathcal{B}_i(p_i, t_i)| = \mathcal{Z}(r_i) \geq 0$, and we apply the same argument as above to show that $\mathcal{Z}(r_i^P) \geq 0$.

[1] Notice that $\mathcal{Z}(r)$ is defined for all $r \geq |p_{i-1}t_i|/2$.

□

2.8 PROOFS OF LEMMAS 2.3.8 AND 2.3.9 - ANALYZING $\Phi(C_{i-1}, C_i)$

In this section, we want to prove Lemmas 2.3.8 and 2.3.9. In other words, we wish to show $\Phi(C_{i-1}, C_i) \leq 0$, where

$$\Phi(C_{i-1}, C_i) = |\mathcal{A}_i(p_{i-1}, t_i)| - |\mathcal{A}_{i-1}(p_{i-1}, t_i)| - \lambda|s_{i-1}s_i| - (\mu - \lambda)|t_{i-1}t_i| \quad (2.8)$$
when p_{i-1} is above st, and
$$\Phi(C_{i-1}, C_i) = |\mathcal{B}_i(p_{i-1}, t_i)| - |\mathcal{B}_{i-1}(p_{i-1}, t_i)| - \lambda|s_{i-1}s_i| - (\mu - \lambda)|t_{i-1}t_i| \quad (2.9)$$
when p_{i-1} is below st.

Since these two cases are symmetric, for the remainder of the proof, we assume that p_{i-1} is above st, thus we focus on proving (5.1a).

We can rewrite $-\lambda|s_{i-1}s_i|$ as

$$\begin{aligned} -\lambda|s_{i-1}s_i| &= -\lambda(x(s_i) - x(s_{i-1})) \\ &= -\lambda(x(t_i) - 2r_i - x(t_{i-1}) + 2r_{i-1}) \\ &= -\lambda|t_{i-1}t_i| - 2\lambda(r_{i-1} - r_i). \end{aligned}$$

Thus we can rewrite $\Phi(C_{i-1}, C_i)$ as

$$\Phi(C_{i-1}, C_i) = |\mathcal{A}_i(p_{i-1}, t_i)| - |\mathcal{A}_{i-1}(p_{i-1}, t_{i-1})| - 2\lambda(r_{i-1} - r_i) - \mu|t_{i-1}t_i|.$$

Recall that Lemmas 2.3.8 and 2.3.9 were introduced in Section 2.3.3, where we assumed that c_{i-1} and c_i lie on the x-axis, with $x(c_i) > x(c_{i-1})$, and p_{i-1} and q_i lie on the y-axis. Therefore $x(p_{i-1}) = x(q_i) = 0$.

The following lemma is a useful result.

Lemma 2.8.1. *Let us fix C_{i-1}, C_i, p_{i-1} and t_i. Consider all line segments st such that t_i is on st, st intersects C_{i-1}, and c_{i-1} is on or above st. Among all such line segments st, $\Phi(C_{i-1}, C_i)$ is maximized when c_{i-1} is on st.*

Proof. Consider the case where c_{i-1} is above st. We rotate st until it contains c_{i-1} and observe the changes in $\Phi(C_{i-1}, C_i)$.

During the rotation of st, r_{i-1}, r_i, and t_i remain fixed, whereas t_{i-1} is changing. Note that $|t_{i-1}t_i|$ is minimized when st contains c_{i-1}. Thus $-\mu|t_{i-1}t_i|$ is increasing. We also

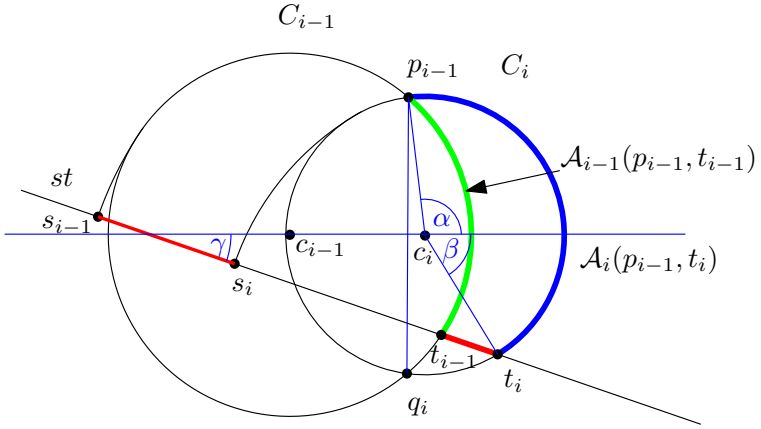

Figure 2.16: c_{i-1} and c_i lie on the x-axis, and (p_{i-1}, q_i) lies along the y-axis.

note that $-|\mathcal{A}_{i-1}(p_{i-1}, t_{i-1})|$ is increasing, while $|\mathcal{A}_i(p_{i-1}, t_i)|$ remains constant. Thus, for all cases where c_{i-1} is on or above st, $\Phi(C_{i-1}, C_i)$ is maximized when c_{i-1} is on st. □

Thus, for the rest of the proof, we assume that c_{i-1} is either on or below st.

Let α (respectively β) be the angle (respectively the signed angle) defined by the line segment $c_i p_{i-1}$ (respectively $c_i t_i$) and the x-axis such that $|\mathcal{A}_i(p_{i-1}, t_i)| = (\alpha + \beta) r_i$ (refer to Fig. 2.16). Thus $0 \leq \alpha \leq \pi$ and $-\alpha \leq \beta \leq \alpha$. Let γ be the signed angle between the x-axis and st such that $-\pi/2 < \gamma < \pi/2$. Observe that $-\pi/2 < \beta - \gamma < \pi/2$.

First, recall the definition of Transformation 2.3.10. As we apply Transformation 2.3.10, we update the values of α, β, and γ. Observe that, after we have completed Transformation 2.3.10, we have $C_i = C_{i-1}$ and thus $\Phi(C_{i-1}, C_i) = 0$. If we can show that $\Phi(C_{i-1}, C_i)$ was increasing while $x(c_i)$ decreased, then it must be that $\Phi(C_{i-1}, C_i) \leq 0$ before Transformation 2.3.10. Thus we wish to find the change in $\Phi(C_{i-1}, C_i)$ with respect to the change in $x(c_i)$ during Transformation 2.3.10. Therefore we wish to calculate the derivative of $\Phi(C_{i-1}, C_i)$ with respect to $x(c_i)$.

We define a function $\tau(\alpha, \beta, \gamma) = \frac{d\Phi(C_{i-1}, C_i)}{dx(c_i)}$. Thus if we show $\tau(\alpha, \beta, \gamma) \leq 0$, we can apply Lemma 2.3.11 and we are done.

However, this does not always work, as we sometimes encounter degenerate cases where $\frac{d\Phi(C_{i-1}, C_i)}{dx(c_i)} > 0$ at some point during Transformation 2.3.10. For the cases when this happens, we use a different argument to show that, before applying Transformation 2.3.10, when C_{i-1} and C_i are balanced, $\Phi(C_{i-1}, C_i) \leq 0$.

Thus we use a combination of Lemma 2.3.11, intermediate circles, and geometric proofs to show that $\Phi(C_{i-1}, C_i) \leq 0$ in all cases when C_{i-1} and C_i are balanced.

In Appendix 2.8.1 we compute $\tau(\alpha, \beta, \gamma) = \frac{d\Phi(C_{i-1}, C_i)}{dx(c_i)}$. In Appendix 2.8.2 we simplify and analyze this function. In Appendix 2.8.3 we identify the different cases we need to

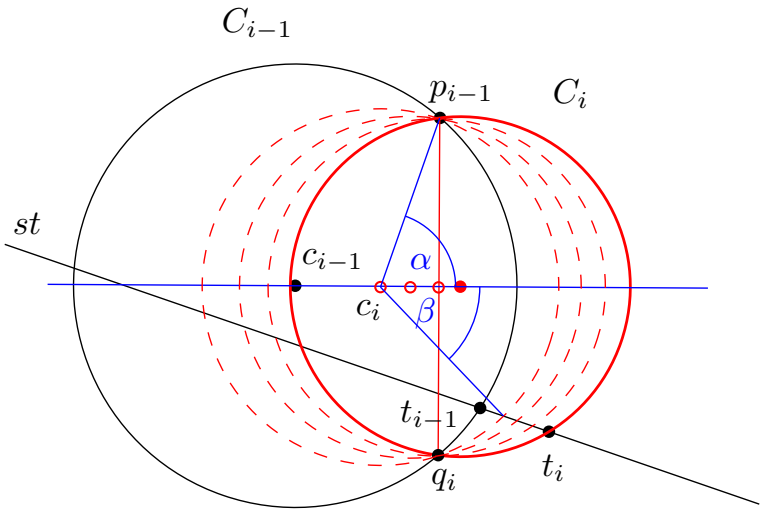

Figure 2.17: Transformation 2.3.10. We fix p_{i-1} and q_i and translate c_i towards c_{i-1}.

consider to prove Lemmas 2.3.8 and 2.3.9, and then apply the appropriate techniques to prove them.

2.8.1 *Analyzing* $\frac{d\Phi(C_{i-1},C_i)}{dx(c_i)}$

We compute $\frac{d\Phi(C_{i-1},C_i)}{dx(c_i)}$ piece by piece. Note that $x(c_i) = -r_i \cos\alpha$ and $y(p_{i-1}) = r_i \sin\alpha$.

$$\frac{dr_i}{dx(c_i)} = \frac{d\sqrt{x(c_i)^2 + y(p_{i-1})^2}}{dx(c_i)} = \frac{x(c_i)}{\sqrt{x(c_i)^2 + y(p_{i-1})^2}} = \frac{x(c_i)}{r_i} = -\cos\alpha \tag{2.10}$$

$$\frac{d\alpha}{dx(c_i)} = \frac{d(\pi/2 + \arctan(\frac{x(c_i)}{y(p_{i-1})}))}{dx(c_i)} = \frac{y(p_{i-1})}{x(c_i)^2 + y(p_{i-1})^2} = \frac{y(p_{i-1})}{r_i^2} = \frac{\sin\alpha}{r_i}$$

$$\frac{d(\alpha r_i)}{dx(c_i)} = \alpha\frac{dr_i}{dx(c_i)} + r_i\frac{d\alpha}{dx(c_i)} = \sin\alpha - \alpha\cos\alpha$$

To calculate $\frac{d|t_{i-1}t_i|}{dx(c_i)}$ and $\frac{d\beta}{dx(c_i)}$ we need the total chain rule, or total derivative. We consider $|t_{i-1}t_i|$ as a function of $x(c_i)$ and r_i. However, r_i is also a function of $x(c_i)$. Thus we can express the change in $|t_{i-1}t_i|$ with respect to the change in $x(c_i)$ as:

$$\frac{d|t_{i-1}t_i|}{dx(c_i)} = \frac{\partial|t_{i-1}t_i|}{\partial x(c_i)}\frac{dx(c_i)}{dx(c_i)} + \frac{\partial|t_{i-1}t_i|}{\partial r_i}\frac{dr_i}{dx(c_i)} = \frac{\partial|t_{i-1}t_i|}{\partial x(c_i)} + \frac{\partial|t_{i-1}t_i|}{\partial r_i}\frac{dr_i}{dx(c_i)}$$

Geometrically, $\partial x(c_i)$ represents translating c_i along the x-axis while fixing the radius r_i. ∂r_i represents changing the radius r_i of C_i, while keeping $x(c_i)$ fixed. See Fig. 2.18. However, the change in r_i is dependent on $x(c_i)$, hence we multiply by $\frac{dr_i}{dx(c_i)}$.

The partial derivatives $\frac{\partial|t_{i-1}t_i|}{\partial x(c_i)}$ and $\frac{\partial|t_{i-1}t_i|}{\partial r_i}$ can be individually determined using simple geometry. We determine $\frac{d\beta}{dx(c_i)}$ using the same technique.

2.8.1.1 *Calculating* $\frac{d|t_{i-1}t_i|}{dx(c_i)}$

In Fig. 2.20a we examine the geometry of $\frac{\partial|t_{i-1}t_i|}{\partial x(c_i)}$. Applying the sine rule yields

$$\frac{\sin(\pi/2+\beta-\gamma)}{\partial x(c_i)} = \frac{\sin(\pi/2-\beta)}{\partial|t_{i-1}t_i|}$$
$$\frac{\partial|t_{i-1}t_i|}{\partial x(c_i)} = \frac{\sin(\pi/2-\beta)}{\sin(\pi/2+\beta-\gamma)} = \frac{\cos\beta}{\cos(\beta-\gamma)}$$

In Fig. 2.19b we examine the geometry of $\frac{\partial|t_{i-1}t_i|}{\partial r_i}$. Applying the sine rule yields

$$\frac{\sin(\pi/2-\beta+\gamma)}{\partial r_i} = \frac{\sin(\pi/2)}{\partial|t_{i-1}t_i|}$$
$$\frac{\partial|t_{i-1}t_i|}{\partial r_i} = \frac{1}{\sin(\pi/2+\beta-\gamma)} = \frac{1}{\cos(\beta-\gamma)}$$

.

From (2.10) we have $\frac{dr_i}{dx(c_i)} = -\cos\alpha$. Thus

$$\begin{aligned}\frac{d|t_{i-1}t_i|}{dx(c_i)} &= \frac{\partial|t_{i-1}t_i|}{\partial x(c_i)} + \frac{\partial|t_{i-1}t_i|}{\partial r_i}\frac{dr_i}{dx(c_i)} \\ &= \frac{\cos\beta}{\cos(\beta-\gamma)} - \frac{1}{\cos(\beta-\gamma)}\cos\alpha \\ &= \frac{\cos\beta-\cos\alpha}{\cos(\beta-\gamma)}. \end{aligned} \tag{2.11}$$

2.8.1.2 *Calculating* $\frac{d\beta}{dx(c_i)}$

The total derivative of $\frac{d\beta}{dx(c_i)}$ is

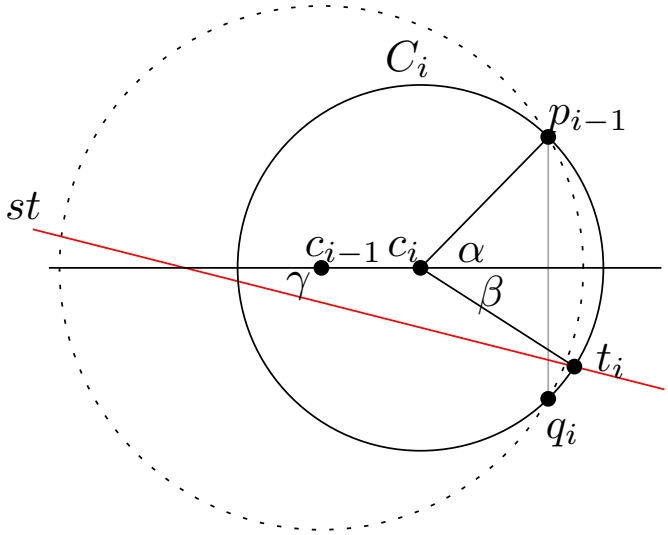

(a) Initial orientation of C_{i-1} and C_i.

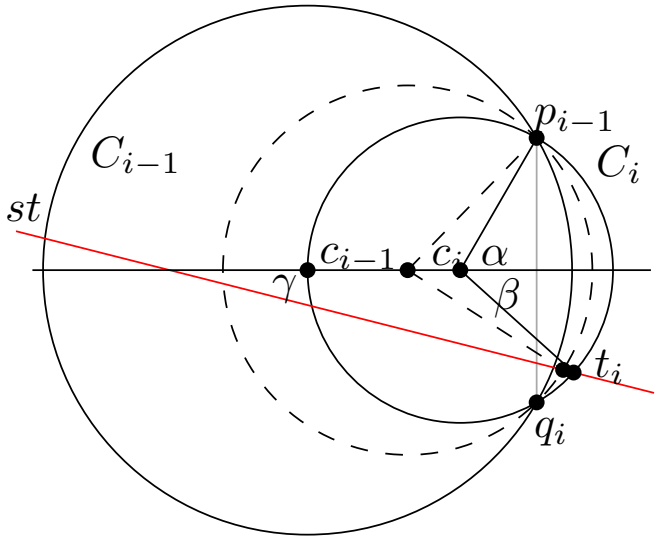

(b) The change in $x(c_i)$ represents moving c_i while fixing p_{i-1} and q_i.

Figure 2.18

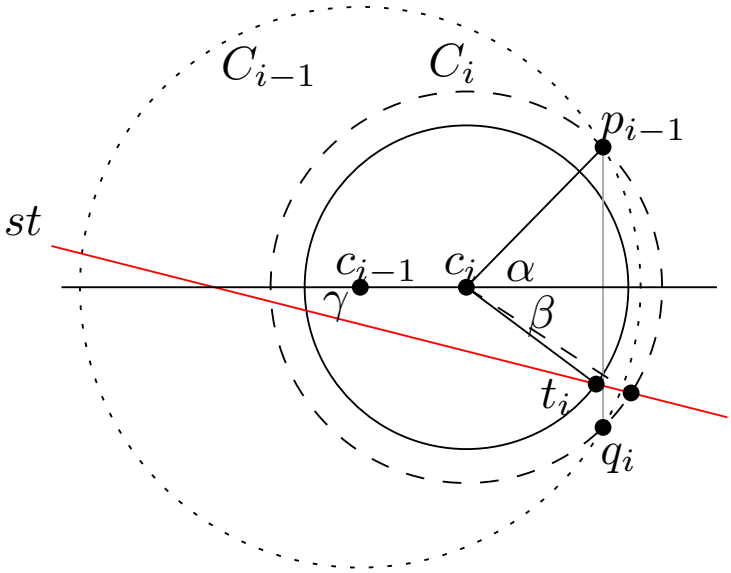

(a) In this case, $\frac{\partial |t_{i-1}t_i|}{\partial r_i}$ is obtained by fixing $x(c_i)$ and decreasing r_i.

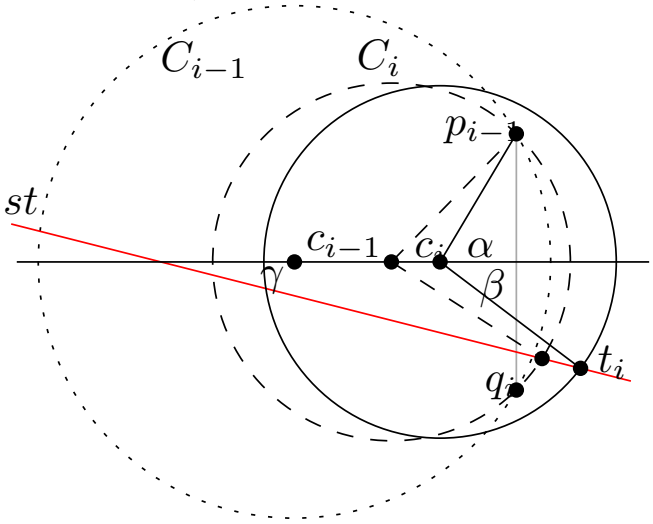

(b) $\frac{\partial |t_{i-1}t_i|}{\partial x(c_i)}$ is found by moving c_i while fixing r_i.

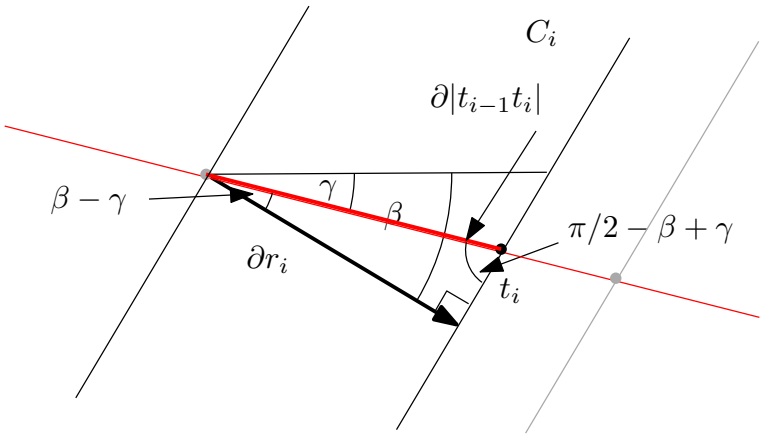

(a) $\dfrac{\partial|t_{i-1}t_i|}{\partial r_i}$.

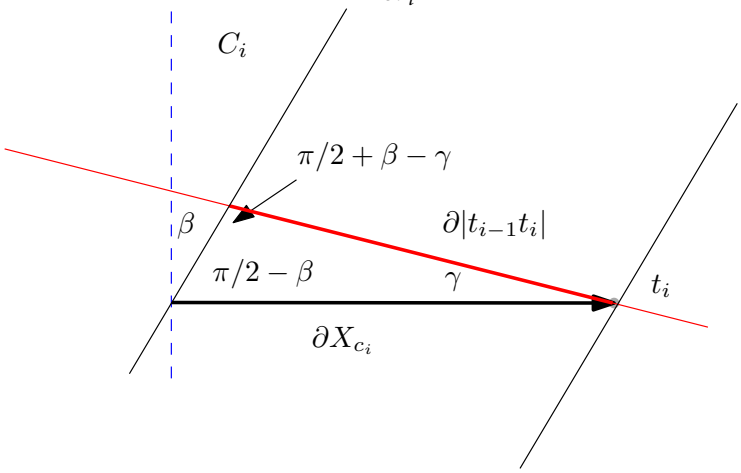

(b) $\dfrac{\partial|t_{i-1}t_i|}{\partial x(c_i)}$.

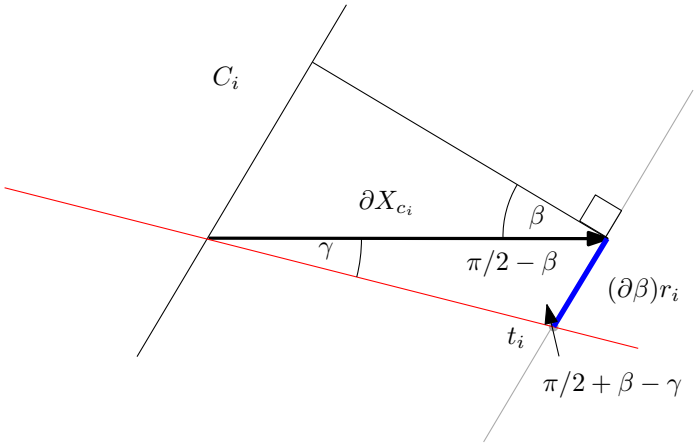

(a) The change in βr_i with $x(c_i)$. Note when $\gamma < \beta$, the change in βr_i with respect to $x(c_i)$ is positive.

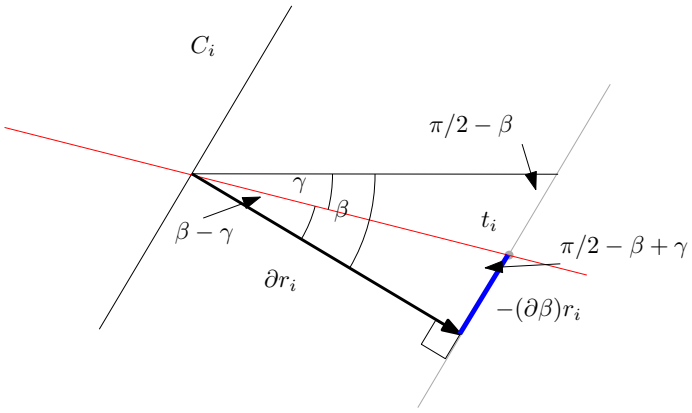

(b) The change in βr_i with r_i. Note when $\gamma < \beta$, the change in βr_i with respect to r_i is negative.

$$\frac{d\beta}{dx(c_i)} = \frac{\partial\beta}{\partial x(c_i)}\frac{dx(c_i)}{dx(c_i)} + \frac{\partial\beta}{\partial r_i}\frac{dr_i}{dx(c_i)} = \frac{\partial\beta}{\partial x(c_i)} + \frac{\partial\beta}{\partial r_i}\frac{dr_i}{dx(c_i)}$$

Fig. 2.21a shows the geometry of $\frac{\partial\beta}{\partial x(c_i)}$). Applying the sine rule yields

$$\frac{(\partial\beta)r_i}{\sin\gamma} = \frac{\partial x(c_i)}{\sin(\pi/2+\beta-\gamma)} \tag{2.12}$$

$$\frac{\partial\beta}{\partial x(c_i)} = \frac{\sin\gamma}{r_i\cos(\beta-\gamma)}. \tag{2.13}$$

Fig. 2.21b shows the geometry of $\frac{\partial\beta}{\partial x(r_i)}$. Applying the sine rule yields

$$\begin{aligned}\frac{\sin(\pi/2-\beta+\gamma)}{\partial x(r_i)} &= \frac{\sin(\beta-\gamma)}{-(\partial\beta)r_i}\\ \frac{(\partial\beta)r_i}{\partial x(r_i)} &= -\frac{\sin(\beta-\gamma)}{\sin(\pi/2+\beta-\gamma)}\\ \frac{\partial\beta}{\partial x(r_i)} &= -\frac{\sin(\beta-\gamma)}{\cos(\beta-\gamma)r_i}.\end{aligned} \tag{2.14}$$

Thus the total derivative is:

$$\begin{aligned}\frac{d\beta}{dx(c_i)} &= \frac{\partial\beta}{\partial x(c_i)} + \frac{\partial\beta}{\partial x(r_i)}\frac{dr_i}{dx(c_i)}\\ &= \frac{\sin\gamma}{\cos(\beta-\gamma)r_i} - \frac{\sin(\beta-\gamma)}{\cos(\beta-\gamma)r_i}(-\cos\alpha)\\ &= \frac{\sin\gamma+\cos\alpha\sin(\beta-\gamma)}{\cos(\beta-\gamma)r_i}\end{aligned}$$

The change in βr_i with $x(c_i)$ is

$$\begin{aligned}\frac{d(\beta r_i)}{dx(c_i)} &= \frac{\sin\gamma+\cos\alpha\sin(\beta-\gamma)}{\cos(\beta-\gamma)r_i}r_i - \beta\cos\alpha\\ &= \frac{\sin\gamma+\cos\alpha\sin(\beta-\gamma)}{\cos(\beta-\gamma)} - \beta\cos\alpha.\end{aligned}$$

Thus

$$\begin{aligned}\frac{d|\mathcal{A}_i(p_{i-1}, t_i)|}{dx(c_i)} &= \frac{d(\alpha+\beta)r_i}{dx(c_i)} \\ &= \sin\alpha - \alpha\cos\alpha + \frac{\cos\alpha\sin(\beta-\gamma)+\sin\gamma}{\cos(\beta-\gamma)} - \beta\cos\alpha \\ &= \sin\alpha - (\alpha+\beta)\cos\alpha + \frac{\cos\alpha\sin(\beta-\gamma)+\sin\gamma}{\cos(\beta-\gamma)}.\end{aligned}$$

The change in $(r_{i-1} - r_i)$ with respect to $x(c_i)$ is

$$\frac{d(r_{i-1}-r_i)}{dx(c_i)} = \frac{dr_{i-1}}{dx(c_i)} - \frac{dr_i}{dx(c_i)} \tag{2.15}$$

$$= \cos\alpha. \tag{2.16}$$

Thus the change in $\Phi(C_{i-1}, C_i)$ with respect to the change in $x(c_i)$ is given by

$$\begin{aligned}&\frac{d\Phi(C_{i-1}, C_i)}{dx(c_i)} \\ &= \frac{d(|\mathcal{A}_i(p_{i-1}, t_i)| - |\mathcal{A}_{i-1}(p_{i-1}, t_{i-1})| - 2\lambda(r_{i-1}-r_i) - \mu|t_{i-1}t_i|)}{dx(c_i)} \\ &= \frac{d(\alpha+\beta)r_i}{dx(c_i)} - \frac{d2\lambda(r_{i-1}-r_i)}{dx(c_i)} - \frac{d\mu|t_{i-1}t_i|}{dx(c_i)} \\ &= \sin\alpha - (\alpha+\beta)\cos\alpha + \frac{\cos\alpha\sin(\beta-\gamma)+\sin\gamma}{\cos(\beta-\gamma)} - 2\lambda\cos\alpha - \mu\left(\frac{\cos\beta-\cos\alpha}{\cos(\beta-\gamma)}\right) \\ &= \sin\alpha - (\alpha+\beta+2\lambda)\cos\alpha + \frac{\cos\alpha\sin(\beta-\gamma)+\sin\gamma}{\cos(\beta-\gamma)} - \mu\left(\frac{\cos\beta-\cos\alpha}{\cos(\beta-\gamma)}\right)\end{aligned}$$

2.8.2 *Simplifying* $\frac{d\Phi(C_{i-1}, C_i)}{dx(c_i)}$

Define a function:

$$\tau(\alpha, \beta, \gamma) = \sin\alpha - (\alpha+\beta+2\lambda)\cos\alpha + \frac{\cos\alpha\sin(\beta-\gamma)+\sin\gamma}{\cos(\beta-\gamma)} - \mu\left(\frac{\cos\beta-\cos\alpha}{\cos(\beta-\gamma)}\right)$$

In this section our goal is to find values of α, β, and γ for which $\tau(\alpha, \beta, \gamma) \leq 0$. We study each parameter separately, and then conclude. In Section 2.8.2.1 we analyze $\tau(\alpha, \beta, \gamma)$ with respect to γ. In Section 2.8.2.2 we analyze $\tau(\alpha, \beta, \gamma)$ with respect to β. Finally, in Section 2.8.2.3 we analyze $\tau(\alpha, \beta, \gamma)$ with respect to α.

2.8.2.1 *Maximizing $\tau(\alpha, \beta, \gamma)$ With Respect to γ.*

To find the value of γ that maximizes $\tau(\alpha, \beta, \gamma)$, we find $\frac{d\tau(\alpha,\beta,\gamma)}{d\gamma}$.

$$\begin{aligned}\frac{d\tau(\alpha,\beta,\gamma)}{d\gamma} &= \frac{-\cos\alpha + \cos\gamma\cos(\beta-\gamma) - \sin\gamma\sin(\beta-\gamma) + \mu\sin(\beta-\gamma)(\cos\beta-\cos\alpha)}{\cos^2(\beta-\gamma)} \\ &= \frac{\cos\beta - \cos\alpha + \mu\sin(\beta-\gamma)(\cos\beta-\cos\alpha)}{\cos^2(\beta-\gamma)} \\ &= \frac{(1+\mu\sin(\beta-\gamma))(\cos\beta-\cos\alpha)}{\cos^2(\beta-\gamma)}\end{aligned}$$

To maximize $\tau(\alpha, \beta, \gamma)$, let γ^* be the value for which $(1 + \mu\sin(\beta - \gamma^*)) = 0$, in other words, $\gamma^* = \beta - \arcsin(-1/\mu)$. The ranges of α, β, and γ give us that $\frac{\cos\beta-\cos\alpha}{\cos^2(\beta-\gamma)} \geq 0$. Therefore $\frac{d\tau(\alpha,\beta,\gamma)}{d\gamma} = 0$ when $\gamma = \gamma^*$, and it is positive when $\gamma < \gamma^*$ and it is negative when $\gamma > \gamma^*$. Thus $\tau(\alpha, \beta, \gamma) \leq \tau(\alpha, \beta, \gamma^*)$ for all $0 \leq \alpha \leq \pi$ and $-\alpha \leq \beta \leq \alpha$.

We can rewrite $\tau(\alpha, \beta, \gamma^*)$ as:

$$\begin{aligned}&\tau(\alpha,\beta,\gamma^*) \\ &= \cos(\beta-\gamma^*)(\sin\alpha - (\alpha+\beta+2\lambda)\cos\alpha) + \cos\alpha\sin(\beta-\gamma^*) + \sin\gamma^* - \mu(\cos\beta-\cos\alpha) \\ &= \sqrt{1-(1/\mu)^2}(\sin\alpha - (\alpha+\beta+2\lambda)\cos\alpha) - \frac{\cos\alpha}{\mu} + \sin\left(\beta - \arcsin\left(\frac{-1}{\mu}\right)\right) - \mu(\cos\beta-\cos\alpha) \\ &= \sqrt{1-(1/\mu)^2}(\sin\alpha - (\alpha+\beta+2\lambda)\cos\alpha) - \frac{\cos\alpha}{\mu} + \sin\beta\sqrt{1-(1/\mu)^2} + \frac{\cos\beta}{\mu} - \mu(\cos\beta-\cos\alpha) \\ &= \sqrt{1-(1/\mu)^2}(\sin\alpha + \sin\beta - (\alpha+\beta+2\lambda)\cos\alpha) - \left(\mu - \frac{1}{\mu}\right)(\cos\beta-\cos\alpha).\end{aligned}$$

Let $A = \sqrt{1-(1/\mu)^2} = \frac{\sqrt{1+\sin(1)}}{\sqrt{2}}$ and let $B = \left(\mu - \frac{1}{\mu}\right) = A\left(\frac{1+\sin(1)}{\cos(1)}\right)$. Then we have

$$\tau(\alpha, \beta, \gamma^*) = A(\sin\alpha + \sin\beta - (\alpha + \beta + 2\lambda)\cos\alpha) - B(\cos\beta - \cos\alpha).$$

2.8.2.2 *Maximizing $\tau(\alpha, \beta, \gamma^*)$ With Respect to β.*

To see how $\tau(\alpha, \beta, \gamma^*)$ behaves with respect to β, we calculate:

$$\frac{d\tau(\alpha, \beta, \gamma^*)}{d\beta} = A(\cos\beta - \cos\alpha) + B(\sin\beta).$$

We can now prove the following lemma.

Lemma 2.8.2. *For a fixed α, $\tau(\alpha, \beta, \gamma^*)$, as a function of β, is unimodal and $\tau(\alpha, \beta, \gamma^*) \leq \max\{\tau(\alpha, -\alpha, \gamma^*), \tau(\alpha, \alpha, \gamma^*)\}$.*

Proof. The expression $A(\cos\beta - \cos\alpha)$ is always positive, since $|\beta| \leq \alpha$. Moreover $B(\sin\beta)$ has the same sign as β. Thus $\frac{d\tau(\alpha, \beta, \gamma^*)}{d\beta}$ is convex in β, which means it is maximized at the lowest and highest values of β, i.e., $\tau(\alpha, \beta, \gamma^*) \leq \max\{\tau(\alpha, -\alpha, \gamma^*), \tau(\alpha, \alpha, \gamma^*)\}$. □

2.8.2.3 $\tau(\alpha, \sin\alpha, \gamma^*) \leq 0$

In this section we prove the following lemma.

Lemma 2.8.3. *$\tau(\alpha, \sin\alpha, \gamma^*) \leq \tau(\pi/2, \sin(\pi/2), \gamma^*) = 0$, for all $0 \leq \alpha \leq \pi$.*

First we prove the equality. When $\alpha = \pi/2$, we have

$$\tau(\pi/2, \sin(\pi/2), \gamma^*) = A(1 + \sin(1)) - B\cos(1) = 0. \tag{2.17}$$

Note that we obtain the value μ by letting $A = \sqrt{1 - (1/\mu)^2}$ and $B = \left(\mu - \frac{1}{\mu}\right)$ and then solving (2.17) for μ.

Now we show that $\tau(\alpha, \sin\alpha, \gamma^*) \leq \tau(\pi/2, \sin(\pi/2), \gamma^*)$. Observe that $\tau(\alpha, \sin\alpha, \gamma^*)$ is a function of a single variable α. We find the derivative of $\tau(\alpha, \sin\alpha, \gamma^*)$ with respect to α. Let $\eta = \frac{d\tau(\alpha, \sin\alpha, \gamma^*)}{d\alpha}$. Then

$$\begin{aligned}\eta =& \frac{d}{d\alpha} A(\sin\alpha + \sin(\sin\alpha) - (\alpha + \sin\alpha + 2\lambda)\cos\alpha) - B(\cos(\sin\alpha) - \cos\alpha) \\ =& A(\cos(\sin\alpha)\cos\alpha - \cos^2\alpha + (\alpha + \sin\alpha + 2\lambda)\sin\alpha) + B(\sin(\sin\alpha)\cos\alpha - \sin\alpha).\end{aligned}$$

Let $\eta_1 = \cos\alpha(A(\cos(\sin\alpha) - \cos\alpha))$ and let $\eta_2 = A(\alpha + \sin\alpha + 2\lambda)\sin\alpha + B\sin(\sin\alpha)\cos\alpha - B\sin\alpha$. Thus $\eta = \eta_1 + \eta_2$. Note that $\eta_1 > 0$ when $0 \leq \alpha < \pi/2$, $\eta_1 = 0$ when $\alpha = \pi/2$, and $\eta_1 < 0$ when $\pi/2 < \alpha \leq \pi$. We wish to show that η_2 exhibits the same behaviour. To this end, we define the function:

$$\eta_2' = A(\alpha + \sin\alpha + 2\lambda)\sin\alpha + B\sin(1)\sin\alpha\cos\alpha - B\sin\alpha.$$

Lemma 2.8.4. *The function $\eta_2' > 0$ for $0 \leq \alpha < \pi/2$, $\eta_2' = 0$ when $\alpha = \pi/2$, and $\eta_2' < 0$ when $\pi/2 < \alpha \leq \pi$.*

Proof. Let $\eta_3 = \dfrac{\eta_2'}{\sin\alpha} = A(\alpha + \sin\alpha + 2\lambda) + B\sin(1)\cos\alpha - B$. We take the second derivative of η_3 with respect to α.

$$\begin{aligned}\frac{d^2\eta_3}{d\alpha^2} &= \frac{d^2}{d\alpha^2}A(\alpha + \sin\alpha + 2\lambda) + B\sin(1)\cos\alpha - B \\ &= \frac{d}{d\alpha}A(1 + \cos\alpha) - B\sin(1)\sin\alpha) \\ &= -A\sin\alpha - B\sin(1)\cos\alpha.\end{aligned}$$

For $0 \leq \alpha \leq \pi/2$, $\dfrac{d^2\eta_3}{d\alpha^2} < 0$. For $\pi/2 < \alpha \leq \pi$, the first term is increasing until it reaches 0 at $\alpha = \pi$. The second term becomes positive and increases until it's maximized at $\alpha = \pi$. Thus $\dfrac{d^2\eta_3}{d\alpha^2}$ is negative followed by positive, which implies that η_3 is concave followed by convex. At $\alpha = 0$ we have $A(\alpha + \sin\alpha + 2\lambda) + B\sin(1)\cos\alpha - B = 2A\lambda + B(\sin(1) - 1) > 0.28$ which is positive. At $\alpha = \pi$ we have $A(\pi + 2\lambda) - B(\sin(1) + 1) < -2.20$ which is negative. This, together with the fact that $\dfrac{d^2\eta_3}{d\alpha^2}$ is concave followed by convex implies that η_3 intersects the x-axis in only one place. We know $\sin\alpha = 0$ when $\alpha = 0$ and when $\alpha = \pi$, and $\sin\alpha > 0$ when $0 < \alpha < \pi$. Since $\eta_2' = \eta_3\sin\alpha$, $\eta_2' = 0$ when $\alpha = 0$ or π. Thus η_2' intersects the x-axis at 0, π, and one other place.

When $\alpha = \pi/2$, we have

$$\begin{aligned}
\eta_2' &= A(\alpha + \sin\alpha + 2\lambda)\sin\alpha + B\sin(1)\sin\alpha\cos\alpha - B\sin\alpha \\
&= A(\pi/2 + 1 + 2\lambda) - B \qquad (2.18) \\
&= A\left(\pi/2 + 1 + 2\left(\frac{1+\sin(1)}{\cos(1)} - \pi/2 - 1\right)/2\right) - A\left(\frac{1+\sin(1)}{\cos(1)}\right) \\
&= A\left(\frac{1+\sin(1)}{\cos(1)}\right) - A\left(\frac{1+\sin(1)}{\cos(1)}\right) \\
&= 0.
\end{aligned}$$

□

Note that (2.18) is where we obtain the value for λ.

The function η_2' is η_2 with the term $\cos\alpha\sin(\sin\alpha)$ replaced by the term $\cos\alpha\sin(1)\sin\alpha$. To relate η_2' to η_2 we show the following:

Lemma 2.8.5. $\cos\alpha\sin(1)\sin\alpha \leq \cos\alpha\sin(\sin\alpha)$ *for* $0 \leq \alpha \leq \pi/2$, *and* $\cos\alpha\sin(1)\sin\alpha \geq \cos\alpha\sin(\sin\alpha)$ *for all* $\pi/2 < \alpha \leq \pi$.

Proof. To prove the claim, let $\theta = \sin\alpha$. Since $\cos\alpha$ is positive for $0 \leq \alpha < \pi/2$, and negative for $\pi/2 < \alpha \leq \pi$, proving Lemma 2.8.5 is equivalent to proving $\theta\sin(1) \leq \sin\theta$, for all $0 \leq \theta \leq 1$. We note that $\theta\sin(1)$ is a linear function with a slope of $\sin(1)$, while $\sin\theta$ is a convex function in the given interval. They intersect at $\theta = 0$ and $\theta = 1$, and $\sin\theta$ contains $\theta\sin(1)$ from $0 \leq \theta \leq 1$. Thus $\theta\sin(1) \leq \sin\theta$, for all $0 \leq \theta \leq 1$. □

As a consequence we get the following corollaries:

Corollary 2.8.6. $\eta_2' \leq \eta_2$ *for all* $0 \leq \alpha < \pi/2$ *and* $\eta_2' \geq \eta_2$ *for all* $\pi/2 < \alpha \leq \pi$, *and* $\eta_2' = \eta_2$ *for all* $\alpha = \pi/2$

which leads to

Corollary 2.8.7. *The function* $\eta_2 > 0$ *when* $0 \leq \alpha < \pi/2$, $\eta_2 = 0$ *when* $\alpha = \pi/2$, *and* $\eta_2 < 0$ *when* $\pi/2 < \alpha \leq \pi$.

Note that $\eta_1 = 0$ when $\alpha = 0$ and $\pi/2$, is positive when $0 < \alpha < \pi/2$, and negative for $\pi/2 < \alpha \leq \pi$. This implies that $\eta = 0$ when $\alpha = 0$ and $\pi/2$, is positive for $0 < \alpha < \pi/2$, and negative for $\pi/2 < \alpha \leq \pi$. This implies that $\tau(\alpha, \sin\alpha, \gamma^*)$ is maximized when $\alpha = \pi/2$.

We can now prove Lemma 2.8.3.

Proof of Lemma 2.8.3. Corollary 2.8.7 implies that $\tau(\alpha, \sin\alpha, \gamma^*)$ is maximized when $\alpha = \pi/2$. Thus

$$\tau(\alpha, \sin\alpha, \gamma^*) \leq \tau(\pi/2, 1, \gamma^*) = \sqrt{1-(1/\mu)^2}(1+\sin(1)) - \left(\mu - \frac{1}{\mu}\right)\cos(1) \leq 0 \quad (2.19)$$

for $\lambda = \left(\frac{1+\sin(1)}{\cos(1)} - \pi/2 - 1\right)/2 \approx 0.42$ and $\mu = \sqrt{\frac{2}{1-\sin(1)}} < 3.56$. □

2.8.3 *Proofs of Lemmas 2.3.8 and 2.3.9*

Recall that $\tau(\alpha, \beta, \gamma^*)$ is unimodal with respect to β (refer to Lemma 2.8.2). We now simplify it further.

Lemma 2.8.8. *For $0 \leq \beta \leq \sin\alpha$, $\tau(\alpha, \beta, \gamma^*) \leq \tau(\alpha, \sin\alpha, \gamma^*)$.*

Proof. Recall that

$$\frac{d\tau(\alpha, \beta, \gamma^*)}{d\beta} = A(\cos\beta - \cos\alpha) + B(\sin\beta). \quad (2.20)$$

Note that $\frac{d\tau(\alpha, \beta, \gamma^*)}{d\beta} > 0$ when β is positive. Thus we have that $\tau(\alpha, \beta, \gamma) \leq \tau(\alpha, \sin\alpha, \gamma^*)$.

□

In order to enumerate all the cases we need to consider to prove $\Phi(C_{i-1}, C_i) \leq 0$, we distinguish between *starting conditions* and *events*. Given circles C_{i-1} and C_i, starting conditions refer to the locations of C_{i-1}, C_i, and st before applying Transformation 2.3.10. By extension, this includes the value of $y(t_{i-1})$ and the angles α, β, and γ. Recall that as we apply Transformation 2.3.10, we update α, β, γ, as well as the lengths of the arcs of C_{i-1} and the position of t_i. Thus an event refers to an angle entering, exiting, or staying within some range, or any other condition that occurs during the transformation.

2.8.3.1 *Proof of Lemma 2.3.8*

Lemma 2.3.8 assumes that $y(t_{i-1}) \leq 0$. Proving Lemma 2.3.8 is equivalent to proving the following two lemmas.

Lemma 2.8.9. *Consider any starting condition where C_{i-1} and C_i are such that $y(t_{i-1}) \leq 0$ and $0 \leq \alpha \leq \pi/2$. Then $\Phi(C_{i-1}, C_i) \leq 0$.*

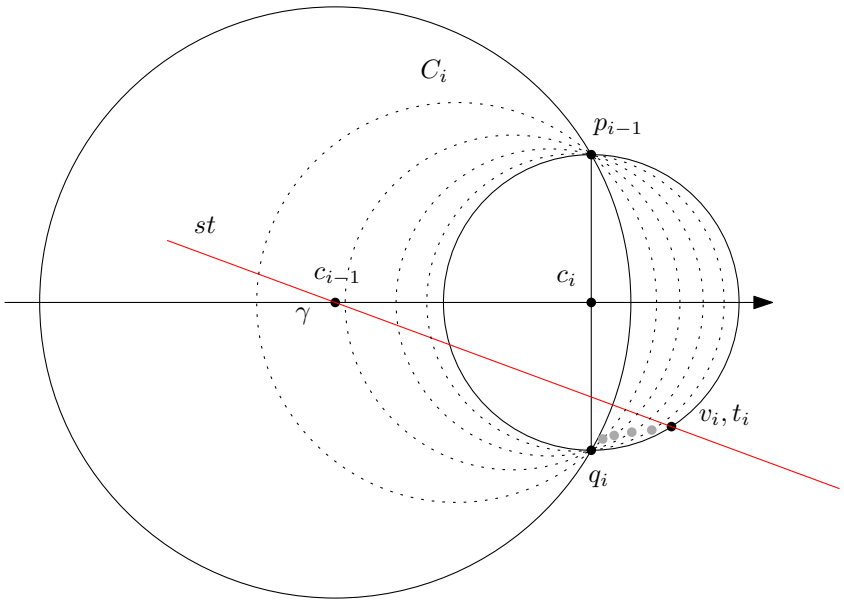

Figure 2.22: The gray dots represent the path of v_i.

Lemma 2.8.10. *Consider any starting condition where C_{i-1} and C_i are such that $y(t_{i-1}) \leq 0$ and $\pi/2 < \alpha \leq \pi$. Then $\Phi(C_{i-1}, C_i) \leq 0$.*

Observe that C_i and C_{i-1} being balanced implies the starting condition $y(t_i) < 0$, which implies that during Transformation 2.3.10, the event $\beta < 0$ does not occur. We need the following lemma to prove Lemma 2.8.9.

Lemma 2.8.11. *Consider any starting condition where C_{i-1} and C_i are such that $\alpha \leq \pi/2$ and $\beta \leq \sin\alpha$. Then, during Transformation 2.3.10, $\beta \leq \sin\alpha$.*

Proof. Let v_i be the point on C_i where $|\mathcal{A}_i(p_{i-1}, v_i)| = |p_{i-1}q_i| + |\mathcal{B}_i(q_i, v_i)|$. We show that v_i does not go above st during Transformation 2.3.10, which implies the lemma.

Since c_{i-1} is on or below st, the slope of st is negative. Let e_i be the rightmost (East-most) point of C_i. Let $\beta' = \angle(v_i c_i e_i)$. During Transformation 2.3.10, since $\beta' r_i = |\mathcal{A}_i(e_i, v_i)| = |p_{i-1}q_i|/2$ is constant, but r_i is increasing and β' is decreasing ($\mathcal{A}_i(e_i, v_i)$ is getting flatter), v_i moves downwards. Since v_i is below c_i, v_i moves left as c_i moves left. Thus the path of v_i (from left to right) maintains a positive slope. Since st has a negative slope, and v_i intersects st initially (that is, $v_i = t_i$), this implies that v_i cannot go above st during Transformation 2.3.10. See Fig. 2.22. □

We can now prove Lemma 2.8.9.

Proof of Lemma 2.8.9. The proof follows from Lemmas 2.8.11, 2.8.3 and 2.3.11. □

Note that, given the starting conditions of Lemma 2.8.10, if the event $\beta > \sin\alpha$ does not occur, then Lemmas 2.8.3 and 2.3.11 imply Lemma 2.8.10. In the following lemma, we identify a starting condition for which $\beta > \sin\alpha$ never occurs during Transformation 2.3.10.

Lemma 2.8.12. *Let w_i be the leftmost (West-most) point of C_i. Consider any starting condition where C_{i-1} and C_i are such that $\alpha > \pi/2$, $\beta \leq \sin\alpha$ and st is on or above w_i. Then during Transformation 2.3.10, $\beta \leq \sin\alpha$.*

Proof. Note that $\beta = \sin\alpha$ if and only if $\beta r_i = r_i \sin\alpha = |p_{i-1}q_i|/2$. Since $|p_{i-1}q_i|/2$ stays constant during Transformation 2.3.10, and $\beta r_i \leq r_i \sin\alpha = |p_{i-1}q_i|/2$ before Transformation 2.3.10, it is enough to show that βr_i is decreasing during Transformation 2.3.10 while $\alpha > \pi/2$. If $\alpha \leq \pi/2$ during the transformation, we apply Lemma 2.8.11. Let C_K be any intermediate circle through p_{i-1} and q_i during Transformation 2.3.10. Fixing t_i, if we increase γ, β on C_K will decrease. Thus the greatest value for β on C_K is when γ is minimized. Since we assume that w_i is on or below st, it is enough to show that βr_i is increasing during Transformation 2.3.10 when st is on w_i. Recall that

$$\frac{d\beta r_i}{dx(c_i)} = \frac{\cos\alpha \sin(\beta-\gamma) + \sin\gamma}{\cos(\beta-\gamma)} - \beta\cos\alpha. \tag{2.21}$$

Since $\alpha > \pi/2$ and $\beta > 0$, we have $-\beta\cos\alpha > 0$. Also recall that $-\pi/2 \leq \beta - \gamma \leq \pi/2$, thus $\cos(\beta-\gamma) > 0$. Therefore to show that $\frac{d\beta r_i}{dx(c_i)}$ is non-negative, it is sufficient to show that $\sin\gamma \geq \sin(\beta-\gamma)$, or $\gamma \geq \beta/2$ (since $\gamma \leq \pi/2$). This is true when w_i is on or below st, as required. □

This leads to the following Corollary.

Corollary 2.8.13. *Consider any starting condition where C_{i-1} and C_i are such that $\alpha > \pi/2$ and c_{i-1} is inside C_i. Then during Transformation 2.3.10, $\beta \leq \sin\alpha$.*

It remains to prove Lemma 2.8.10 when the event $\beta > \sin\alpha$ occurs. Since C_{i-1} and C_i are balanced, one of the starting conditions is $\beta = \sin\alpha$. Recall that c_{i-1} is assumed to be on or below st. Corollary 2.8.13 tells us we can assume c_{i-1} is outside of C_i. We look at two cases with the following starting conditions.

$\alpha > \pi/2, c_{i-1}$ is outside of C_i and $r_i \geq r_{i-1}$ (refer to Lemma 2.8.14).
$\alpha > \pi/2, c_{i-1}$ is outside of C_i and $r_i < r_{i-1}$ (refer to Lemma 2.8.15).

Lemma 2.8.14. *Consider any starting condition where C_{i-1} and C_i are such that $\alpha > \pi/2$, c_{i-1} is outside of C_i, and $r_i \geq r_{i-1}$. Then $\Phi(C_{i-1}, C_i) \leq 0$.*

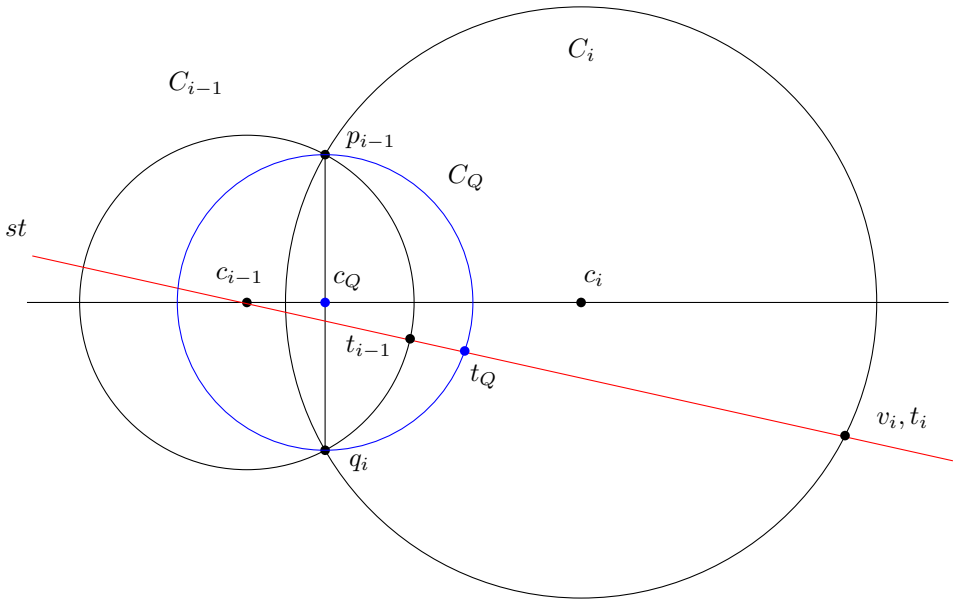

Figure 2.23: Lemma 2.8.14

Proof. See Fig. 2.23. Let C_Q be a circle through p_{i-1} and q_i with radius $r_Q = |p_{i-1}q_i|/2$. First we show that s_Q is between s_{i-1} and s_i on st. Let u_i be the intersection of C_i and the line through t_i and c_i, where $u_i \neq t_i$. Lemma 2.3.7 tells us that s_Q is between s_{i-1} and s_i on st, if u_k and u_i are left of $p_{i-1}q_i$, which is true if $|y(t_Q)| \leq y(p_{i-1})$ and $|y(t_i)| \leq y(p_{i-1})$. Since c_{i-1} is on or below st, the slope of st is negative, and since $y(t_{i-1}) \leq 0$, we have $|y(t_Q)| < |y(t_i)|$. We have $y(p_{i-1}) = r_i \sin\alpha$, and $|y(t_i)| = r_i \sin(\sin\alpha) \leq r_i \sin\alpha = y(p_{i-1})$ when $\alpha \leq \pi/2$, and thus s_Q is between s_{i-1} and s_i on st.

Thus we have $\Phi(C_{i-1}, C_i) = \Phi(C_{i-1}, C_Q) + \Phi(C_Q, C_i)$, and it is sufficient to prove that $\Phi(C_{i-1}, C_Q) \leq 0$ and $\Phi(C_Q, C_i) \leq 0$.

If st is below c_Q, then $\Phi(C_Q, C_i)$ is increased when st goes through c_Q, so we assume that c_Q is on or below st. We apply Transformation 2.3.10 to C_i and C_Q. Since $y(t_{i-1}) \leq 0$, and $y(t_i) \leq 0$, we have $y(t_Q) \leq 0$, and thus $\beta \geq 0$ during Transformation 2.3.10. Since c_Q is inside C_i, Corollary 2.8.13 tells us that $\beta \leq \sin\alpha$ during Transformation 2.3.10. Together with the fact that $\tau(\alpha, \beta, \gamma) \leq 0$ when $0 \leq \beta \leq \sin\alpha$, this implies that $\Phi(C_Q, C_i) \leq 0$ by Lemma 2.3.11.

We now apply Transformation 2.3.10 to C_{i-1} and C_Q. Since $\alpha = \pi/2$ before Transformation 2.3.10, Lemma 2.8.11 tells us that $\beta \leq \sin\alpha$ during Transformation 2.3.10 if $\beta \leq \sin\alpha$ initially. Proving that initially we have $\beta \leq \sin\alpha$ is equivalent to proving that t_Q is above v_Q, or equivalently, that v_Q is below st.

Let C_K be a circle through p_{i-1} and q_i such that t_K is between t_{i-1} and t_i. Notice that C_K is any intermediate circle encountered during Transformation 2.3.10. If we fix t_i, then

β is maximized on C_K when γ is minimized. Since we assume c_{i-1} is on or below st, we conclude γ is minimized when st intersects c_{i-1}. To minimize γ further we move c_{i-1} as far left as it can go, i.e., to the point where $r_i = r_{i-1}$. Thus it is sufficient to show v_Q is below st when $r_i = r_{i-1}$.

Let p'_{i-1} and q'_i be the points on C_i that mirror p_{i-1} and q_i in the vertical line through c_i. Note that the line segment $c_{i-1}q'_i$ is below the line segment $c_{i-1}t_i$, which is part of st. Thus, showing that v_Q is below $c_{i-1}q'_i$ shows that v_Q is below st.

We begin by showing that if v_Q is below $c_{i-1}q'_i$ when $r_i = r_{i-1}$ and c_{i-1} intersects C_i, then v_Q is below $c_{i-1}q'_i$ for any c_{i-1} outside of C_i where $r_i = r_{i-1}$.

See Fig. 2.24. Note that $x(q_i) - x(c_{i-1}) = x(c_i) - x(q_i) = x(q'_i) - x(c_i)$, thus $2(x(q_i) - x(c_{i-1})) = x(q'_i) - x(q_i)$. Thus one third of $c_{i-1}q'_i$ is to the left of $p_{i-1}q_i$, while two thirds of $c_{i-1}q'_i$ is to the right. Since $y(c_{i-1})$ and $y(q'_i)$ are constant, this implies that as $c_{i-1}q'_i$ grows it pivots at the intersection of itself and $p_{i-1}q_i$. Thus v_Q being under $c_{i-1}q'_i$ when c_{i-1} and C_i intersect implies that it is always under $c_{i-1}q'_i$. Thus it is enough to show that v_Q is under $c_{i-1}q'_i$ when c_{i-1} intersects C_i.

See Figs. 2.25 and 2.26. Assume that $r_i = r_{i-1} = 1$, which implies that $r_Q = \sin(\pi/3)$, and $|c_{i-1}c_Q| = 1/2$. Note that when Transformation 2.3.10 gets to ${}^2C_Q$, we have $\alpha = \pi/2$, thus we need to prove that $\beta \leq \sin\alpha = 1$. Let t'_Q be the intersection of $c_{i-1}q'_i$ and C_Q. Since $c_{i-1}q'_i$ lies under st, and $\angle(t'_Q c_Q c_i) > \beta$, it is sufficient to show that $\angle(t'_Q c_Q c_i) < 1$.

Let $\theta = \angle(c_Q t'_Q c_{i-1})$, and note that $\angle(q'_i c_{i-1} c_Q) = \pi/6$. We can find θ using the sine rule. Thus $\sin\theta = \dfrac{\sin(\pi/6)}{2\sin(\pi/3)}$, and $\theta < 0.3$. We see that $\angle(t'_Q c_Q c_i) = \theta + \pi/6 < 0.82 < 1$, as required.

□

Lemma 2.8.15. *If $r_i < r_{i-1}$, $\alpha > \pi/2$ and c_{i-1} is outside of C_i, then $\Phi(C_{i-1}, C_i) \leq 0$.*

Proof. Let C_P be the circle with radius r_i through p_{i-1} and q_i such that $C_P \neq C_i$. Notice that C_P is one of the intermediate circles encountered during Transformation 2.3.10. See Fig. 2.27. We have $\Phi(C_{i-1}, C_i) = \Phi(C_{i-1}, C_P) + \Phi(C_P, C_i)$, and thus it is sufficient to prove that $\Phi(C_{i-1}, C_P) \leq 0$ and $\Phi(C_P, C_i) \leq 0$. We do this by applying Transformation 2.3.10 to C_i and C_P, and then to C_P and C_{i-1}.

Since $r_P = r_i$, we have $\Phi(C_P, C_i) \leq 0$ by Lemma 2.8.14. Since we assumed that c_{i-1} is on or below st, we know that st has a negative slope. Thus $y(t_P) > y(t_i)$, which implies that ${}^2\beta$ as defined by C_P is less than β as defined by C_i. Thus when applying Transformation 2.3.10 to C_P and C_{i-1}, we know that $0 \leq \beta < \sin\alpha$ by Lemma 2.8.11, and thus $\Phi(C_{i-1}, C_P) \leq 0$ by Lemma 2.3.11. □

Proof of Lemma 2.8.10. The proof follows from Lemmas 2.8.14 and 2.8.15. □

[2] Recall that, as we apply Transformation 2.3.10, we update the values of α, β, and γ.

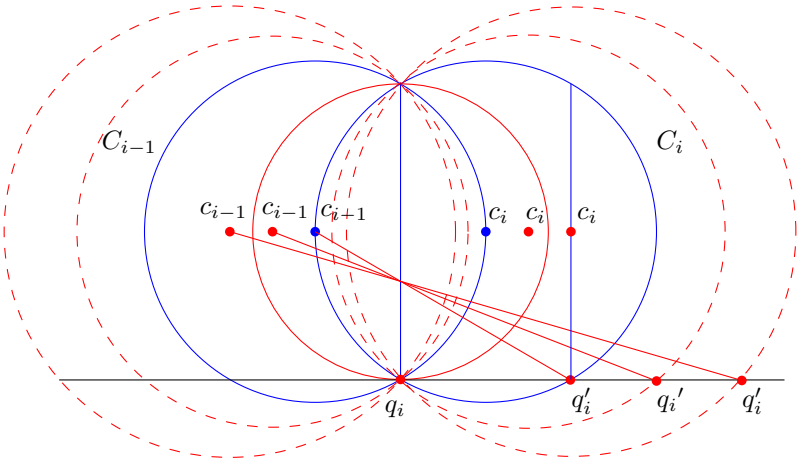

Figure 2.24: Line segment $c_{i-1}q_i'$ as we increase r_i and r_{i-1}.

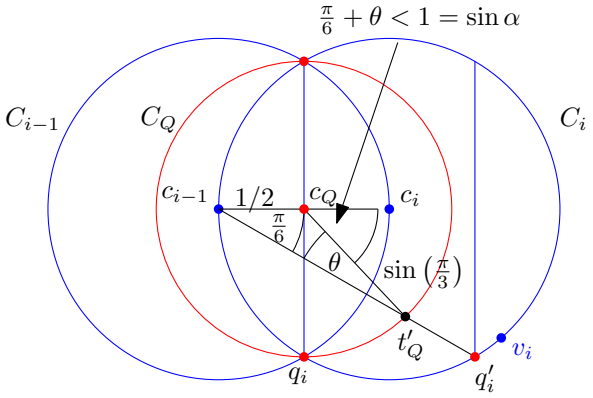

Figure 2.25: Computing an upper bound on β on C_Q.

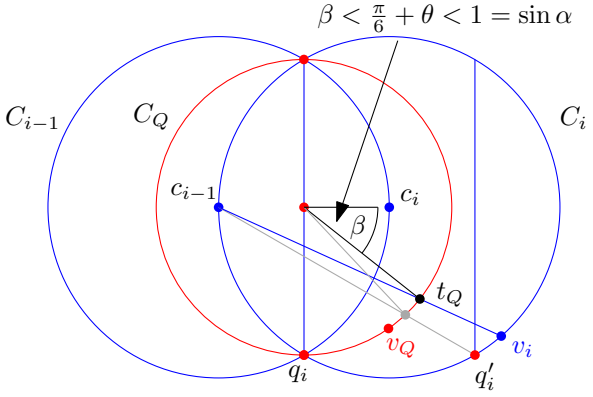

Figure 2.26: Since $\beta < 1 = \sin\alpha$ on circle C_Q, v_Q is below st.

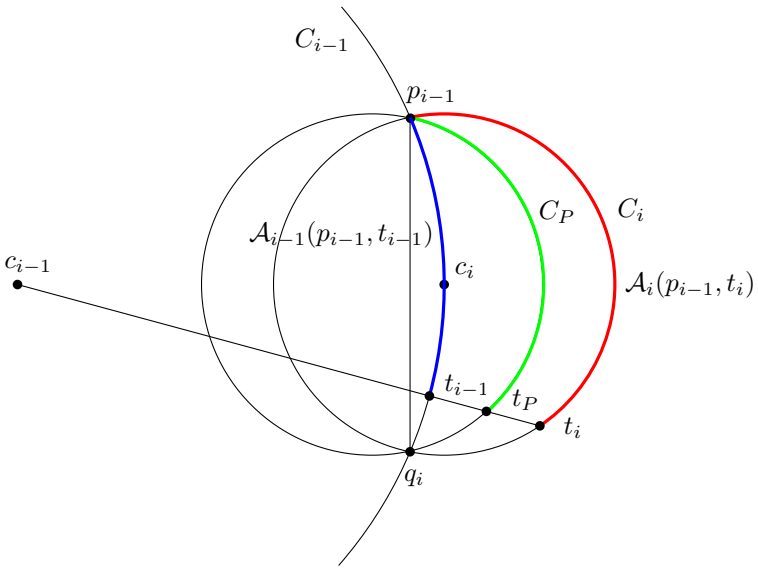

Figure 2.27: The case where $\alpha > \pi/2$ and $r_{i-1} > r_i$.

2.8.3.2 *Proof of Lemma 2.3.9*

First observe the following.

Lemma 2.8.16. *For $0 \leq \alpha \leq \pi/2$, $\tau(\alpha, -\alpha, \gamma^*) \leq 0$.*

Proof.

$$\begin{aligned}\tau(\alpha, -\alpha, \gamma^*) &= A(\sin\alpha + \sin(-\alpha) - (\alpha - \alpha + 2\lambda)\cos\alpha) - B(\cos(-\alpha) - \cos\alpha) \\ &= -2\lambda\cos\alpha \\ &\leq 0.\end{aligned}$$

□

We now break Lemma 2.3.9 into the two lemmas.

Lemma 2.8.17. *Consider any starting condition where C_{i-1} and C_i are such that $y(t_{i-1}) > 0$ and $0 \leq \alpha \leq \pi/2$. Then $\Phi(C_{i-1}, C_i) \leq 0$.*

Proof. We know $\tau(\alpha, \beta, \gamma^*)$ is unimodal with respect to β by Lemma 2.8.2. The starting condition $0 \leq \alpha \leq \pi/2$ together with Lemma 2.8.11 imply that $-\alpha \leq \beta \leq \sin\alpha$. Thus the proof follows from Lemmas 2.8.16, 2.8.3, and 2.3.11. □

We are thus left to prove the following lemma in order to prove Lemma 2.8.10. Note that in this case, instead of working on $\tau(\alpha, \beta, \gamma^*)$, we use a geometric proof.

Lemma 2.8.18. *Consider any starting condition where C_{i-1} and C_i are such that $y(t_{i-1}) > 0$ and $\pi/2 < \alpha \leq \pi$. Then $\Phi(C_{i-1}, C_i) \leq 0$.*

Proof. If c_{i-1} is left of $p_{i-1}q_i$, then let C_Q be a circle through p_{i-1} and q_i with diameter $|p_{i-1}b_i|$. Otherwise let $C_Q = C_{i-1}$. We will show that $\Phi(C_{i-1}, C_i) \leq \Phi(C_{i-1}, C_Q) + \Phi(C_Q, C_i) \leq 0$.

Note that since t_{i-1} is inside C_i, and $y(t_{i-1}) > 0$, Lemma 2.8.12 implies that β as defined by C_Q[3] is less than $\sin\alpha$, where α as defined by C_Q is $\pi/2$. Lemma 2.8.12 implies the event $\beta \leq \sin\alpha$. This implies that $\Phi(C_{i-1}, C_Q) \leq 0$ by Lemmas 2.8.3, 2.8.16 and 2.3.11. Thus we need only show that $\Phi(C_Q, C_i) \leq 0$. Note that if $y(t_Q) \leq 0$, then $\Phi(C_Q, C_i) \leq 0$ by Lemma 2.3.8. Thus we assume that $y(t_Q) > 0$.

To show $\Phi(C_Q, C_i) \leq 0$ in this case we will show three inequalities.

$$|\mathcal{A}_i(p_{i-1}, t_i)| \leq \pi/2|p_{i-1}t_i|, \tag{2.22}$$

$$|\mathcal{A}_Q(p_{i-1}, t_Q)| + \mu|t_Qt_i| \geq \frac{\mu\sin(1)+1}{\sin(1)+1}|p_{i-1}t_i|, \tag{2.23}$$

$$2(r_i - r_Q) \leq |p_{i-1}t_i|. \tag{2.24}$$

See Fig. 2.28. Assuming (2.22), (2.23), and (2.24) are true, we substitute these values into $\Phi(C_Q, C_i)$ and get

$$\begin{aligned}
\Phi(C_Q, C_i) =& |\mathcal{A}_i(p_{i-1}, t_i)| - |\mathcal{A}_Q(p_{i-1}, t_Q)| - 2\lambda(r_Q - r_i) - \mu|t_Qt_i| \\
&\leq \left(\pi/2 + 1 + \lambda - \frac{(\mu-1)\sin(1)}{\sin(1)+1}\right)|p_{i-1}t_i| \\
&\leq \left(\pi/2 + \lambda - \frac{\mu\sin(1)+1}{\sin(1)+1}\right)|p_{i-1}t_i| \\
&\leq (2 - 2.16)|p_{i-1}t_i| \\
&\leq 0.
\end{aligned}$$

Inequality (2.22) is satisfied whenever $|\mathcal{A}_i(p_{i-1}, t_i)| = |p_{i-1}q_i| + |\mathcal{B}_i(q_i, t_i)|$, which is always the case initially when C_{i-1} and C_i are balanced.

For inequality (2.23), note that $|\mathcal{A}_Q(p_{i-1}, t_Q)| \geq |p_{i-1}t_Q|$, and $|p_{i-1}t_Q| + |t_Qt_i| \geq |p_{i-1}t_i|$ by the triangle inequality. Thus it remains to show that $|t_Qt_i| \geq |p_{i-1}t_i|\frac{sin(1)}{sin(1)+1}$.

Recall that $y(t_Q) > 0$. If we increase $y(t_Q)$, observe that $|t_Qt_i|$ also increases. Notice that the minimum value of $|t_Qt_i|$ is when t_Q corresponds to the intersection of st and the x-axis. Thus for the minimum value of $|t_Qt_i|$, we will assume that $y(t_Q) = 0$.

[3] Recall that, as we apply Transformation 2.3.10, we update the values of α, β, and γ.

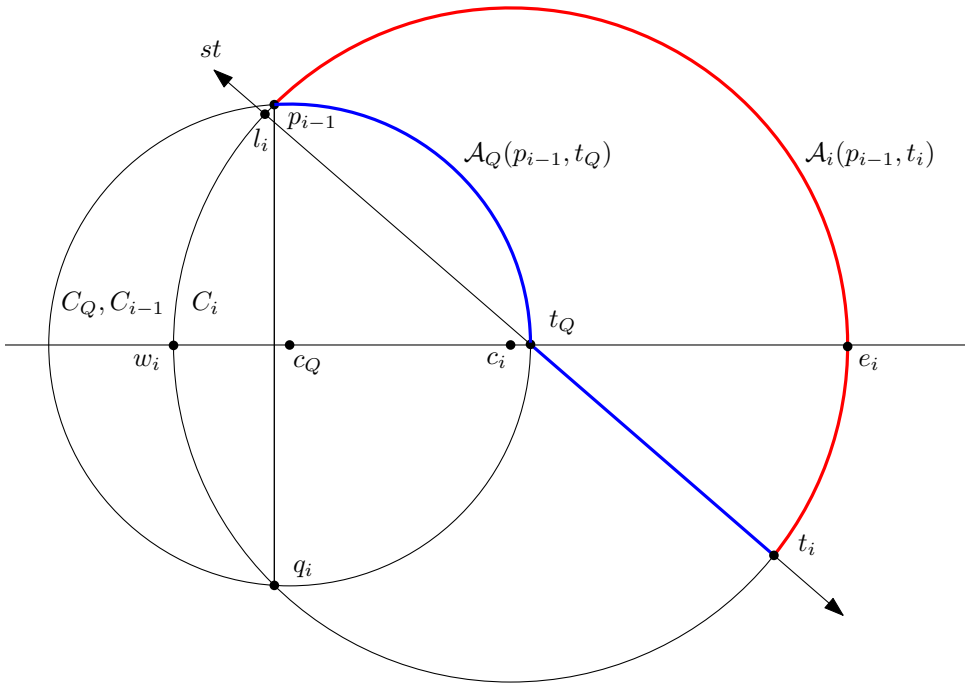

Figure 2.28: $\Phi(C_Q, C_i) \leq 0$ when $y(t_Q) > 0$.

Recall that l_i is the leftmost intersection of C_i and st, and e_i is the rightmost point of C_i. If $|y(t_i)| \geq |y(l_i)|$, then $y(t_Q) = 0$ implies that $|t_Q t_i| \geq r_i \geq |p_{i-1}t_i|/2 \geq |p_{i-1}t_i|\frac{sin(1)}{sin(1)+1}$ as required. So assume that $|y(t_i)| < |y(l_i)|$, which implies that c_i is below st, and thus below $l_i t_i$, which is a segment of st. Observe that since p_{i-1} is a vertex, it is above st. Since c_i is below $l_i t_i$, but $p_{i-1}t_i$ is above $l_i t_i$, this implies that $|l_i t_i| \geq |p_{i-1}t_i|$. This means that it is sufficient to prove $|t_Q t_i| \geq |l_i t_i|\frac{sin(1)}{sin(1)+1}$. Note that $|t_Q t_i|$ is the part of $|l_i t_i|$ below the x-axis. Thus $|t_Q t_i|/|l_i t_i| = |y(t_i)|/(|y(l_i)| + |y(t_i)|)$. This expression is minimized when $|y(t_i)|/|y(l_i)|$ is smallest. Also $|y(l_i)|$ is largest when $l_i = p_{i-1}$. Note that $|y(p_{i-1})| = r_i \sin\alpha$, and that $|y(t_i)| = r_i \sin(\sin\alpha)$. Thus $|y(t_i)|/|y(l_i)| = \sin(\sin\alpha)/\sin\alpha$, which is minimized when $\alpha = \pi/2$. This implies that $|y(t_i)|/(|y(l_i)| + |y(t_i)|) = |t_Q t_i|/|l_i t_i| \geq \sin(1)/(\sin(\pi/2) + \sin(1)) = \sin(1)/(\sin(1) + 1)$. Thus $|t_Q t_i| \geq |l_i t_i|\frac{\sin(1)}{\sin(1)+1} \geq |p_{i-1}t_i|\frac{\sin(1)}{\sin(1)+1}$ as required.

Let us now prove (2.24). Observe that c_i is right of $|p_{i-1}q_i|$, which is right of $|p_{i-1}w_i|$. Together with the fact that $|p_{i-1}q_i|$ and $|p_{i-1}w_i|$ are both chords of C_i, then $|p_{i-1}w_i| < |p_{i-1}q_i|$. Moreover, c_i is below $p_{i-1}t_i$, which is below $p_{i-1}e_i$. Together with the fact that

$|p_{i-1}t_i|$ and $|p_{i-1}e_i|$ are both chords of C_i, then $|p_{i-1}e_i| \leq |p_{i-1}t_i|$. Finally, since p_{i-1} and q_i both lie on C_Q, then $|p_{i-1}q_i| \leq 2r_Q$. Thus we have

$$\begin{aligned} 2r_i &= |w_i e_i| \\ &\leq |p_{i-1}e_i| + |p_{i-1}w_i| && \text{by the triangle inequality,} \\ &\leq |p_{i-1}e_i| + |p_{i-1}q_i| \\ &\leq |p_{i-1}t_i| + 2r_Q, \end{aligned}$$

from which we have $2(r_i - r_Q) \leq |p_{i-1}t_i|$, as required.

□

BIBLIOGRAPHY

[1] Nicolas Bonichon, Prosenjit Bose, Jean-Lou De Carufel, Ljubomir Perković, and André van Renssen. Upper and lower bounds for online routing on Delaunay triangulations. In Nikhil Bansal and Irene Finocchi, editors, *Algorithms - ESA 2015*, volume 9294 of *Lecture Notes in Computer Science*, pages 203–214. Springer Berlin Heidelberg, 2015.

[2] Nicolas Bonichon, Prosenjit Bose, Jean-Lou De Carufel, Ljubomir Perković, and André van Renssen. Upper and lower bounds for online routing on Delaunay triangulations. *Discrete & Computational Geometry*, 58(2):482–504, Sep 2017.

[3] Nicolas Bonichon, Cyril Gavoille, Nicolas Hanusse, and Ljubomir Perković. Tight stretch factors for L_1 and L_∞ Delaunay triangulations. *Computational Geometry*, 48(3):237 – 250, 2015.

[4] Prosenjit Bose, Jean-Lou De Carufel, Stephane Durocher, and Perouz Taslakian. Competitive online routing on Delaunay triangulations. In R. Ravi and Inge Li Gørtz, editors, *Algorithm Theory - SWAT 2014 - 14th Scandinavian Symposium and Workshops, Copenhagen, Denmark, July 2-4, 2014. Proceedings*, volume 8503 of *Lecture Notes in Computer Science*, pages 98–109. Springer, 2014.

[5] Prosenjit Bose, Rolf Fagerberg, André van Renssen, and Sander Verdonschot. Competitive routing in the half-theta-6-graph. In *Proceedings of the Twenty-third Annual ACM-SIAM Symposium on Discrete Algorithms*, SODA '12, pages 1319–1328. SIAM, 2012.

[6] Prosenjit Bose and Pat Morin. Online routing in triangulations. In *Algorithms and Computation*, volume 1741 of *Lecture Notes in Computer Science*, pages 113–122. Springer Berlin Heidelberg, 1999.

[7] Timothy M. Chan, editor. *Proceedings of the Thirtieth Annual ACM-SIAM Symposium on Discrete Algorithms, SODA 2019, San Diego, California, USA, January 6-9, 2019*. SIAM, 2019.

[8] L. Paul Chew. There is a planar graph almost as good as the complete graph. In *Proceedings of the Second Annual Symposium on Computational Geometry*, SCG '86, pages 169–177, New York, NY, USA, 1986. ACM.

[9] L. Paul Chew. There are planar graphs almost as good as the complete graph. *Journal of Computer and System Sciences*, 39(2):205 – 219, 1989.

[10] Michael Dennis, Ljubomir Perković, and Duru Türkoglu. The stretch factor of hexagon-Delaunay triangulations. *CoRR*, abs/1711.00068, 2017.

[11] David P. Dobkin, Steven J. Friedman, and Kenneth J. Supowit. Delaunay graphs are almost as good as complete graphs. *Discrete & Computational Geometry*, 5(1):399–407, 1990.

[12] J. Mark Keil and Carl A. Gutwin. Classes of graphs which approximate the complete euclidean graph. *Discrete & Computational Geometry*, 7(1):13–28, 1992.

[13] Giri Narasimhan and Michiel Smid. *Geometric Spanner Networks*. Cambridge University Press, New York, NY, USA, 2007.

[14] Ge Xia. Improved upper bound on the stretch factor of Delaunay triangulations. In *Proceedings of the Twenty-seventh Annual Symposium on Computational Geometry*, SoCG '11, pages 264–273, New York, NY, USA, 2011. ACM.

[15] Ge Xia and Liang Zhang. Toward the tight bound of the stretch factor of Delaunay triangulations. In *Proceedings of the Canadian Conference on Computational Geometry*, CCCG '11, 2011.

3

ON THE SPANNING AND ROUTING RATIO OF THETA-FOUR

ABSTRACT

We present a routing algorithm for the Θ_4-graph that computes a path between any two vertices s and t having length at most 17 times the Euclidean distance between s and t. To compute this path, at each step, the algorithm only uses knowledge of the location of the current vertex, its (at most four) outgoing edges, the destination vertex, and one additional bit of information in order to determine the next edge to follow. This provides the first known online, local, competitive routing algorithm with constant routing ratio for the Θ_4-graph, as well as improving the best known upper bound on the spanning ratio of these graphs from 237 to 17. We also show that without this additional bit of information, the routing ratio increases to $\sqrt{290} \approx 17.03$.

This chapter appeared in the proceedings of the Symposium of Discrete Algorithms (SODA19) [6] and was presented there.

3.1 INTRODUCTION

Finding a path in a graph is a fundamental problem in computer science. Typically, algorithms that compute paths in graphs have at their disposal knowledge of the whole graph. The problem of finding a path in a graph is more difficult in the online setting, when the routing algorithm must explore the graph as it attempts to find a path. Moreover, the situation is even more challenging if the routing algorithm only has a constant amount of working memory, i.e. it can only remember a constant size subgraph of the portion of the graph it has explored. Specifically, an online routing algorithm attempting to find a path from one vertex to another is called *local* if at each step, the only information it can use to make its forwarding decision is the location of the current vertex and its neighbouring vertices, plus a constant amount of additional information.

For a routing algorithm A and a given graph G from a class $\mathcal{G}$ of graphs, let $\mathcal{P}_G^A(s,t)$ be the path found by A from s to t. The class of graphs we focus on are a subclass of weighted geometric graphs. A weighted geometric graph $G = (P, E)$ consists of a set P of points in the plane and a set E of (directed or undirected) edges between pairs of points, where the weight of an edge (p, q) is equal to the Euclidean distance $L_2(p, q)$

between its endpoints (i.e., distance in the L_2-metric). For a pair of vertices s and t in P, let $\mathcal{P}_G(s,t)$ be the shortest path from s to t in G, and let $L_2(\mathcal{P}_G(s,t))$ be the length of $\mathcal{P}_G(s,t)$ with respect to the L_2-metric. The spanning ratio of a graph G is the minimum value c such that $L_2(\mathcal{P}_G(s,t)) \leq c \cdot L_2(s,t)$ over all pairs of points s and t in G. A graph is called a *c-spanner*, or just a *spanner*, if its spanning ratio is at most some constant c. The routing ratio of a local online routing algorithm A on $\mathcal{G}$ is the maximum value c' such that $L_2(\mathcal{P}_G^A(s,t)) \leq c' \cdot L_2(s,t)$ for all $G \in \mathcal{G}$ and all pairs s and t in G. When c' is a constant, such an algorithm is called *competitive* on the class $\mathcal{G}$. Note that the routing ratio on a class of graphs $\mathcal{G}$ is an upper bound on the spanning ratio of $\mathcal{G}$, since the routing ratio proves the existence of a bounded-length path.

3.1.1 Θ-*graphs*

Let $k \geq 3$ be an integer and for each i with $0 \leq i < k$, let $\mathcal{R}_i$ be the ray emanating from the origin that makes an angle of $2\pi i/k$ with the negative y-axis. Let $\mathcal{R}_k = \mathcal{R}_0$. The Θ_k-graph of a given set P of points is the directed graph that is obtained in the following way. The vertex set is the set P. Each vertex v has at most k outgoing edges: For each i with $0 \leq i < k$, let $\mathcal{R}_i^v$ be the ray emanating from v parallel to $\mathcal{R}_i$. Let C_i^v be the cone consisting of all points in the plane that are strictly between the rays $\mathcal{R}_i^v$ and $\mathcal{R}_{i+1}^v$ or on $\mathcal{R}_{i+1}^v$. If C_i^v contains at least one point of $P \setminus \{v\}$, then let w_i be such a point whose perpendicular projection onto the bisector of C_i^v is closest to v (where closest refers to the Euclidean distance). Then the Θ_k-graph contains the directed edge (v, w_i). See Figure 3.1 for an example with $k = 4$.

Θ_k-graphs were introduced simultaneously by Keil and Gutwin[18, 19], and Clarkson[17]. Both papers gave a spanning ratio of $1/(\cos\theta - \sin\theta)$, where $\theta = 2\pi/k$ is the angle defined by the cones. Observe this gives a constant spanning ratio for $k \geq 9$. Ruppert and Seidel[23] improved this to $1/(1 - 2\sin(\theta/2))$, which applies to Θ_k-graphs with $k \geq 7$. Bose et al. [7] give a tight bound of 2 for $k = 6$. In the same paper are the current best bounds on the spanning ratio of a large range of values of k. For $k = 5$, Bose et al. [12] showed a spanning ratio of ≈ 9.96, and a lower bound of ≈ 3.78. For $k = 4$, Barba et al. [1] showed a spanning ratio of ≈ 237, with a lower bound of 7. For $k = 3$, [21] showed that there is no constant c for which Θ_3 is a c-spanner.

3.1.2 *Local Routing*

Local Routing has been studied extensively in variants of the Delaunay graph as well as Θ_k-graphs (see [11, 5, 20, 15, 16, 9, 22, 14, 13]). There is an intimate connection between Θ_k-graphs and variants of the Delaunay triangulation. For example, the existence of an

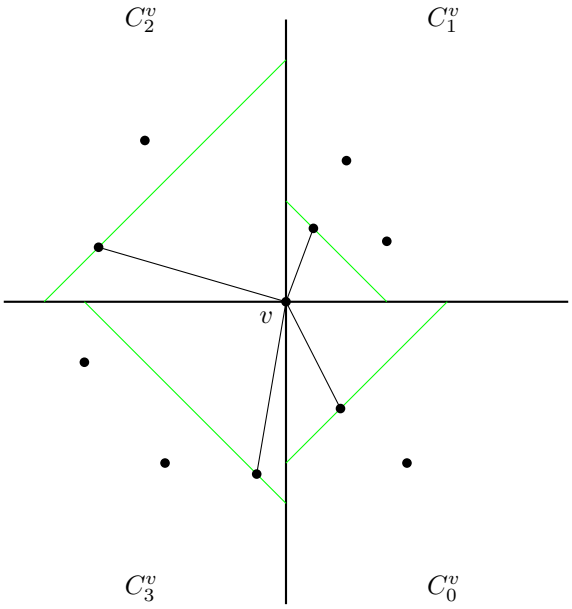

Figure 3.1: Neighbours of v in the Θ_4-graph.

edge in a Θ_k-graph implies the existence of an empty triangle containing the edge (refer to Fig. 3.1). In a Delaunay triangulation, the existence of an edge implies the existence of an empty disk containing the edge (or some empty convex shape when considering variants of the Delaunay graph). Moreover, the Delaunay graph where the empty convex shape is an equilateral triangle (this is often referred to as the TD-Delaunay graph [4]) is a subgraph of the Θ_6-graph.

Chew [15] proved that the L_1-Delaunay graph has bounded spanning ratio by providing a local routing algorithm whose routing ratio is at most $\sqrt{10}$. Bose and Morin[10] provide a competitive local routing algorithm that works on triangulations that have the *diamond property*. This includes such graphs as the L_2-Delaunay triangulation, the greedy triangulation, and the minimum weight triangulation. Bose and Morin[11] show that there are no routing algorithms that will work on any arbitrary graph. This implies that we must pair routing algorithms with particular classes of geometric graphs in order to route competitively. They also provide the first deterministic competitive routing algorithm on the L_2-Delaunay graphs. Bonichon et al. [3] showed that we could route competitively on the L_2-Delaunay triangulation with a routing ratio of around 5.9, using a generalization of Chew's [15] algorithm. This was the best known routing ratio for L_2-Delaunay triangulations until Bonichon et al. [2] gave a new algorithm with a routing ratio of 3.56, which is currently the best known. Bose et al. [8] show that the half-θ_6 graph, which is identical to the TD-Delaunay graph, has a routing ratio of $5/\sqrt{3}$, and this is shown to be tight. Since the spanning ratio of this graph is 2, local routing

cannot guarantee finding the shortest path, and we see a separation between routing and spanning ratios in this graph.

For Θ_k-graphs, there is a simple routing algorithm called *cone-routing* that is competitive for $k \geq 7$. To route from a vertex s to a vertex t, let C_i^s be the cone of s that contains t. We forward the packet from s to its neighbour in C_i^s. Let $\theta = 2\pi/k$, then for $k \geq 7$ cone routing gives a routing ratio of $1/(1 - 2\sin(\theta/2))$. Cone routing also has the advantage of only utilizing outgoing edges, so each vertex needs only to store the location of at most k neighbours. For $k < 7$, cone-routing does not necessarily give a short path, however, for $k = 6$, Bose et al. [8] show that a different local online routing algorithm gives a routing ratio of 2. There are currently no known competitive routing algorithms for $k = 5$ and $k = 4$.

3.1.3 *Our Results*

In this paper we improve the upper bound of the spanning ratio of Θ_4 from 237 to 17. We do this by providing a local online routing algorithm with a routing ratio of at most 17. This is the first local routing algorithm on Θ_k-graphs for $k = 4$, bringing us one step closer to obtaining competitive routing strategies on all Θ_k-graphs with $k > 3$. At the time of the writing of this paper, $k = 5$ is all that remains. This algorithm is a modified version of cone routing, where, instead of always taking the edge in the cone that contains the destination, we sometimes take a step in an orthogonal cone. The algorithm is simple, and only uses knowledge of the destination vertex, the current vertex v, the neighbours of v, and one bit of additional information. If we forgo that bit of information, then the routing ratio increases to $\sqrt{290} \approx 17.03$. Additionally, like cone-routing, we route using only outgoing edges, so each vertex only needs to store the location of its at most 4 outgoing neighbours. For the remainder of the paper, all edges (u, v) are considered directed outgoing edges from u to v, and when we refer to the neighbour v of a vertex u in a cone C_i^u, we are referring to the outgoing edge (u, v) of u.

The rest of the paper is organized as follows. Section 3.2 gives the details of the routing algorithm that is used to navigate the Θ_4-graph. In Section 3.3 we analyze the length of the path found by the algorithm, and show an upper bound of 17 on the routing ratio. In Section 3.4 we give an example of a path that shows this approach cannot do any better than a routing ratio of 17. In Section 3.5 we show how routing with only knowledge of the destination vertex increases the routing ratio to $\sqrt{290} \approx 17.03$. Section 3.6 concludes the paper and gives some directions for future work.

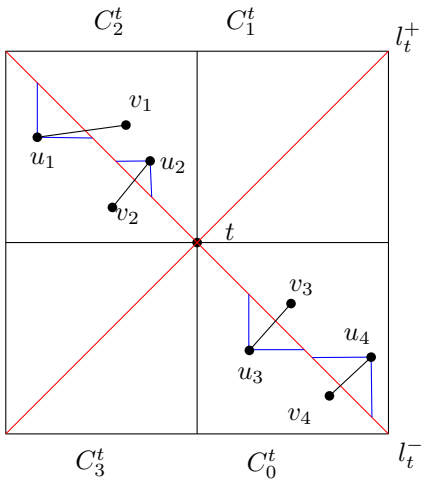

Figure 3.2: Vertices u_1, u_2, u_3, and u_4 are all clean with respect to ℓ_t^-.

3.2 ALGORITHM

In this section, we present our 17-competitive local online routing algorithm on Θ_4-graphs. Before doing so, we introduce some concepts. Let t be an arbitrary point in the plane, and let ℓ_t^- be the line through t with slope -1. Similarly let ℓ_t^+ be the line through t with slope 1. We refer to these as the *diagonals* of t. Examples can be seen in Figs. 3.2, 3.3, and 3.4. To ease our analysis and avoid tedious tie-breaking, we make a general position assumption that no two vertices have the same x- or y-coordinates, and no two vertices lie on a common diagonal. Let t and u be arbitrary vertices and consider a diagonal of t. Without loss of generality, we consider the diagonal ℓ_t^-. Let $\mathcal{R}_i^u$ and $\mathcal{R}_{i+1}^u$ be the rays emanating from u that intersect ℓ_t^-. Recall that $\mathcal{R}_i^u$ and $\mathcal{R}_{i+1}^u$ delineate the cone C_i^u. Let the triangle $T(u, \ell_t^-)$ be the intersection of the halfplane of ℓ_t^- containing u and the cone C_1^u. If $T(u, \ell_t^-)$ is empty of vertices, then we say that u is *clean with respect to* ℓ_t^-. See Fig. 3.2. If the diagonal is clear from the context, we say that u is *clean*. If u is not clean with respect to ℓ_t^-, then let v be the vertex in $T(u, \ell_t^-)$ for which (u, v) is an edge in the Θ_4-graph. We will refer to following the edge from u to v as *taking a sweeping step towards* ℓ_t^-. (See Fig. 3.3.) Let i be the index such that the vertex t is in the cone C_i^u. Let v be the vertex in C_i^u for which (u, v) is an edge in the Θ_4-graph. We will refer to following the edge from u to v as *taking a greedy step towards* t. (See Fig. 3.4.)

We now define the algorithm. Let s be the source vertex and t the target vertex. We assume that t lies at the point $(0, 0)$. We choose a diagonal as follows: if $s \in C_0^t \cup C_2^t$, we choose ℓ_t^-, otherwise we choose ℓ_t^+. Intuitively we choose the diagonal "closer" to s. Without loss of generality, assume that s is in C_2^t under ℓ_t^-, thus we choose ℓ_t^-. Let v be

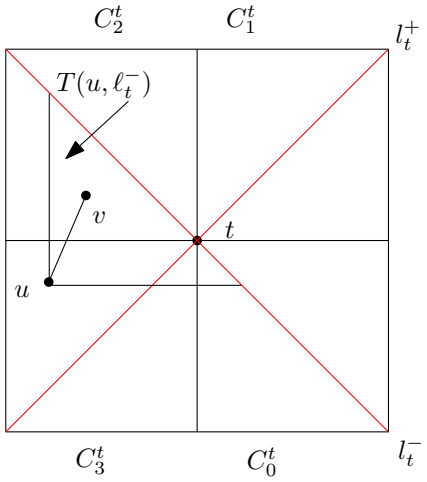

Figure 3.3: A sweeping step towards ℓ_t^-.

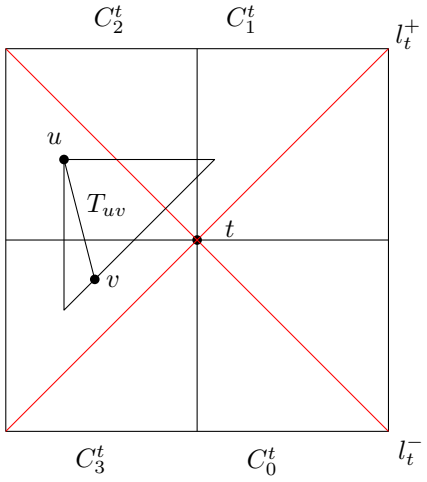

Figure 3.4: A greedy step towards t.

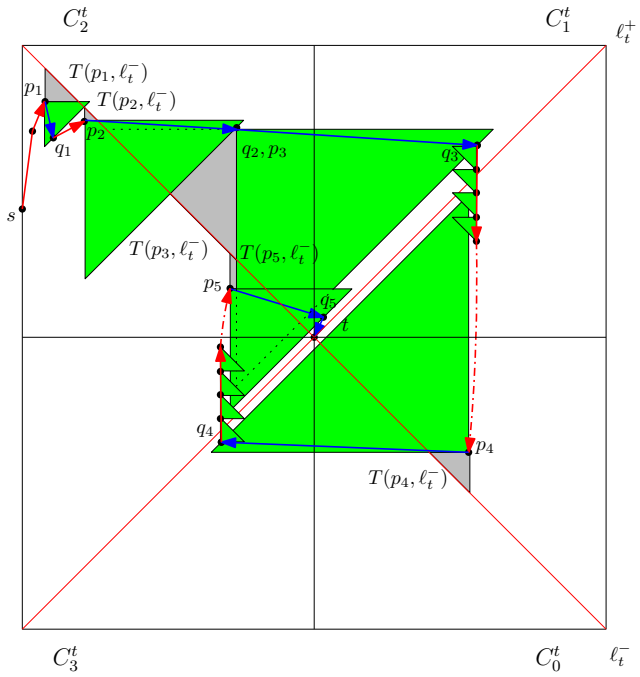

Figure 3.5: Canonical triangles and cleaned triangles. Blue lines are greedy steps towards t, red lines are sweeping steps towards ℓ_t^-.

the current vertex. Then the algorithm is:

Algorithm 1: The Greedy/Sweep Algorithm on Θ_4

```
v = s;                                          ▷ v is the current vertex
while v ≠ t do
    if v is not clean with respect to ℓ_t^- then
        take a sweeping step towards ℓ_t^-;
    else
        take a greedy step towards t;
    end
end
```

Observe that our algorithm requires knowledge of the current vertex v, its 4 outgoing edges, the destination vertex t, and one additional bit of information (signifying the chosen diagonal of t) in order to route to t. See Fig. 3.5 for an example of a path from s to t computed by Algorithm 1.

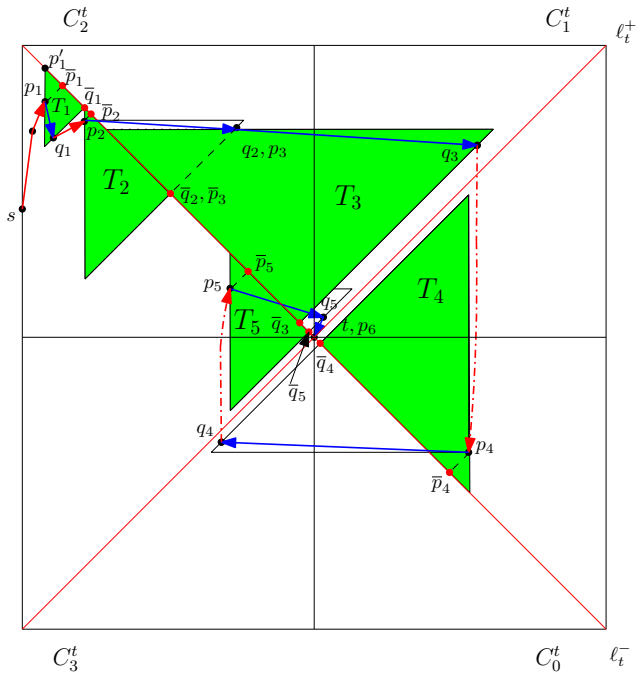

Figure 3.6: The bounding triangles. Blue lines are greedy steps towards t, red lines are sweeping steps towards ℓ_t^-.

3.3 ANALYSIS

In this section, we prove that our routing algorithm terminates and that it has a routing ratio of 17. Without loss of generality, we assume that s is in C_2^t under ℓ_t^-. Thus ℓ_t^- is the closest diagonal of t to s. For two arbitrary points u and v, let $d_x(u,v)$ and $d_y(u,v)$ be the distance between them along the x-axis and y-axis respectively. Let $L_1(u,v)$ be the L_1 distance between u and v (i.e., $L_1(u,v) = d_x(u,v) + d_y(u,v)$), and let $L_\infty(u,v)$ be the L_∞ distance from u to v (i.e., $L_\infty(u,v) = \max\{d_x(u,v), d_y(u,v)\}$). To simplify our analysis, most of our intermediate measurements will be in the L_1-metric. In the final analysis we will express the length in the L_2-metric. Let $\mathcal{P}(s,t)$ be the sequence of directed edges produced by our algorithm. For vertices u and v in $\mathcal{P}(s,t)$, with u occurring before v, let $\mathcal{P}\langle u,v\rangle$ be the subpath of $\mathcal{P}(s,t)$ from u to v.

We divide the area around t into *quadrants*. The *Northern* quadrant is the area above ℓ_t^- and ℓ_t^+, while the *Southern* quadrant is the area below ℓ_t^- and ℓ_t^+. The *Western* quadrant is the area to the left of ℓ_t^- and ℓ_t^+, while the *Eastern* quadrant is the area to the right of ℓ_t^- and ℓ_t^+.

We note the following about the path found by the algorithm:

Lemma 3.3.1. *Let u and v be two consecutive vertices on $\mathcal{P}(s,t)$. Then $L_\infty(u,t) > L_\infty(v,t)$.*

Proof. Let u be a vertex in the Western quadrant. Observe that through rotations or flips along a diagonal of t, this can be generalized to any quadrant and routing with respect to either diagonal. Since u is below ℓ_t^- and above ℓ_t^+, $L_\infty(u,t) = d_x(u,t)$. If v is in the Western quadrant, observe that for both a greedy step and a sweeping step, $d_x(u,t) > d_x(v,t)$, which implies that $L_\infty(u,t) > L_\infty(v,t)$, as required.

Assume v is not in the Western quadrant. For v to be in the Eastern quadrant, (u,v) must cross both diagonals of t. Observe that a greedy step does not cross ℓ_t^+, while a sweeping step does not cross ℓ_t^-. Thus v can only be in the Northern or Southern quadrant, and $L_\infty(v,t) = d_y(v,t)$. Observe that if v is in the Southern quadrant, then (u,v) was a sweeping step, and if v is in the Northern quadrant, then (u,v) was a greedy step. In both cases, $d_y(u,t) > d_y(v,t)$. Thus $L_\infty(u,t) = d_x(u,t) > d_y(u,t) > d_y(v,t) = L_\infty(v,t)$, as required. See Figs. 3.3 and 3.4. □ □

This leads to the following corollary.

Corollary 3.3.2. *The algorithm terminates, i.e., it reaches t.*

Note that when the current vertex v is in C_3^t or C_1^t, a greedy step towards t and a sweeping step towards ℓ_t^- are the same. However, by our definition of *clean*, this step is defined as a sweeping step. Let $((p_1,q_1),(p_2,q_2),\ldots,(p_{m-1},q_{m-1}))$ be the sequence of edges produced by greedy steps of the algorithm, with $t = p_m$. We refer to the path from a vertex p_i to a vertex p_{i+1}, for $1 \leq i < m$ as a *phase* f_i of the algorithm. That is, a phase consists of a single greedy step followed by a (possibly empty) sequence of sweeping steps. Note that the first phase is preceded by a (possibly empty) sequence of sweeping steps from s to p_1. Let $L_2(f_i)$ represent the length of phase f_i. Then observe that $\mathcal{P}(s,t) = \mathcal{P}\langle s,p_1\rangle + \sum_{i=1}^{m-1} f_i$, where the $+$ operator on paths is concatenation of the paths. Note that if each vertex on $\mathcal{P}\langle u,v\rangle$ is in the same cone $i, 0 \leq i \leq 3$ of all preceding vertices, then $\mathcal{P}\langle u,v\rangle$ is x- and y-monotone, and $L_2(\mathcal{P}\langle u,v\rangle) \leq L_1(u,v)$. This implies that $L_2(\mathcal{P}\langle q_i,p_{i+1}\rangle) \leq L_1(q_i,p_{i+1})$, for all $1 \leq i < m-1$.

Let v be the neighbour of an arbitrary vertex u in the cone C_i^u. Let the *canonical triangle* T_{uv} be the triangle formed by the boundaries of C_i^u and the line through v perpendicular to the bisector of C_i^u. Note that T_{uv} is empty of vertices in its interior. See Fig. 3.4.

Definition 3.3.3. *Consider the edge (p_i,q_i) of f_i. If p_i is in the Northern or Southern quadrant, then let $\mathcal{L}$ be the horizontal line through p_i, otherwise $\mathcal{L}$ is the vertical line through p_i. Let the* bounding triangle *T_i be the triangle formed by the lines ℓ_t^-, $\mathcal{L}$, and $\ell_{q_i}^+$. See Figs. 3.7, 3.8, and 3.9.*

Lemma 3.3.4. *The bounding triangle T_i is empty of vertices.*

Proof. Since (p_i,q_i) is a greedy step, p_i is clean with respect to ℓ_t^-, and $T(p_i,\ell_t^-)$ and $T_{p_iq_i}$ are both empty of vertices. Observe that T_i lies completely in one of the half-planes of ℓ_t^-.

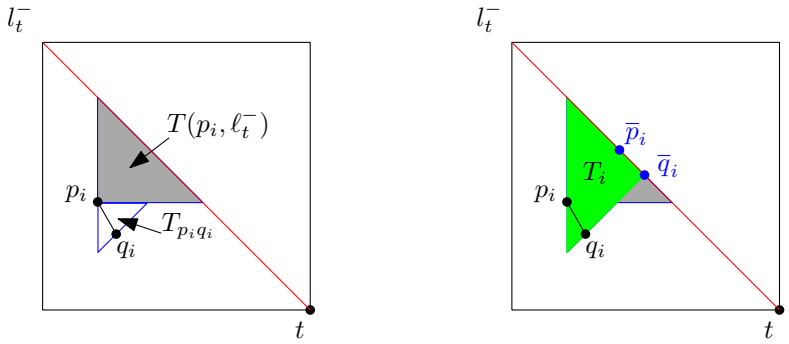

Figure 3.7: $T_{p_iq_i}$ does not intersect ℓ_t^-.

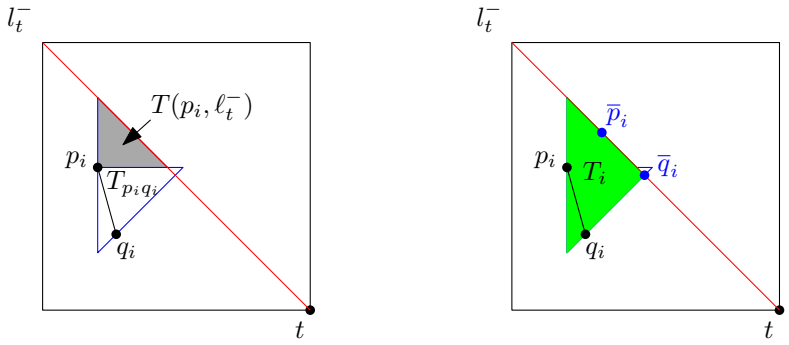

Figure 3.8: $T_{p_iq_i}$ intersects ℓ_t^-, and q_i lies on T_i.

If $T_{p_iq_i}$ does not intersect ℓ_t^-, then $T_{p_iq_i} \subseteq T_i$ and $T(p_i, \ell_t^-) \nsubseteq T_i$. See Fig. 3.7. If $T_{p_iq_i}$ does intersect ℓ_t^-, then observe that $T(p_i, \ell_t^-) \subseteq T_i$ and $T_{p_iq_i} \nsubseteq T_i$. In this case, q_i can be on the same side of ℓ_t^- as p_i, and thus lie on T_i (Fig. 3.8), or it can be on the opposite side of ℓ_t^-, and not lie on T_i (Fig. 3.9). In all cases observe that $T_i \subseteq T_{p_iq_i} \cup T(p_i, \ell_t^-)$, and thus T_i is empty of vertices. □ □

Notice that a bounding triangle T_i cannot be on both sides of ℓ_t^- by construction, and cannot be on both sides of ℓ_t^+ since that would imply that t is within $T_{p_iq_i}$. This implies that a bounding triangle T_i can only intersect the interior of a single quadrant.

Lemma 3.3.1 has strong implications about the positions of bounding triangles relative to one another in the same quadrant. For a vertex p, let $\overline{p}$ be the intersection of ℓ_t^- and ℓ_p^+.

Lemma 3.3.5. *If T_i and T_j are two bounding triangles in the same quadrant, then $\overline{p}_j\overline{q}_j$ and $\overline{p}_i\overline{q}_i$ are disjoint segments lying along ℓ_t^-.*

Proof. Without loss of generality, assume that $i < j$. Note that for a point $\overline{v}$ lying on ℓ_t^-, $L_1(\overline{v}, t) = \sqrt{2} \cdot L_2(\overline{v}, t)$. That is, the L_1- and L_2-distances are proportional. Then

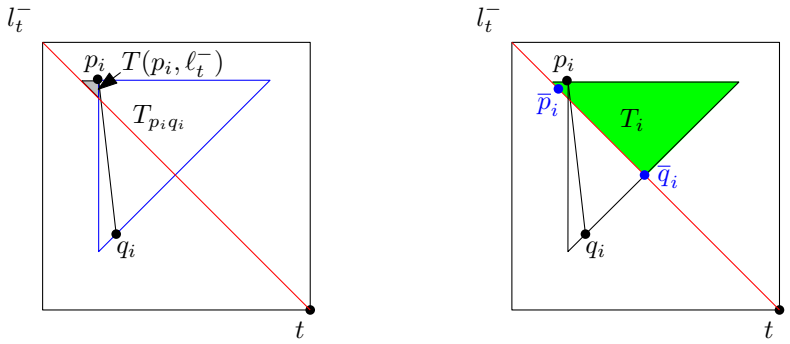

Figure 3.9: $T_{p_i q_i}$ intersects ℓ_t^-, and q_i does not lie on T_i.

Lemma 3.3.5 is true if $L_1(\overline{p}_i, t) > L_1(\overline{q}_i, t) > L_1(\overline{p}_j, t) > L_1(\overline{q}_j, t)$ is true. Assume without loss of generality T_i and T_j are in the Western quadrant. See Fig. 3.10. Note that $L_1(\overline{p}_i, t) - L_1(\overline{q}_i, t) = L_1(\overline{p}_i, \overline{q}_i) = L_1(p_i, q_i)$, since q_i is in the same cone of p_i as t. Thus $L_1(\overline{p}_i, t) > L_1(\overline{q}_i, t)$ and $L_1(\overline{p}_j, t) > L_1(\overline{q}_j, t)$ are true. It remains to show $L_1(\overline{q}_i, t) > L_1(\overline{p}_j, t)$. Lemma 3.3.1 implies $L_\infty(p_i, t) > L_\infty(p_j, t)$, and both points are in the Western quadrant (by the definition of bounding triangle), thus p_j cannot be left of p_i. This, and the fact that T_i is empty, implies p_j must be below $\ell_{q_i}^+$, which implies $\ell_{p_j}^+$ is below $\ell_{q_i}^+$, which implies $L_1(\overline{q}_i, t) > L_1(\overline{p}_j, t)$. □ □

Fig. 3.10 shows two consecutive bounding triangles in the Western quadrant, and the associated segments $\overline{p}_i\overline{q}_i$ and $\overline{p}_{i+1}\overline{q}_{i+1}$.

Let p_1' be the vertical projection of p_1 onto ℓ_t^-. Then the following inequality is true.

Corollary 3.3.6. $\sum_{i=1}^{m-1} L_1(\overline{p}_i, \overline{q}_i) \leq 4 \cdot L_1(p_1', t)$.

Proof. Lemma 3.3.1 implies that $L_1(p_1', t) > L_1(\overline{p}_i, t)$ for all $1 \leq i \leq m-1$. This combined with Lemma 3.3.5 and the fact that there are four quadrants implies the lemma. □ □

Lemma 3.3.7. $L_2(f_i) \leq L_1(p_i, q_i) + L_1(q_i, p_{i+1})$.

Proof. This follows from the fact that (p_i, q_i) is an edge, and $\mathcal{P}\langle q_i, p_{i+1}\rangle$ is x- and y-monotone. □ □

Each of the bounding triangles T_i are associated with the segment $\overline{p}_i\overline{q}_i$ and the phase f_i. A natural approach is to try and bound the length of the phase $L_2(f_i)$ to the length of the segment $\overline{p}_i\overline{q}_i$. This does not quite work. However, by using a potential function we are able to make it work. We define the potential function $\Phi(p_i, p_{i+1}) = L_1(p_i, q_i) + L_1(q_i, \overline{p}_{i+1}) - L_1(p_i, \overline{p}_i)$ for all $1 \leq i < m-1$.

Lemma 3.3.8. $\Phi(p_i, p_{i+1}) \leq 2 \cdot L_1(\overline{p}_i, \overline{q}_i)$.

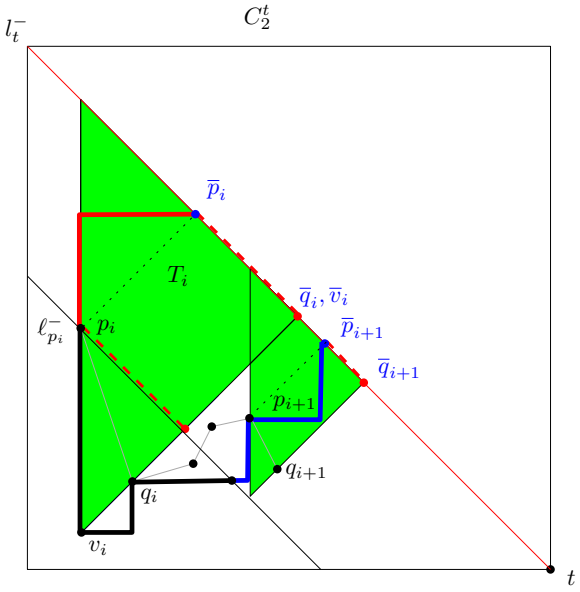

Figure 3.10: The red path from p_i to $\overline{p}_i$ is the same length as the blue path. Thus $\Phi(p_i, p_{i+1})$ is equal to the length of the black path.

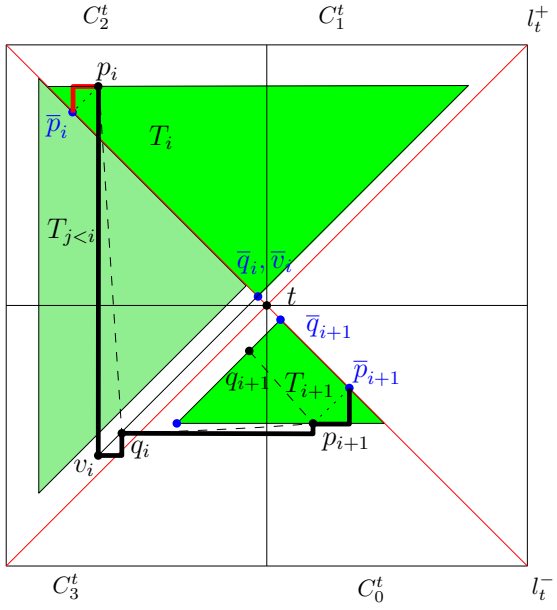

Figure 3.11: $L_1(q_i, \overline{p}_{i+1}) < L_1(p_i, q_i)$, since p_i is in $C_2^{q_i}$ and on the opposite side of ℓ_t^- as q_i.

Proof. Without loss of generality, assume that q_i is in the Western quadrant. Since greedy steps can only originate in C_2^t and C_0^t, and a greedy step cannot cross ℓ_t^+, p_i is in C_2^t in either the Western or Northern quadrant (Figs. 3.10 and 3.11 respectively). Let v_i be the bottommost point of $T_{p_i q_i}$. Since v_i is on $\ell_{q_i}^+$, we have $\overline{v_i} = \overline{q_i}$. Since both p_i and $\overline{p}_i$ are on $\ell_{p_i}^+$, and both v_i and $\overline{v}_i$ are on $\ell_{v_i}^+$, we have $L_1(p_i, v_i) = L_1(\overline{p}_i, \overline{v_i}) = L_1(\overline{p}_i, \overline{q_i})$. Thus it is enough to prove that $\Phi(p_i, p_{i+1}) \leq 2 \cdot L_1(p_i, v_i)$. Observe that $L_1(p_i, v_i) + L_1(v_i, q_i) \geq L_1(p_i, q_i)$ by the triangle inequality.

If p_i is in the Western quadrant, we have that $L_1(v_i, \overline{p}_i) = L_1(v_i, p_i) + L_1(p_i, \overline{p}_i)$ and $L_1(v_i, \overline{p}_{i+1}) = L_1(v_i, q_i) + L_1(q_i, \overline{p}_{i+1})$. Since both $\overline{p}_i$ and $\overline{p}_{i+1}$ lie in $C_1^{v_i}$ on ℓ_t^-, we have $L_1(v_i, \overline{p}_i) = L_1(v_i, \overline{p}_{i+1})$. Thus

$$\begin{aligned}
\Phi(p_i, p_{i+1}) &= L_1(p_i, q_i) + L_1(q_i, \overline{p}_{i+1}) - L_1(p_i, \overline{p}_i) \\
&\leq L_1(p_i, v_i) + L_1(v_i, \overline{p}_{i+1}) - L_1(p_i, \overline{p}_i) \\
&= L_1(p_i, v_i) + L_1(v_i, \overline{p}_i) - L_1(p_i, \overline{p}_i) \\
&= 2 \cdot L_1(p_i, v_i)
\end{aligned}$$

as required. Otherwise p_i is in the Northern quadrant. Observe that p_i and $\overline{p}_{i+1}$ are both in $C_1^{v_i}$, but p_i is above ℓ_t^- while $\overline{p}_{i+1}$ is on it, thus $L_1(p_i, v_i) > L_1(v_i, \overline{p}_{i+1})$. Thus

$$\begin{aligned}
\Phi(p_i, p_{i+1}) &= L_1(p_i, q_i) + L_1(q_i, \overline{p}_{i+1}) - L_1(p_i, \overline{p}_i) \\
&\leq L_1(p_i, v_i) + L_1(v_i, \overline{p}_{i+1}) \\
&\leq 2 \cdot L_1(p_i, v_i)
\end{aligned}$$

as required. □ □

We can now prove the main theorem.

Theorem 3.3.9. *The path produced by Algorithm 1 has length at most* $17 \cdot L_2(s, t)$.

Proof. Recall that $t = p_m$. Thus $L_1(p_m, \overline{p}_m) = 0$, and

$$\sum_{i=1}^{m-1} (L_1(p_{i+1}, \overline{p}_{i+1}) - L_1(p_i, \overline{p}_i)) = -L_1(p_1, \overline{p}_1). \tag{3.1}$$

Since p_1 is in C_1^s, and $\overline{p}_1$ is in $C_1^{p_1}$, we have that $\overline{p}_1$ is in C_1^s. Since we assume that ℓ_t^- is the closest diagonal to s, that gives us

$$L_1(s, \overline{p}_1) \leq L_\infty(s, t) \leq L_2(s, t). \tag{3.2}$$

Additinally, since p'_1 is a point on ℓ_t^-, we have $L_1(p'_1, t) = 2L_\infty(p'_1, t)$. Observe that $L_\infty(s,t) > L_\infty(p_1,t) = L_\infty(p'_1,t)$, thus $L_1(p'_1,t) \le 2L_\infty(s,t)$, and $L_\infty(s,t) \le L_2(s,t)$. That gives us

$$L_1(p'_1, t) \le 2 \cdot L_\infty(s,t) \le 2 \cdot L_2(s,t). \tag{3.3}$$

Thus $L_2(\mathcal{P}(s,t))$ is equal to

$$\begin{aligned}
&L_2(\mathcal{P}\langle s, p_1\rangle) + \sum_{i=1}^{m-1} L_2(f_i) \\
\le &L_1(s,p_1) + \sum_{i=1}^{m-1} (L_1(p_i,q_i) + L_1(q_i,p_{i+1})) && \text{(Lemma 3.3.7)} \\
= &L_1(s,p_1) + L_1(p_1,\overline{p}_1) - L_1(p_1,\overline{p}_1) \\
&+ \sum_{i=1}^{m-1} (L_1(p_i,q_i) + L_1(q_i,p_{i+1})) \\
= &L_1(s,\overline{p}_1) + \sum_{i=1}^{m-1} (L_1(p_{i+1},\overline{p}_{i+1}) - L_1(p_i,\overline{p}_i)) \\
&+ \sum_{i=1}^{m-1} (L_1(p_i,q_i) + L_1(q_i,p_{i+1})) && \text{(by (3.1))} \\
= &L_1(s,\overline{p}_1) + \sum_{i=1}^{m-1} (L_1(p_i,q_i) + L_1(q_i,\overline{p}_{i+1}) - L_1(p_i,\overline{p}_i)) \\
= &L_1(s,\overline{p}_1) + \sum_{i=1}^{m-1} \Phi(p_i,p_{i+1}) \\
\le &L_1(s,\overline{p}_1) + 2\sum_{i=1}^{m-1} L_1(\overline{p}_i,\overline{q}_i) && \text{(Lemma 3.3.8)} \\
\le &L_1(s,\overline{p}_1) + 8 \cdot L_1(p'_1,t) && \text{(Corollary 3.3.6)} \\
\le &L_2(s,t) + 16 \cdot L_2(s,t) && \text{(by (3.2) and (3.3))} \\
\le &17 \cdot L_2(s,t)
\end{aligned}$$

as required. □ □

3.4 LOWER BOUND

In this section, we show that our analysis of the routing ratio of Algorithm 1 is tight: We will construct a set of points, together with two vertices s and t, such that the routing

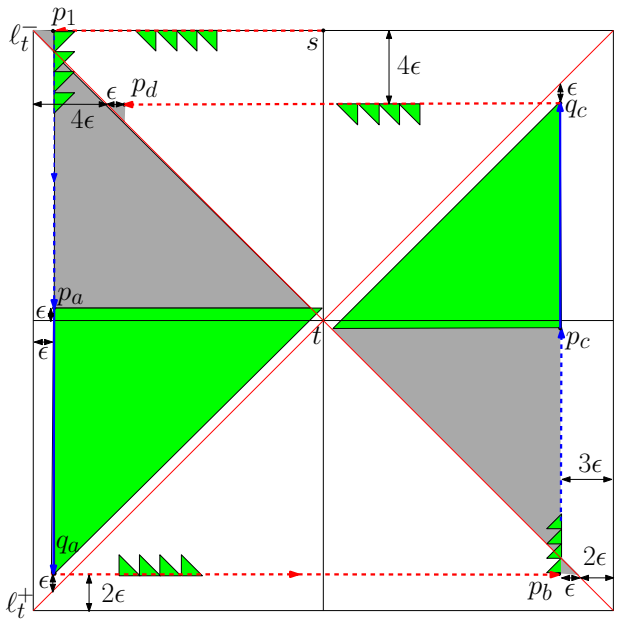

Figure 3.12: The path from s to p_d. Blue lines are greedy steps, red are sweeping steps towards ℓ_t^-.

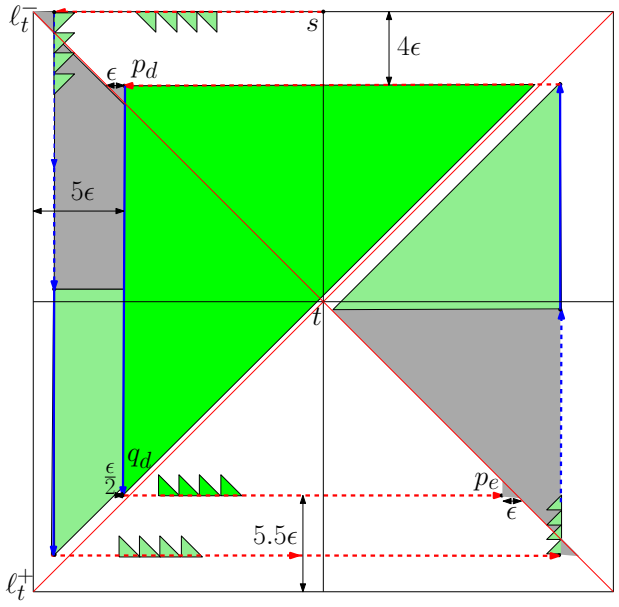

Figure 3.13: The path from p_d to p_e.

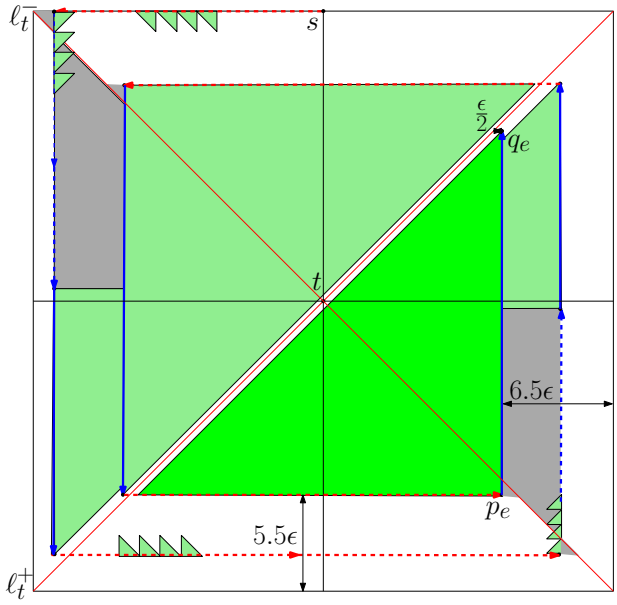

Figure 3.14: The last greedy edge (p_e, q_e).

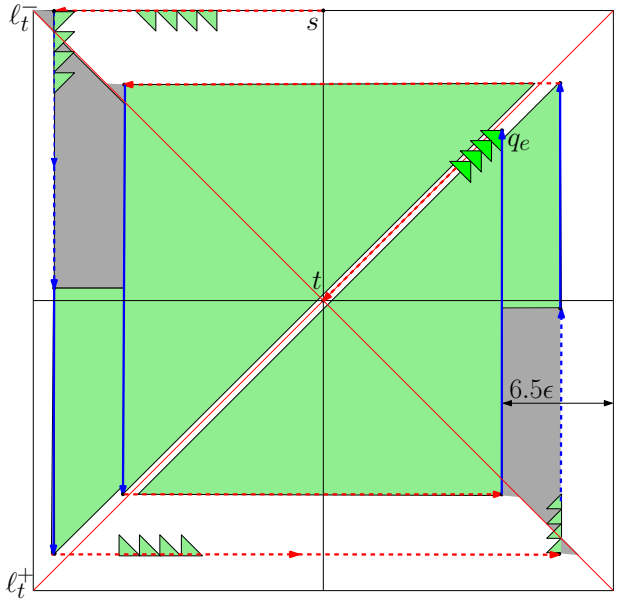

Figure 3.15: The final path from q_e to t.

ratio of Algorithm 1 is arbitrarily close to 17. The construction is illustrated in Figs. 3.12, 3.13, 3.14, and 3.15. We forgo our general position assumption in order to make the demonstration of the lower bound simpler. For this particular example, if a vertex is on the boundary between two cones or two quadrants, we say that that vertex is in the *counter-clockwise* of the two cones or quadrants. Let $\epsilon > 0$ be an arbitrarily small number. Let $1 < a < b < c < d < e$ be (not necessarily consecutive) integers.

Let t be at coordinates $(0, 0)$. Let s be at coordinates $(0, 1)$. Vertex p_1 is at $(-1 + \epsilon, 1)$. See Fig. 3.12. There is a sequence of vertices directly left of s at coordinates $(-\epsilon, 1), (-2\epsilon, 1), (-3\epsilon, 1)..., (-1 + \epsilon, 1) = p_1$. This implies that s is not clean, so we take sweeping steps along this sequence of vertices (red dashed line) until we reach p_1. The path from s to p_1 has length $(1 - \epsilon)$.

Directly below p_1 (and thus in $C_0^{p_1}$) there is a sequence of vertices at coordinates $(-1 + \epsilon, 1 - \epsilon), (-1 + \epsilon, 1 - 2\epsilon), ..., (-1 + \epsilon, \epsilon) = p_a$, all of which are clean. Since p_1 is clean with respect to ℓ_t^-, we take greedy steps along this sequence to p_a (blue dashed line). Directly below p_a is vertex $q_a = (-1 + \epsilon, -1 + 2\epsilon)$. Vertex p_a is clean, so the next greedy step takes us to q_a (blue edge). The path from p_1 to q_a has length $2 - 2\epsilon$.

To the right of q_a is a sequence of vertices at coordinates $(-1 + 2\epsilon, -1 + 2\epsilon), (-1 + 3\epsilon, -1 + 2\epsilon), ..., (1 - 3\epsilon, -1 + 2\epsilon) = p_b$. The path from q_a to p_b has length $2 - 4\epsilon$.

There is a sequence of vertices directly above p_b at coordinates $(1 - 3\epsilon, -1 + 3\epsilon), (1 - 3\epsilon, -1 + 4\epsilon), ..., (1 - 3\epsilon, -\epsilon) = p_c$, all of which are clean. Thus we proceed along these vertice in a sequence of greedy steps from p_b to p_c (blue dashed path). From p_c we take a greedy step to $q_c = (1 - 3\epsilon, 1 - 4\epsilon)$ (blue edge). The path from p_b to q_c has length $2 - 6\epsilon$.

There is a sequence of vertices left of q_c at coordinates $(1 - 4\epsilon, 1 - 4\epsilon), (1 - 5\epsilon, 1 - 4\epsilon), ..., (-1 + 5\epsilon, 1 - 4\epsilon) = p_d$. The path from q_c to p_d has length $2 - 8\epsilon$.

In Fig. 3.13 we take a greedy step from p_d to $q_d = (-1 + 5\epsilon, -1 + 5.5\epsilon)$ (blue edge). This edge has length $2 - 9.5\epsilon$.

To the right of q_d is a sequence of vertices at coordinates $(-1 + 6\epsilon, -1 + 5.5\epsilon), (-1 + 7\epsilon, -1 + 5.5\epsilon), ..., (1 - 6\epsilon, -1 + 5.5\epsilon) = p_e$. The path from q_d to p_e has length $2 - 11.5\epsilon$.

In Fig. 3.14 we take a greedy step from p_e to $q_e = (1 - 6.5\epsilon, 1 - 7\epsilon)$ (blue edge). The edge (p_e, q_e) has length $2 - 12.5\epsilon$.

In Figs. 3.15 and 3.16 there are a sequence of vertices at $(1 - 7\epsilon, 1 - 7\epsilon), (1 - 7\epsilon + \epsilon', 1 - 7.5\epsilon), (1 - 7.5\epsilon, 1 - 7.5\epsilon), (1 - 7.5\epsilon + \epsilon', 1 - 8\epsilon)...(0, 0) = t$. We will define ϵ' in a moment. A sequence of clearing steps takes us from q_e to t along these vertices. Let $\delta + 1$ be the number of horizontal edges in this sequence, and let γ be the number of edges with a vertical component. Let $\epsilon' = \epsilon/\delta$. Observe that $d_x(q_e, t) = 1 - 6.5\epsilon = (\delta + 1) \cdot \epsilon/2$. The first horizontal edge has length $\epsilon/2$, and the remaining δ horizontal edges have length $\epsilon/2 - \epsilon'$. Thus the total length of the horizontal edges is $1 - 6.5\epsilon - \delta\epsilon' = 1 - 6.5\epsilon - \epsilon = 1 - 7.5\epsilon$.

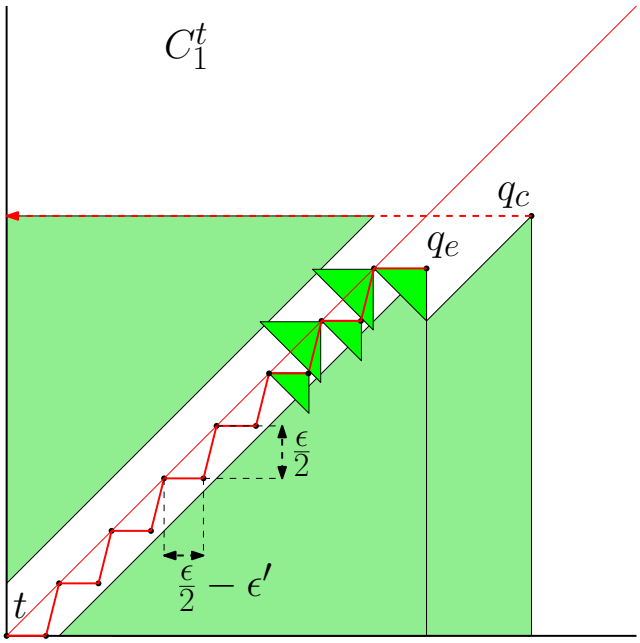

Figure 3.16: Details of the final path from q_e to t.

Observe that $d_y(q_e, t) = 1 - 7\epsilon = \gamma \cdot \epsilon/2$. Each of the γ vertical edges has length $> \epsilon/2$, since their vertical distance is $\epsilon/2$ and they are skewed from vertical, thus the total length of the vertical steps is at least $1 - 7\epsilon$. Thus the path from q_e to t has length at least $2 - 14.5\epsilon$.

The total length of these paths is at least $L_2(s, p_1) + L_2(p_1, q_a) + L_2(q_a, p_b) + L_2(p_b, q_c) + L_2(q_c, p_d) + L_2(p_d, q_d) + L_2(q_d, p_e) + L_2(p_e, q_e) + d_x(q_e, t) - \epsilon + d_y(q_e, t) = 1 - \epsilon + 2 - 2\epsilon + 2 - 4\epsilon + 2 - 6\epsilon + 2 - 8\epsilon + 2 - 9.5\epsilon + 2 - 11.5\epsilon + 2 - 12.5\epsilon + 2 - 14.5\epsilon = 17 - 69\epsilon$. Since $L_2(s, t) = 1$, by letting ϵ tend to 0 we can make the path arbitrarily close to $17 \cdot L_2(s, t)$.

3.5 REMOVING THE DIAGONAL-BIT

The algorithm, as presented in Section 3.2 uses one single bit to remember the diagonal of the destination t that is closest to the start vertex s. In this section, we show that without this single bit, the routing ratio increases to $\sqrt{290} < 17.03$.

We modify Algorithm 1 by always using the same diagonal, say ℓ_t^-. The changes that have to be made in the analysis are Inequality (3.2), which becomes

$$L_1(s, \overline{p}_1) \leq d_y(s, t) + L_\infty(s, t), \tag{3.4}$$

and Inequality (3.3), which becomes

$$L_1(p'_1, t) \leq 2 \cdot L_\infty(s, t). \tag{3.5}$$

If we replace (3.4) and (3.5) by (3.2) and (3.3) respectively in our proof of Theorem 4.2 we get $L_2(\mathcal{P}\langle s, t\rangle) \leq d_y(s, t) + 17 \cdot L_\infty(s, t)$. Let $\gamma = (d_y(s, t) + 17 \cdot L_\infty(s, t))/L_2(s, t)$. The routing ratio is thus the maximum of γ. Let u be the point at $(d_x(s), d_y(t))$, and let $\theta = \angle uts$. We can rewrite γ as $\sin\theta + 17 \cdot \cos\theta = \sqrt{17^2 + 1^2} \cdot \sin(\theta + \arctan(17))$ for $0 \leq \theta \leq \pi/4$. This is maximized at $\theta = \arctan(\frac{1}{17})$ with a value of $\sqrt{290}$. Thus we have the following theorem.

Theorem 3.5.1. *With no bits of memory, and using a fixed diagonal ℓ_t^-, Algorithm 1 outputs a path from s to t with length at most $\sqrt{290} \cdot L_2(s, t)$.*

If we refer to the lower bound proof in Section 3.4, we can adjust it to this new bound by moving s to the right until st forms an angle of $\arctan(\frac{1}{17})$ with the positive y-axis. Thus, in this case, we can get arbitrarily close to $\sqrt{290}$.

3.6 CONCLUSION

We have presented a simple online local routing algorithm for Θ_4-graphs that achieves a routing ratio of 17 using knowledge of the destination and one bit of information, and $\sqrt{290} < 17.03$ using only knowledge of the destination. Although we have presented the first such algorithm on Θ_4-graphs and also improved the spanning ratio of Θ_4-graphs from 237 down to 17, we conjecture that this upper bound both on the routing ratio and spanning ratio is not tight. Given that 7 [1] is the best known lower bound for the spanning ratio of Θ_4, the actual spanning ratio remains unknown.

BIBLIOGRAPHY

[1] Luis Barba, Prosenjit Bose, Jean-Lou De Carufel, André van Renssen, and Sander Verdonschot. On the stretch factor of the theta-4 graph. *CoRR*, abs/1303.5473, 2013.

[2] Nicolas Bonichon, Prosenjit Bose, Jean-Lou De Carufel, Vincent Despré, Darryl Hill, and Michiel H. M. Smid. Improved routing on the delaunay triangulation. In *ESA*, volume 112 of *LIPIcs*, pages 22:1–22:13. Schloss Dagstuhl - Leibniz-Zentrum fuer Informatik, 2018.

[3] Nicolas Bonichon, Prosenjit Bose, Jean-Lou De Carufel, Ljubomir Perkovic, and André van Renssen. Upper and lower bounds for online routing on delaunay triangulations. *Discrete & Computational Geometry*, 58(2):482–504, 2017.

[4] Nicolas Bonichon, Cyril Gavoille, Nicolas Hanusse, and David Ilcinkas. Connections between theta-graphs, delaunay triangulations, and orthogonal surfaces. In *WG*, volume 6410 of *Lecture Notes in Computer Science*, pages 266–278, 2010.

[5] Prosenjit Bose, Paz Carmi, and Stephane Durocher. Bounding the locality of distributed routing algorithms. *Distributed Computing*, 26(1):39–58, 2013.

[6] Prosenjit Bose, Jean-Lou De Carufel, Darryl Hill, and Michiel H. M. Smid. On the spanning and routing ratio of theta-four. In Timothy M. Chan, editor, *Proceedings of the Thirtieth Annual ACM-SIAM Symposium on Discrete Algorithms, SODA 2019, San Diego, California, USA, January 6-9, 2019*, pages 2361–2370. SIAM, 2019.

[7] Prosenjit Bose, Jean-Lou De Carufel, Pat Morin, André van Renssen, and Sander Verdonschot. Towards tight bounds on theta-graphs: More is not always better. *Theor. Comput. Sci.*, 616:70–93, 2016.

[8] Prosenjit Bose, Rolf Fagerberg, André van Renssen, and Sander Verdonschot. Competitive routing in the half-theta-6-graph. In *SODA*, pages 1319–1328. SIAM, 2012.

[9] Prosenjit Bose, Rolf Fagerberg, André van Renssen, and Sander Verdonschot. Optimal local routing on delaunay triangulations defined by empty equilateral triangles. *SIAM J. Comput.*, 44(6):1626–1649, 2015.

[10] Prosenjit Bose and Pat Morin. Competitive online routing in geometric graphs. *Theor. Comput. Sci.*, 324(2-3):273–288, 2004.

[11] Prosenjit Bose and Pat Morin. Online routing in triangulations. *SIAM J. Comput.*, 33(4):937–951, 2004.

[12] Prosenjit Bose, Pat Morin, André van Renssen, and Sander Verdonschot. The theta-5-graph is a spanner. *CoRR*, abs/1212.0570, 2012.

[13] Nicolas Broutin, Olivier Devillers, and Ross Hemsley. Efficiently navigating a random delaunay triangulation. *Random Struct. Algorithms*, 49(1):95–136, 2016.

[14] Dan Chen, Luc Devroye, Vida Dujmovic, and Pat Morin. Memoryless routing in convex subdivisions: Random walks are optimal. *Computational Geometry - Theory and Applications*, 45(4):178–185, 2012.

[15] Paul Chew. There is a planar graph almost as good as the complete graph. In *Symposium on Computational Geometry*, pages 169–177. ACM, 1986.

[16] Paul Chew. There are planar graphs almost as good as the complete graph. *J. Comput. Syst. Sci.*, 39(2):205–219, 1989.

[17] Kenneth L. Clarkson. Approximation algorithms for shortest path motion planning (extended abstract). In *STOC*, pages 56–65. ACM, 1987.

[18] J. Mark Keil. Approximating the complete euclidean graph. In *SWAT*, volume 318 of *Lecture Notes in Computer Science*, pages 208–213. Springer, 1988.

[19] J. Mark Keil and Carl A. Gutwin. Classes of graphs which approximate the complete euclidean graph. *Discrete & Computational Geometry*, 7:13–28, 1992.

[20] Evangelos Kranakis, Harvinder Singh, and Jorge Urrutia. Compass routing on geometric networks. In *CCCG*, 1999.

[21] Nawar M. El Molla. *Yao spanners for wireless ad-hoc networks*. PhD thesis, Villanova University, 2009.

[22] Stefan Ruhrup. Theory and practice of geographic routing. *Chapter 5 in Ad Hoc and Sensor Wireless Networks: Architectures, Algorithms and Protocols*, 2009.

[23] Jim Ruppert and Raimund Seidel. Approximating the d-dimensional complete Euclidean graph. In *Proceedings of the 3rd Canadian Conference on Computational Geometry*, CCCG 1991.

4

THE SPANNING RATIO OF CONVEX POLYHEDRA WHOSE VERTICES ARE ON A SPHERE

ABSTRACT

Let P_C be a convex simplicial polyhedron in $\mathbb{R}^3$. Let the *skeleton* of P_C, denoted $skel(P_C)$, be the graph whose vertex and edge sets are equal to the vertex and edge sets of P_C, respectively. Xia has shown that the Delaunay triangulation in $\mathbb{R}^2$ is a 1.998-spanner of the complete graph. We make use of this result to prove that, if the vertices of P_C are on a sphere, then the skeleton of P_C is a 0.999π-spanner.

This chapter is part of a paper that appeared in the Journal of Computational Geometry [5].

A geometric graph G in Euclidean space is a set of points S and a set of edges E consisting of pairs of points of S. Let $|pq|$ be the Euclidean distance between points p and q, and let $|uv|$ then be the weight of an edge uv of E. A graph G is a t-spanner, or just spanner, if there exists a constant t such that, for every pair of points p and q in S, there is a path $\mathcal{P}_G(p,q)$ whose length $|\mathcal{P}_G(p,q)|$ is at most $t \cdot |pq|$. The value t is also known as the *spanning ratio* of G.

If we restrict the points of S to the plane, then a well-known t-spanner of S is the Delaunay triangulation. The Delaunay triangulation was first proven to be spanner by Dobkin *et al.* [2], who showed it had a spanning ratio of $(1+\sqrt{5})\pi/2 \approx 5.08$. This was improved to $4\pi\sqrt{3}/9 \approx 2.42$ by Keil and Gutwin[3], before Xia[6] showed the current upper bound on the spanning ratio of 1.998.

If we restrict the points of S to the surface of a sphere, then let P_C be the convex simplicial polyhedron, i.e., all faces are triangles, whose vertices are the points of S. Let the *skeleton* of P_C, denoted $skel(P_C)$, be the graph whose vertex and edge sets are equal to the vertex and edge sets of P_C. Brown[1] was the first to observe that the polyhedron P_C has the same combinatorial structure as the spherical Delaunay triangulation of S. Using this observation and Dobkin *et al.*'s [2] result, Bose et al. [4] showed that $skel(P_C)$ is a spanner with a spanning ratio of $3\pi(\pi/2+1)/2 < 12.12$.

In this paper we improve the spanning ratio $skel(P_C)$ to $0.999 \cdot \pi < 3.14$. Our proof relies on a result by Xia [6] that gives the best known spanning ratio of the Delaunay

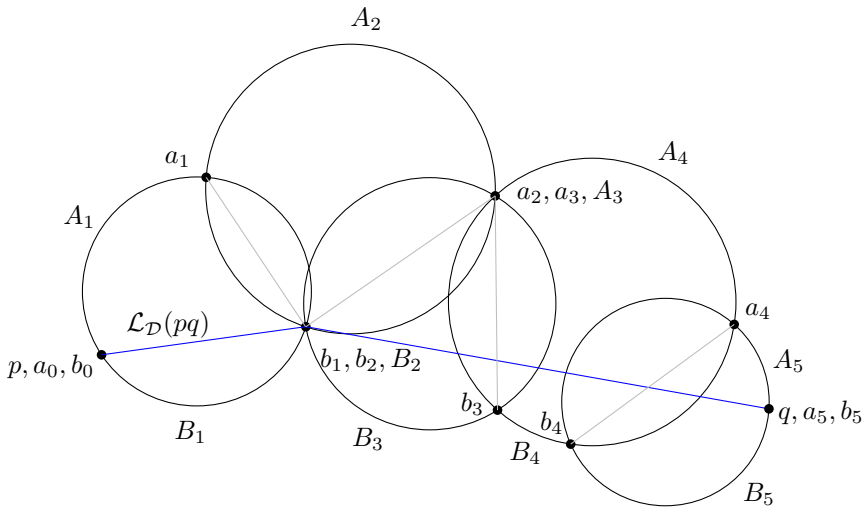

Figure 4.1: A chain of disks.

triangulation. In Section 4.1 we first present the main ideas behind Xia's [6] result. In Section 4.2 we show how we can use Xia's result to show an upper bound on the spanning ratio of $skel(P_C)$ when vertices are on a sphere. In Section 5.6 we give the conclusion along with open problems.

4.1 CHAINS OF DISKS

One of the strengths of Xia's [6] is a well chosen model. In particular, he finds the spanning ratio of a *chain of disks*, and this provides an upper bound on the spanning ratio of the Delaunay triangulation. Let $\mathcal{D} = (D_1, D_2, ...D_k)$ be a sequence of disks in $\mathbb{R}^2$, where $k \geq 2$. For $2 \leq i \leq k$, let $\Gamma_i^{i-1} = D_{i-1} \cap \partial D_i$, that is, the part of the boundary of D_i that is contained in D_{i-1}, and for $1 \leq i < k$, let $\Gamma_i^{i+1} = D_{i+1} \cap \partial D_i$, that is, the part of the boundary of D_i that is contained in D_{i+1}. Then $\mathcal{D}$ is called a *chain of disks* if

1. for $1 \leq i < k$, the circles ∂D_i and ∂D_{i+1} intersect in exactly one or two points, and
2. for each $1 < i < k$, arcs Γ_i^{i-1} and Γ_i^{i+1} share at most a single point.

See Fig. 4.1.

For a given curve J, let $|J|$ denote the length of J. For two points u and v, let $|uv|$ denote the Euclidean distance from u to v.

Let p be a point on ∂D_1 not in D_2 and let q be a point on ∂D_k not in D_{k-1}. For $1 \leq i < k$, let d_i be the center of disk D_i, and let a_i and b_i be the intersections of ∂D_i and ∂D_{i+1}, where $a_i = b_i$ if the two circles are tangent, otherwise a_i is to the left of

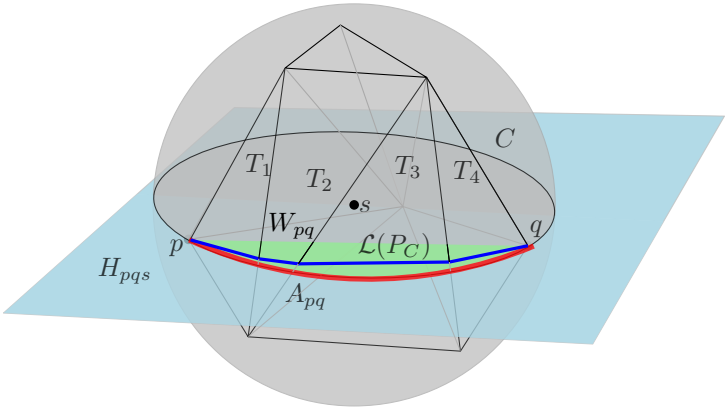

Figure 4.2: Illustration of notation.

the line through d_i and d_{i+1} and b_i is to the right. Let $a_0 = b_0 = p$ and $a_k = b_k = q$. Let $\mathcal{L}_{\mathcal{D}}(pq)$ be the shortest directed polyline from p to q that intersects each (possibly degenerate) segment $a_0b_0, a_1b_1, ..., a_kb_k$ in order. For each i, $1 < i \leq k$, let A_i be the clockwise arc of D_i from a_{i-1} to a_i, and let B_i be the counter-clockwise arc of D_i from b_{i-1} to b_i. Let $E = \{A_1, A_2, ..., A_k\} \cup \{B_1, B_2, ..., B_k\} \cup \{\{a_1, b_1\}, \{a_2, b_2\}, ..., \{a_{k-1}, b_{k-1}\}\}$ be a set of edges, and let $P = \{p, a_1, a_2, ..., a_{k-1}, b_1, b_2, ...b_{k-1}, q\}$ be a set of vertices. Let $G(P, E)$ be the graph formed using the vertices of P and the edges of E. Let $\mathcal{P}_G(p, q)$ be the shortest path from p to q on the graph $G(P, E)$. The following theorem, taken from the paper by Xia [6] on the spanning ratio of the L_2-Delauany triangulation, is central to our result.

Theorem 4.1.1. $|\mathcal{P}_G(p, q)| \leq 1.998 \cdot |\mathcal{L}_{\mathcal{D}}(pq)|$.

Given two vertices u and v in a Delaunay triangulation, the circumcircles of the triangles intersected by uv form a chain of disks. Xia [6] presents the upper bound on the spanning ratio of the L_2-Delaunay triangulation as a corollary to this theorem.

4.2 MAIN THEOREM

Given two vertices p and q in $skel(P_C)$, we define the following notation.

- Let H_{pqs} be the plane through p, q, and s.
- Let A_{pq} be the shorter of the two arcs of $H_{pqs} \cap \mathcal{S}$ from p to q.
- Let W_{pq} be the polygon in H_{pqs} enclosed by A_{pq} and pq.
- Let $\mathcal{T} = (T_1, T_2, ...T_k)$ be the triangles of P_C intersected by W_{pq}.

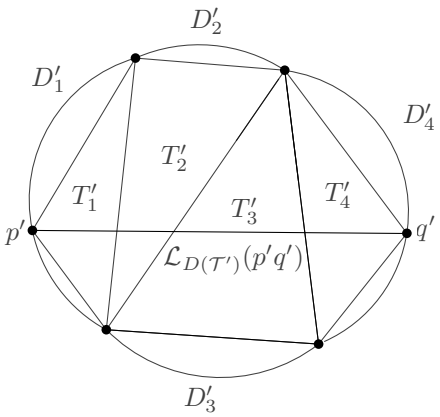

Figure 4.3: $\mathcal{T}$ unfolded into the plane into $\mathcal{T}'$.

- Let $\mathcal{L}(P_C) = P_C \cap W_{pq}$ (thus $\mathcal{T} \cap \mathcal{L}(P_C) = \mathcal{L}(P_C)$).
- Let $\mathcal{T}'$ be $\mathcal{T}$ unfolded into the plane along its edges, where p' and q' are the degree 2 vertices of T'_1 and T'_k respectively.

See Figs. 4.2 and 4.3. The following two lemmas are used to prove the main theorem.

Lemma 4.2.1. *Let $\mathcal{D}(\mathcal{T}') = (D'_1, D'_2, ..., D'_k)$ be the circumcircles of $\mathcal{T}'$. Then $\mathcal{D}(\mathcal{T}')$ forms a chain of disks.*

Recall that $\mathcal{L}_{\mathcal{D}(\mathcal{T}')}(p'q')$ is the shortest polyline such that $\mathcal{L}_{\mathcal{D}(\mathcal{T}')}(p'q') \cap \mathcal{D}(\mathcal{T}') = \mathcal{L}_{\mathcal{D}(\mathcal{T}')}(p'q')$.

Lemma 4.2.2.

$$|\mathcal{L}_{\mathcal{D}(\mathcal{T}')}(p'q')| \leq |\mathcal{L}(P_C)| \leq |A_{pq}| \leq \pi/2|pq|$$

Proof. $\mathcal{L}(P_C)$ represents a geodesic path contained in $\mathcal{T}$. Recall that $\mathcal{L}_{\mathcal{D}(\mathcal{T})}(pq)$ represents the shortest geodesic path contained in $\mathcal{T}$, and thus $|\mathcal{L}_{\mathcal{D}(\mathcal{T})}(pq)| \leq |\mathcal{L}(P_C)|$, and $|\mathcal{L}_{\mathcal{D}(\mathcal{T})}(pq)| = |\mathcal{L}_{\mathcal{D}(\mathcal{T}')}(p'q')|$, which proves the first inequality. The second inequality is true because $\mathcal{L}(P_C)$ and A_{pq} lie in the same plane H_{pqs}, both are convex curves and $\mathcal{L}(P_C)$ lies within A_{pq}. The last inequality is true because A_{pq} is the shorter arc of the circle $H_{pqs} \cap \mathcal{S}$.

□

Lemmas 4.2.1, 4.2.2, and Theorem 4.1.1 imply the main theorem.

Theorem 4.2.3. $|\mathcal{P}_{skel(P_C)}(p,q)| \leq 1.998 \cdot |\mathcal{L}_{\mathcal{D}(\mathcal{T}')}(p'q')| \leq 0.999 \cdot \pi \cdot |pq|$.

It remains to prove Lemma 4.2.1. To prove this requires the following two lemmas.

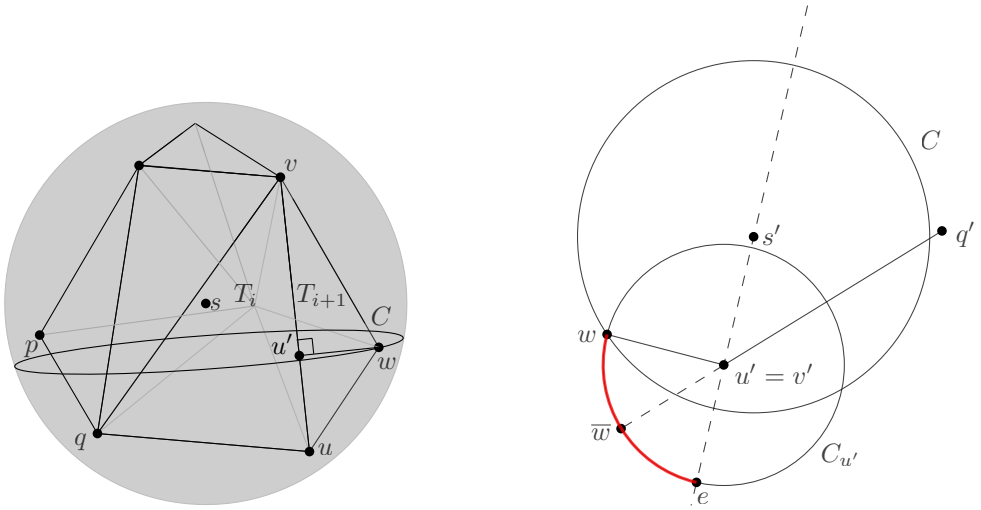

(a) (b)

Figure 4.4: Proof of Lemma 4.2.5.

Lemma 4.2.4. *Let i be an integer for $1 \leq i \leq k$. Then P_C and s are in the same halfspace of the plane through T_i of P_C.*

Proof. The fact that A_{pq} is the shorter of the two arcs of $H_{pqs} \cap S$ implies that s lies in the opposite half-plane of the line through p and q as W_{pq}. Let $e_i = T_i \cap W_{pq}$. Thus e_i and s are in opposite half-planes of the line through p and q, which implies that p, q, s are in the same half-plane of the line supporting e_i. This implies $P_C \cap H_{pqs}$ and s are in the same half-plane of the line supporting e_i, which implies the lemma. □

Lemma 4.2.5. *Let i be an integer with $1 \leq i < k$ and let w be the vertex of T_{i+1} that is not a vertex of T_i. Consider the vertex w' of the unfolded triangle T'_{i+1} that corresponds to w. Then w' is not in the circumdisk D'_i of the unfolded triangle T'_i.*

Proof. Let $T_i = \triangle uvq$ and let $T_{i+1} = \triangle uvw$, thus uv is the edge shared by T_i and T_{i+1}. We will unfold T_{i+1} into the plane H_{uvq} supporting T_i. We will call the resulting triangle $\overline{T}_{i+1} = \triangle uv\overline{w}$, where $\overline{w}$ corresponds to w. Observe that if $\overline{w}$ is outside of D_i, then w' is outside of D'_i, and we are done. Further observe that $D_i = H_{uvq} \cap S$, thus if $\overline{w}$ is outside of D_i it must be outside of S. So we will show that $\overline{w}$ is outside of S.

Assume without loss of generality that uv is parallel to the z-axis. Let C be the cross section of S that goes through w and is orthogonal to uv. Let u', v', q', and s' be the orthogonal projections of u, v, q, and s respectively onto the plane supporting C. Observe that $u' = v'$, and we will henceforth refer to it as u'. Let $C_{u'w}$ be the circle in the plane supporting C centered at u' that goes through w. Thus $\overline{w}$ is the point on $C_{u'w}$

that intersects the line through u' and q' such that $|\overline{w}u'| < |\overline{w}q'|$. See Fig. 4.4b. Let e be the point on $C_{u'}$ that intersects the line through u' and s' that is contained in the angle $\angle wu'q' > \pi$. Lemma 4.2.4 implies that s' lies in $\angle wu'q' < \pi$, thus $|eu'| < |es'|$ and e lies outside of C, otherwise all of $C_{u'}$ lies inside C, which is a contradiction since C and $C_{u'}$ intersect at w. Thus $\overline{w}$ lies on the arc of $C_{u'}$ between w and e that lies outside of C, which implies that $\overline{w}$ lies outside of S, as required. □

We can now prove Lemma 4.2.1.

proof of Lemma 4.2.1. Lemma 4.2.5 implies that, for triangles T'_i and T'_{i+1}, that q' is outside of D'_{i+1} and w' is outside of D'_i, and thus T'_i and T'_{i+1} are locally Delaunay. This implies that all consecutive pairs of triangles of $\mathcal{T}'$ are locally Delaunay, which implies that $\mathcal{D}(\mathcal{T}')$ is a chain of disks. □

4.3 CONCLUSION

The strength of this approach is a result of the flexibility of the model of the chain of disks provided by Xia[6]. It provides a convenient black box that we were able to build a solution around. It remains to be seen if it could be used in other scenarios.

An interesting result presented in the same paper[5] is the fact that, if the vertices of S are nudged even slightly off of $\mathbb{S}^2$, then $skel(P_C)$ is no longer a spanner, even if the points are arranged in an annulus, which allows us to bound the ratio of a geodesic arc between two points to the Euclidean distance between two points. However, we note that the Delaunay triangulation of points in space is a tetrahedralization, the convex hull of which corresponds to $skel(P_C)$, but now has additional Delaunay edges inside of P_C. Is it possible that, for points S in convex position in an annulus, the Delaunay triangulation is a spanner? That is, do the inner edges always provide a short path, even if the outer edges do not?

BIBLIOGRAPHY

[1] Kevin Q. Brown. *Geometric Transforms for Fast Geometric Algorithms*. PhD thesis, Carnegie Mellon University, Pittsburgh, PA, USA, 1979. AAI8012772.

[2] David P. Dobkin, Steven J. Friedman, and Kenneth J. Supowit. Delaunay graphs are almost as good as complete graphs. *Discrete & Computational Geometry*, 5(1):399–407, 1990.

[3] J. Mark Keil and CarlA. Gutwin. Classes of graphs which approximate the complete euclidean graph. *Discrete & Computational Geometry*, 7(1):13–28, 1992.

[4] Simon Pratt, Michiel Smid, and Prosenjit Bose. The convex hull of points on a sphere is a spanner. In *Proceedings of the Canadian Conference on Computational Geometry*, CCCG '14, 2014.

[5] Michiel H. M. Smid, Prosenjit Bose, Paz Carmi, Mirela Damian, Jean-Lou De Carufel, Darryl Hill, Anil Maheshwari, and Yuyang Liu. On the stretch factor of convex polyhedra whose vertices are (almost) on a sphere. *JoCG*, 7(1):444–472, 2016.

[6] Ge Xia. Improved upper bound on the stretch factor of Delaunay triangulations. In *Proceedings of the Twenty-seventh Annual Symposium on Computational Geometry*, SoCG '11, pages 264–273, New York, NY, USA, 2011. ACM.

5

IMPROVED SPANNING RATIO ON THETA-FIVE

ABSTRACT

We show an upper bound on the spanning ratio of the Θ_5-graph of 5.70, improving the previous best upper bound of 9.96 by Bose *et al.* [4]. The key to this improvement is a proof by induction based on Euclidean distances, rather than sizes of the canonical triangles. This requires the analysis of single variable functions, but results in a finer grained analysis overall, bringing the spanning ratio closer to the lower bound of 3.798.

This chapter is a paper being prepared for publication.

5.1 INTRODUCTION

A geometric graph G is a graph whose vertex set is a set of points P in the plane and whose edge set is a set of edges E consisting of pairs of points in P where the weight of an edge uv in E is equal to the Euclidean distance $|uv|$ between u and v. A Θ_k-graph is a geometric graph built in the following way. Around each node v we define k equal angled cones. In each cone, we connect v to their nearest neighbour (we shall define *nearest* later). Such graphs arise naturally in settings like wireless networks, where signals to anyone but your nearest neighbour are likely to be drowned out by interference. Navigating short paths in these types of graphs are also important since signal strength fades quadratically with distance, and thus power requirements are proportional to the distance the signal has to travel squared. This makes many short hops economically superior to one large hop, even if the total resulting distance is longer. Informally the *spanning ratio* of a graph is an upper bound on the length of the shortest path between two points in a graph. In this paper we analyze the Θ_5-graph, which is a graph built by dividing the area around a node into 5 equal angled cones and connecting to the "closest" neighbour in each cone. Using simple geometric observations and techniques, we improve the bound on the spanning ratio from 9.96 [4] to 5.70.

Let $k \geq 3$ be an integer. To construct a Θ_k-graph we do the following. For each i with $0 \leq i < k$, let $\mathcal{R}_i$ be the ray emanating from the origin that makes an angle of $2\pi i/k$ with the negative y-axis. Let $\mathcal{R}_k = \mathcal{R}_0$. The Θ_k-graph of a given set P of points is the directed

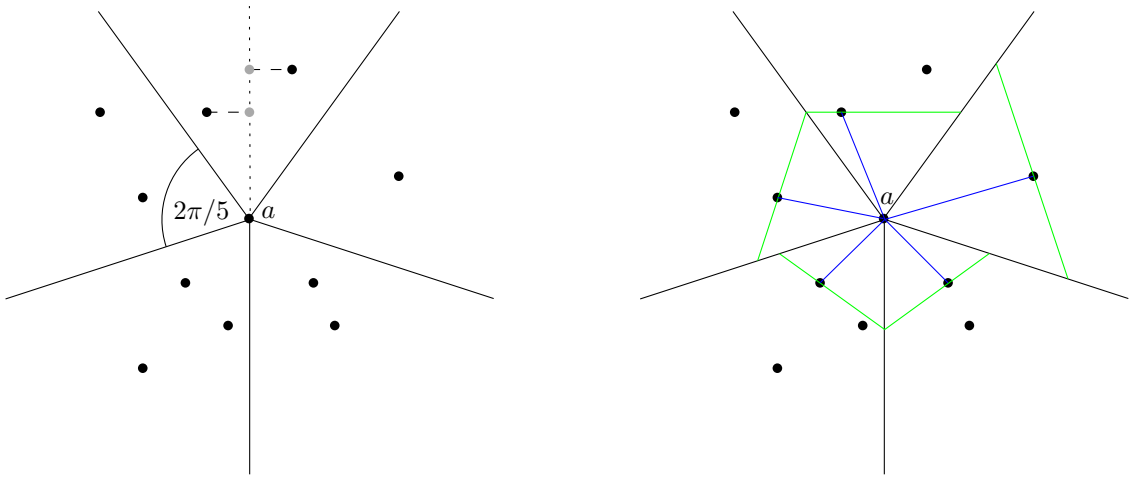

(a) (b)

Figure 5.1: The area around a is divided into cones with angle $2\pi/5$. The top cone in 5.1a illustrates the measurement of "closest" by the distance of the perpendicular projection onto the bisector from a.

graph that is obtained in the following way. The vertex set is the set P. Each vertex v has at most k outgoing edges: For each i with $0 \leq i < k$, let $\mathcal{R}_i^v$ be the ray emanating from v parallel to $\mathcal{R}_i$. Let C_i^v be the cone consisting of all points in the plane that are strictly between the rays $\mathcal{R}_i^v$ and $\mathcal{R}_{i+1}^v$ or on $\mathcal{R}_{i+1}^v$. If C_i^v contains at least one point of $P \setminus \{v\}$, then let w_i be the closest such point to v, where we define "closest" as the point who perpendicular projection onto the bisector of C_i^v is closest to v in Euclidean distance. Then the Θ_k-graph contains the directed edge vw_i. While using directed edges makes our construction more illuminating, in the final Θ_5-graph all edges are considered undirected.

Θ_k-graphs were introduced simultaneously by Keil and Gutwin[6, 7], and Clarkson[5]. Both papers gave a spanning ratio of $1/(\cos\theta - \sin\theta)$, where $\theta = 2\pi/k$ is the angle defined by the cones. Observe this gives a constant spanning ratio for $k \geq 9$. Ruppert and Seidel[9] improved this to $1/(1 - 2\sin(\theta/2))$, which applies to Θ_k-graphs with $k \geq 7$. Bose et al. [3] give a tight bound of 2 for $k = 6$. In the same paper are the current best bounds on the spanning ratio of a large range of values of k. For $k = 5$, Bose et al. [4] showed a spanning ratio of ≈ 9.96, and a lower bound of ≈ 3.78. For $k = 4$, Bose et al. [2] showed a spanning ratio of 17, while Barba et al. [1] gave a lower bound on the spanning ratio of 7. For $k = 3$, El Molla[8] showed that there is no constant c for which Θ_3 is a c-spanner. In this paper we study the spanning ratio of Θ_5 by looking at two arbitrary vertices, a and b, and showing that there must exist a short path between them using induction on the rank of the Euclidean distance $|ab|$ among all pairs of points in P. We show that the shortest path $\mathcal{P}\langle a, b\rangle$ has length at most $K|ab|$, where $K = 5.70$.

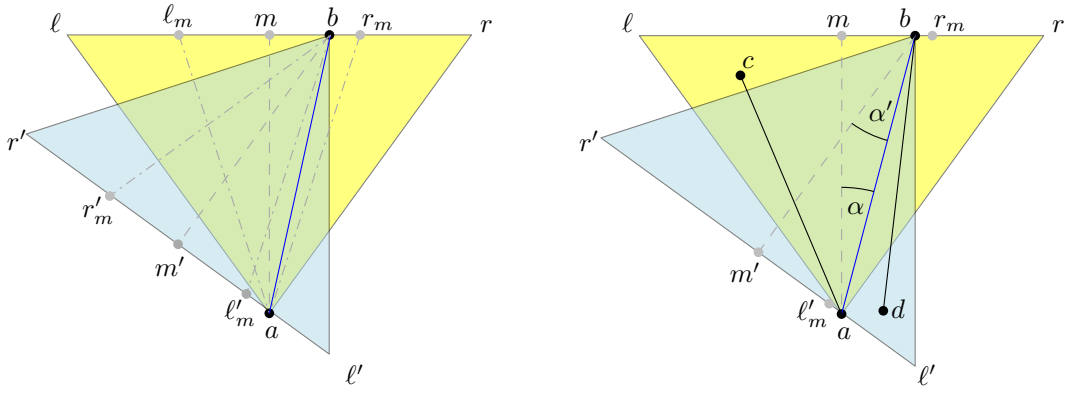

(a) We assume b is in C_2^a and a is in C_4^b.

(b) The angle α.

Figure 5.2

We organize the rest of the paper as follows. In Section 5.2 we introduce concepts and notation, and give some assumptions about the positions of a and b that do not reduce the generality of our arguments. In Section 5.3 we introduce two generic arguments that can then be applied to the Θ_5-graph. In Section 5.4 we use the generic arguments from Section 5.3 to solve all but a small handful of cases. The remaining cases are solved using similar methods, and we show a spanning ratio of $K = 6.16$. In Section 5.5 we observe that only a single case requires $|\mathcal{P}\langle a, b\rangle| \leq K \cdot |ab|$ for $K = 6.16$. We analyze this case in detail to show that $|\mathcal{P}\langle a, b\rangle| \leq K \cdot |ab|$ for $K \geq 5.70$. In Section 5.6 we discuss possible directions for future work.

5.2 PRELIMINARIES

Angles are considered counter-clockwise unless otherwise stated. Let P be a set of points in general position, that is, all distances between pairs of points is unique. Consider two vertices a and b of P. We define the *canonical triangle* T_{ab} to be the triangle bounded by the sides of the cone of a that contains b and the line through b perpendicular to the bisector of that cone. Note that any pair of vertices a and b has two canonical triangles, T_{ab} and T_{ba}. Without loss of generality assume that b is in C_2^a. Let ℓ be the leftmost point of T_{ab} and let r be the rightmost point of T_{ab}. Let m be the midpoint of ℓr. Note that a must be in C_4^b or C_5^b; since the cases are symmetric we consider the case where a is in C_4^b. Thus b is to the right of m. Let r_m be the intersection of ℓr and the bisector of $\angle ram$, and let ℓ_m be the intersection of ℓr and the bisector of $\angle(ma\ell)$. Let ℓ' and r' be the left and right endpoints of T_{ba} respectively. Let m' be the midpoint of $\ell' r'$, and let r'_m and ℓ'_m be the intersections of $\ell' r'$ and the bisector of $\angle \ell' bm'$ and $\angle(m' br')$ respectively. See Fig. 5.2a. Let $\alpha = \angle bam$ and let $\alpha' = \angle abm'$. Note that $\alpha + \alpha' = \pi/5$ since α and α' are

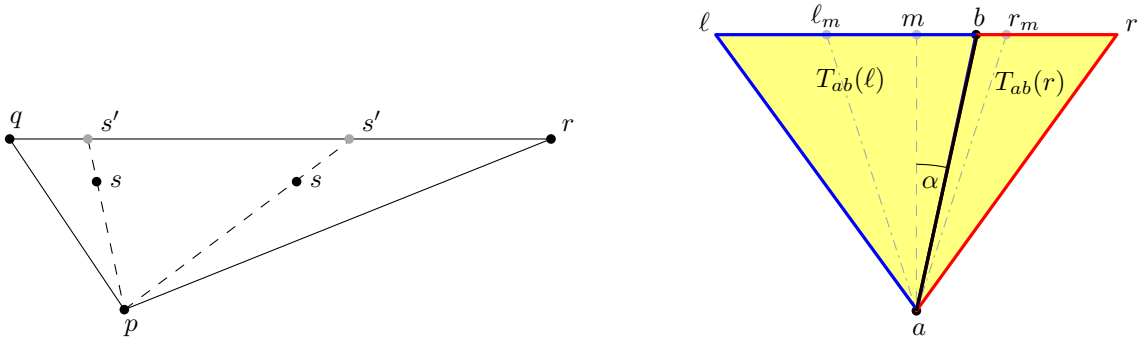

(a) Two examples for the position of s.

(b) The triangles T^{ℓ}_{ab} and T^{r}_{ab}.

Figure 5.3

alternate interior angles. Thus either $\alpha \leq \pi/10$ or $\alpha' \leq \pi/10$. Without loss of generality, we assume $\alpha \leq \pi/10$. Let c be the closest neighbour to a in C^a_0, and let d be the closest neighbour to b in C^b_2. See Fig. 5.2b.

To prove the spanning ratio of Θ_5, we do a proof by induction on the rank of the Euclidean distance between two vertices. To prove the base case we need the following two geometric lemmas.

Lemma 5.2.1. *Let $\mathcal{T}$ be a triangle $\triangle pqr$ with points in counter-clockwise order, and without loss of generality assume that $|pq| \leq |pr|$. Then for all points s inside $\mathcal{T}$, $|ps| \leq |pr|$.*

Proof. Let s' be the intersection of the line through ps onto qr, thus $|ps| \leq |ps'|$ and it is enough to show that $|ps'| \leq |pr|$. See Fig. 5.3a. If $\angle rs'p \geq \pi/2$, then $|ps'| \leq |pr|$ since $|pr|$ is the longest side of $\triangle pqr$. Otherwise $\angle ps'q > \pi/2$, which implies that $|ps'| < |pq| \leq |pr|$. □

Lemma 5.2.2. *Let a and b be the closest pair of points in P. Then the Θ_5-graph of P contains the edge ab.*

Proof. To show this we divide T_{ab} into two triangles by separating T_{ab} along ab into the left triangle T^{ℓ}_{ab} and the right triangle T^{r}_{ab}. See Fig. 5.3b. We then show that for all α, ab is not the shortest edge in T^{ℓ}_{ab}, and ab is not the shortest edge in T^{r}_{ab}. Assuming this is true, Lemma 5.2.1 then implies that for every point p in T_{ab}, either $|pa| \leq |ab|$ or $|pb| \leq |ab|$. Since a and b are the closest pair of points in P, there are no other points of P in T_{ab}, and thus ab is an edge in the Θ_5-graph of P.

Observe that $\pi/10 \leq \angle rab \leq \pi/5$, and $\angle arb = 3\pi/10$, and $\pi/2 \leq \angle abr \leq 3\pi/5$. That means $\angle rab < \angle arb < \angle abr$, and the sine law implies that ab is not the shortest edge in the triangle T^{r}_{ab}. To the left of ab observe that $\angle a\ell b = 3\pi/10$, $2\pi/5 \leq \angle \ell ba \leq \pi/2$, and $\pi/5 \leq \angle ba\ell \leq 3\pi/10$. Thus $\angle ba\ell \leq \angle a\ell b < \angle \ell ba$ and the sine law implies ab is not the shortest edge in the triangle T^{ℓ}_{ab}. □

For a set P of points, we show that the spanning ratio of Θ_5-graph of P is at most K using a proof by induction on the rank of the Euclidean distance between pairs of points in P. To simplify notation, instead of saying "Θ_5-graph of P" we will simply say Θ_5. Recall that $\mathcal{P}\langle a, b\rangle$ denotes the shortest path between points a and b in Θ_5. The base case is when a and b are the closest pair of points in P. Then Lemma 5.2.2 implies that ab is an edge in Θ_5, and thus $|\mathcal{P}\langle a, b\rangle| \leq K|ab|$ holds for any $K \geq 1$. Otherwise we assume that ab is not an edge of Θ_5, and for every pair of points a' and b' in P where $|a'b'| < |ab|$, the shortest path $\mathcal{P}\langle a', b'\rangle$ from a' to b' has length at most $|\mathcal{P}\langle a', b'\rangle| \leq K \cdot |a'b'|$, for some $K \geq 1$. Our goal then is to find the minimum value of K for which our inductive argument will hold. We assume ab is not an edge in Θ_5, otherwise we are done by choosing any $K \geq 1$. Recall that c is the closest point to a in C_2^a and d is the closest point to b in C_4^b. There are three possible paths we will examine, depending on the particular arrangement of a, b, c, and d. They are

(1) $ac + \mathcal{P}\langle c, b\rangle$.

(2) $bd + \mathcal{P}\langle d, a\rangle$.

(3) $ac + \mathcal{P}\langle c, d\rangle + db$.

Below are three sets of constraints. Given the points a, b, c and d we will find a minimum value for $K \geq 1$ that satisfies at least one of the following inequalities.

(A) $|ac| + K \cdot |cb| \leq K \cdot |ab|$.

(B) $|bd| + K \cdot |ba| \leq K \cdot |ab|$.

(C) $|ac| + |bd| + K \cdot |cd| \leq K \cdot |ab|$.

Observe that in all three cases, if we can show the expression holds then our inductive argument follows. For instance, if we prove (A) holds for some value K, the implication is that $|cb| < |ab|$, thus $|\mathcal{P}\langle c, b\rangle| \leq K \cdot |cb|$ by the inductive hypothesis. Thus we can combine (1)-(3) with (A)-(C) as follows.

(a) $|\mathcal{P}\langle a, b\rangle| \leq |ac| + |\mathcal{P}\langle c, b\rangle| \leq |ac| + K \cdot |cb| \leq K \cdot |ab|$.

(b) $|\mathcal{P}\langle a, b\rangle| \leq |bd| + |\mathcal{P}\langle d, a\rangle| \leq |bd| + K \cdot |ba| \leq K \cdot |ab|$.

(c) $|\mathcal{P}\langle a, b\rangle| \leq |ac| + |\mathcal{P}\langle c, d\rangle| + |bd| \leq |ac| + |bd| + K \cdot |cd| \leq K \cdot |ab|$.

Thus for any given arrangement of vertices we prove that at least one of (A), (B), or (C) holds true for some value K, and find the smallest value for which this is true. Our proof relies mainly on case analysis, but some of these cases have similar structure. We extract these similar arguments into a pair of geometric lemmas in Section 5.3. These geometric lemmas, along with additional arguments, are then applied to different arrangements of a, b, c, and d in Section 5.4. For all but one case in Section 5.4 we can show at least one of (a), (b), or (c) holds true for $K \geq 5.70$, but the last case requires $K \geq 6.31$. We can reduce this down to $K \geq 5.70$, but due to the complexity of this last case, we dedicate Section 5.5 to this proof.

5.3 GENERAL TRIANGLES T_1 AND T_2

In this section we introduce two triangles on which we will prove the inequalites (A) and (B).

Lemma 5.3.1. *Consider a triangle $T_1 = \triangle(s, v, u)$ with interior angles $(\frac{\pi}{5}, \frac{\pi}{2}, \frac{3\pi}{10})$. Let t be a point on uv. Then $|sw| + K|wt| \leq K|st|$ for any $K \geq 5.70$.*

Proof. Let $\Phi = |sw| + K|wt| - K|st|$. Showing $\Phi \leq 0$ is equivalent to showing $|sw| + K|wt| \leq K|st|$. Without loss of generality, orient $\triangle svu$ so that s and v share a vertical line with s below v, and v and u share a horizontal line with u left of v. Let w_r be the horizontal projection of w onto st, and let w_ℓ be the horizontal projection of w onto su. See Fig. 5.4a. We have $|ww_r| + |w_rt| \geq |wt|$ by the triangle inequality. We also have that $\angle sww_\ell \geq \pi/2$, which implies that sw_ℓ is the longest edge in triangle sww_ℓ, and thus $|sw_\ell| \geq |sw|$. Since w is on $w_\ell w_r$, we have $|w_\ell w_r| \geq |ww_r|$. Thus

$$\begin{aligned}\Phi &= |sw| + K|wt| - K|st| \\ &\leq |sw_\ell| + K(|ww_r| + |w_rt|) - K(|sw_r| + |w_rt|) \\ &\leq |sw_\ell| + K|w_\ell w_r| - K|sw_r|.\end{aligned}$$

Now observe as we decrease θ, that $|sw_r|$ decreases while $|w_\ell w_r|$ increases and $|sw_\ell|$ stays constant. That means that Φ is maximized when $\theta = 0$, which is when w_r lies on sv. Thus assume that w_r lies on sv and let $|sw_r| = 1$. In order to show $\Phi \leq 0$, we can use the sine law, and it is sufficient to show

$$\begin{aligned}\Phi =& |sw_\ell| + K|w_\ell w_r| - K|sw_r| \\ \leq& \frac{1}{\cos(\pi/5)} + K(\tan(\pi/5) - 1) \leq 0.\end{aligned}$$

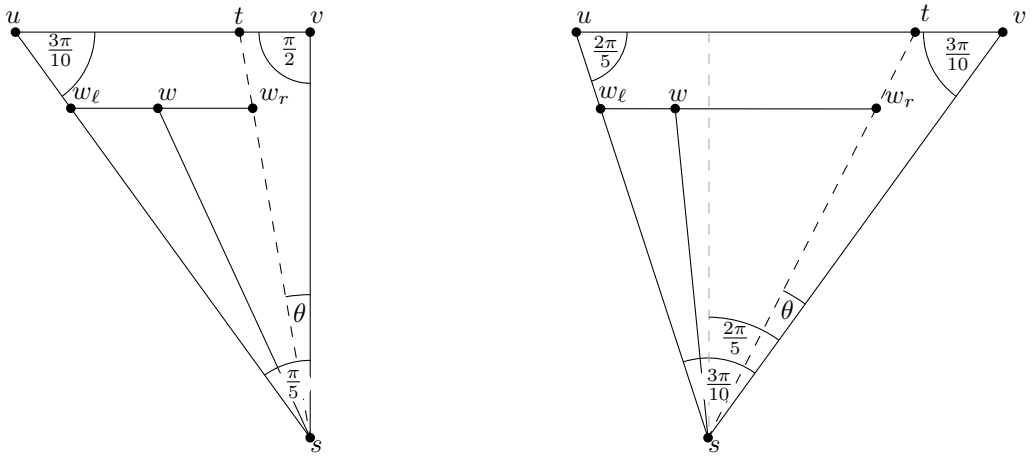

(a) T_1 has angles $(\frac{\pi}{5}, \frac{\pi}{2}, \frac{3\pi}{10})$.

(b) T_2 has angles $(\frac{3\pi}{10}, \frac{3\pi}{10}, \frac{2\pi}{5})$.

Figure 5.4: T_1 and T_2.

We solve for K and get

$$K > 4.53 > \frac{1}{\cos(\pi/5)(1-\tan(\pi/5))}.$$

Thus $\Phi \leq 0$ for any $K \geq 5.70$, as required. □

Lemma 5.3.2. *Let $T_2 = \triangle(s, v, u)$ be a triangle with interior angles $(\frac{3\pi}{10}, \frac{3\pi}{10}, \frac{2\pi}{5})$. Let t be a point on uv such that $0 \leq \angle vst \leq \pi/10$, where $\angle vst$ is the interior angle of $\triangle(s, v, t)$. Then $|sw| + K|wt| \leq K|st|$ for $K \geq 5.70$.*

Proof. Let $\Phi = |sw| + K|wt| - K|st|$. Showing $\Phi \leq 0$ is equivalent to showing $|sw| + K|wt| \leq K|st|$. If $\angle vsw \leq \pi/5$, then let t' be the orthogonal projection of t onto sv. Let u' be the point on the line through t and t' such that $\angle t'su' = \pi/5$. Observe that $\triangle t'su'$ corresponds to T_1 of Lemma 5.3.1 and it contains w. See Fig. 5.5a. Thus Lemma 5.3.1 tells us $\Phi \leq 0$ for any $K \geq 5.70$. Otherwise we assume $\angle vsw > \pi/5$. Without loss of generality, orient $\triangle svu$ so that s and v share a vertical line with s below v, and v and u share a horizontal line. Let w_r be the horizontal projection of w onto st, and let w_ℓ be the horizontal projection of w onto su. See Fig. 5.4b. We have $|ww'| + |w't| \geq |wt|$ by the triangle inequality. We also have that $\angle sww_\ell \geq \pi/2$, which implies that sw_ℓ is the longest

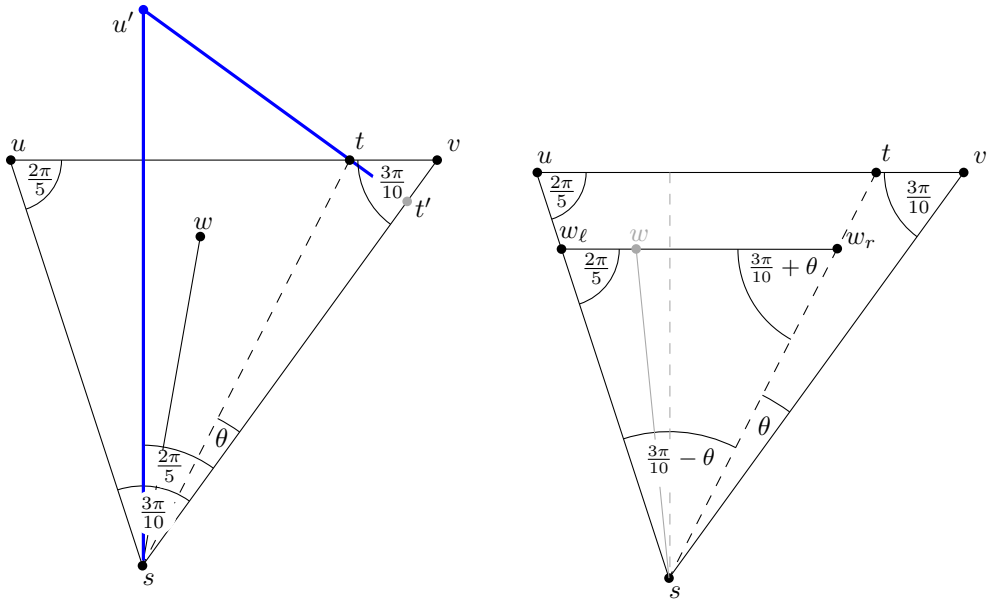

(a) Using T_1 to analyze T_2. (b) Proving $|sw_\ell| + K|w_\ell w_r| \leq K|sw_r|$

Figure 5.5: Analyzing T_2.

edge in triangle sww_ℓ, and thus $|sw_\ell| \geq |sw|$. Since w is on $w_\ell w_r$, we have $|w_\ell w_r| \geq |ww_r|$. Thus

$$\begin{aligned}\Phi &= |sw| + K|wt| - K|st| \\ &\leq |sw_\ell| + K(|ww_r| + |w_r t|) - K(|sw_r| + |w_r t|) \\ &\leq |sw_\ell| + K|w_\ell w_r| - K|sw_r|.\end{aligned}$$

Let $\Phi' = |sw_\ell| + K|w_\ell w_r| - K|sw_r|$. To show $\Phi' \leq 0$ we can use the sine law and write Φ' in terms of θ as follows (see Fig. 5.5b).

$$\Phi' = \sin\left(\frac{3\pi}{10} + \theta\right) + K\sin\left(\frac{3\pi}{10} - \theta\right) - K\sin\left(\frac{2\pi}{5}\right).$$

We take the derivative of Φ' with respect to θ and we get

$$\frac{d\Phi'}{d\theta} = \cos\left(\frac{3\pi}{10} + \theta\right) - K\cos\left(\frac{3\pi}{10} - \theta\right)$$

which is negative for $K \geq 1$. Thus for $K \geq 1$, Φ' is decreasing in θ for $0 \leq \theta \leq \pi/10$, and is thus maximized when $\theta = 0$. Which means

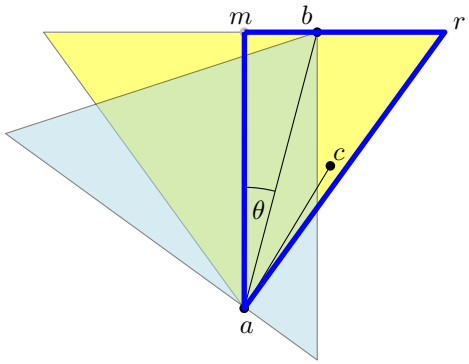

Figure 5.6: Points (a, r, m) correspond to the triangle T_1 with angles $(\frac{\pi}{5}, \frac{\pi}{2}, \frac{3\pi}{10})$ as denoted by the blue triangle. Let $t = b$ and $w = c$, and $\theta = \alpha$, thus $0 \leq \theta \leq \pi/10$.

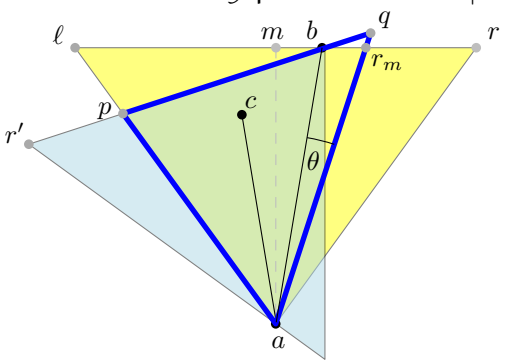

Figure 5.7: Points (a, q, p) correspond to the triangle T_2 with angles $(\frac{3\pi}{10}, \frac{2\pi}{5}, \frac{3\pi}{10})$ as denoted by the blue triangle. Let $t = b$ and $w = c$, and $\theta = \frac{\pi}{10} - \alpha$, which falls in the range of $0 \leq \angle vsu \leq \pi/10$.

$$\Phi' \leq \sin\left(\frac{3\pi}{10}\right) + K\sin\left(\frac{3\pi}{10}\right) - K\sin\left(\frac{2\pi}{5}\right)$$

and thus $\Phi \leq \Phi' \leq 0$ when

$$K \geq 5.70 > \frac{\sin\left(\frac{3\pi}{10}\right)}{\sin\left(\frac{2\pi}{5}\right) - \sin\left(\frac{3\pi}{10}\right)}.$$

□

5.4 ANALYSIS OF $|\mathcal{P}\langle a,b\rangle|$

We give a breakdown of the cases we will analyze. If c or d are right of ab, we can apply T_1 and Lemma 5.3.1 to show the existence of a short path from a to b. When both c and d are left of ab, we consider the following cases. First we consider the possible positions of c, and bound the length of the path $ac \oplus \mathcal{P}\langle c, b\rangle$.

1. c is in the intersection of T_{ab} and T_{ba}.
2. c is above T_{ba} but right of P_5.

Otherwise c must be above T_{ba} and in P_5. Assuming that this is the case, we analyze the length of the path $bd \oplus \mathcal{P}\langle d, a\rangle$ given the following positions of d.

1. d is below br'_m.

2. d is above br'_m but right of P_5.

Otherwise both both c and d are in P_5 and we analyze the length of the path $ac \oplus bd \oplus \mathcal{P}\langle c,d\rangle$. Lemma 5.4.11 gives us a bound on the spanning ratio of $K \geq 6.16$ using a simple proof. However, using a more technical analysis, we can obtain $K \geq 5.70$ when c and d are in P_5. This is proven in Lemma 5.5.4 in Section 5.5.

Lemma 5.4.1. *If c is right of ab, then $|\mathcal{P}\langle a,b\rangle| \leq K|ab|$ for $K \geq 5.70$.*

Proof. Observe that $\triangle(a,r,m)$ has interior angles $(\frac{\pi}{5}, \frac{3\pi}{10}, \frac{\pi}{2})$ at the points (a,r,m) respectively. If we let points $(s,t,w,u,v) = (a,b,c,r,m)$ then they correspond to the triangle T_1 from Lemma 5.3.1, and thus $|ac| + K|cb| \leq K|ab|$ for any $K \geq 5.70$. Then our inductive hypothesis and Lemma 5.3.1 imply that there is a path from a to b with length

$$|\mathcal{P}\langle a,b\rangle| \leq |ac| + |\mathcal{P}\langle c,b\rangle| \leq |ac| + K|cb| \leq K|ab|.$$

See Fig. 5.6. □

Lemma 5.4.2. *If c is left of ab and within $T_{ab} \cup T_{ba}$, then $|\mathcal{P}\langle a,b\rangle| \leq K|ab|$ for $K \geq 5.70$.*

Proof. Let p be the intersection of br' and $a\ell$, and let q be the intersection of the lines through $r'b$ and ar_m. Observe that $0 \leq \angle r_m ab \leq \pi/10$, thus $\angle r_m ab$ has the same range as $\angle vst$ from T_2 in Lemma 5.3.2. If we let points $(s,t,w,u,v) = (a,b,c,p,q)$, then these points correspond to the triangle T_2, and thus $|ac| + K|cb| \leq K|ab|$ for $K \geq 5.70$ by Lemma 5.3.2. Then our inductive hypothesis and Lemma 5.3.2 imply that there is a path from a to b with length

$$|\mathcal{P}\langle a,b\rangle| \leq |ac| + |\mathcal{P}\langle c,b\rangle| \leq |ac| + K|cb| \leq K|ab|.$$

See Fig. 5.7. □

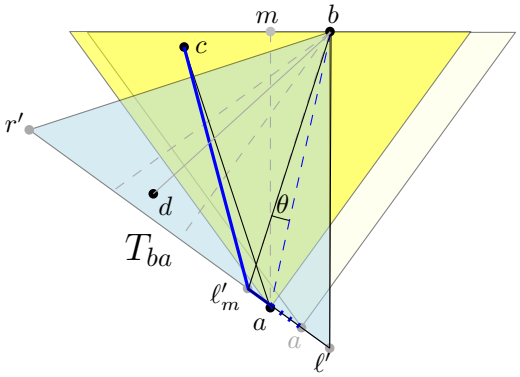

Figure 5.8: Transformation 5.4.3. Note $\theta = \pi/10 - \alpha$.

To proceed further we require a transformation that will allow us to fix the angle α to $\alpha = \pi/10$.

Transformation 5.4.3. *We fix b, c, d, and T_{ba}, and translate a along $r'\ell'$ until $a = \ell'_m$.*

Observe this transformation changes the values of $|ac|$ and $|ab|$, but not $|bd|$, $|cd|$, or $|cb|$. The transformation also changes the value of $|ad|$, but we do not use it in any case that requires analysis of this value. Thus applying Transformation 5.4.3 is functionally equivalent to assuming $\alpha = \pi/10$.

We will show the following.

Lemma 5.4.4. *Let $\Phi = |ac| - K|ab|$. Under Transformation 5.4.3, Φ is maximized when $a = \ell'_m$.*

Proof. See Fig.5.8. Let $\theta = \angle \ell'_m ba$, and observe that $\theta = \pi/10 - \alpha$. Recall that Transformation 5.4.3 fixes T_{ba}. Let $\Phi' = |a\ell'_m| + |\ell'_m c| - K|ab|$. Since $|a\ell'_m| + |\ell'_m c| \geq |ac|$ by the triangle inequality, $\Phi' \geq \Phi$, and observe when $\theta = 0$, that $\Phi = \Phi'$. We will show that Φ' decreases in θ, which proves both Φ and Φ' are maximized when $\theta = 0$. Using sine law, and letting $|a\ell'_m| = 1$, we can express Φ' as a function of θ. We get

$$\begin{aligned}\frac{d\Phi'}{d\theta} &= \frac{d}{d\theta}\left(\frac{\sin\theta - K\sin(\frac{3\pi}{5})}{\sin(\frac{2\pi}{5}-\theta)}\right) \\ &= \frac{\cos\theta\sin(\frac{2\pi}{5}-\theta) + \cos(\frac{2\pi}{5}-\theta)(\sin\theta - K\sin(\frac{3\pi}{5}))}{\sin^2(\frac{2\pi}{5}-\theta)} \\ &= \frac{\sin(\frac{2\pi}{5}) - \cos(\frac{2\pi}{5}-\theta)K\sin(\frac{3\pi}{5})}{\sin^2(\frac{2\pi}{5}-\theta)}.\end{aligned}$$

Observe $\sin^2(\frac{2\pi}{5}-\theta)$ is positive, and the numerator of $\frac{d\Phi'}{d\theta}$ is maximized when $\theta = 0$. Since $\sin(\frac{2\pi}{5}) - \cos(\frac{2\pi}{5})K\sin(\frac{3\pi}{5}) < 0$, $\frac{d\Phi'}{d\theta} \leq 0$, and Φ is decreasing in θ and maximized when $\theta = 0$, which is when $\alpha = \pi/10$.

□

We use Transformation 5.4.3 and Lemma 5.4.4 in the next lemma, which also requires this definition.

Definition 5.4.5. *Let P_5 be the regular pentagon with vertices $(p_0, p_1, p_2, p_3, p_4)$, where $p_2 = r'$ and $p_3 = r'_m$ and p_4 is inside T_{ba}. See Fig. 5.9.*

Observe that P_5 is fixed with respect to T_{ba}, and that this construction puts p_0 and p_1 on a horizontal line with b.

Lemma 5.4.6. *If c is above T_{ba} and right of P_5, then $|\mathcal{P}\langle a,b\rangle| \leq K|ab|$ for any $K \geq 5.70$.*

Proof. Let $\Phi = |ac| + K|cb| - K|ab|$. We apply Transformation 5.4.3. Since c is above T_{ba} it must be left of $b\ell'_m$, thus c remains left of ab. As a moves left, so does the left side of T_{ab}, which means that c remains inside T_{ab}. Thus Lemma 5.4.4 implies that Φ is maximized at $\alpha = \pi/10$, thus we assume this is the case. Observe that $\angle ba\ell_m = \pi/5$, and $\angle \ell_m ba = 2\pi/5 < \pi/2$. Let q be the intersection of the line through b orthogonal to ab and the line through a and ℓ_m. If we let $(s,t,w,u,v) = (a,b,c,b,q)$ then these points correspond to T_1. See Fig. 5.9b. Then Lemma 5.3.1 tells us that $|ac| + K|cb| \leq K|ab|$ and thus $\Phi = |ac| + K|cb| - K|ab| \leq 0$ for $K \geq 5.70$. □

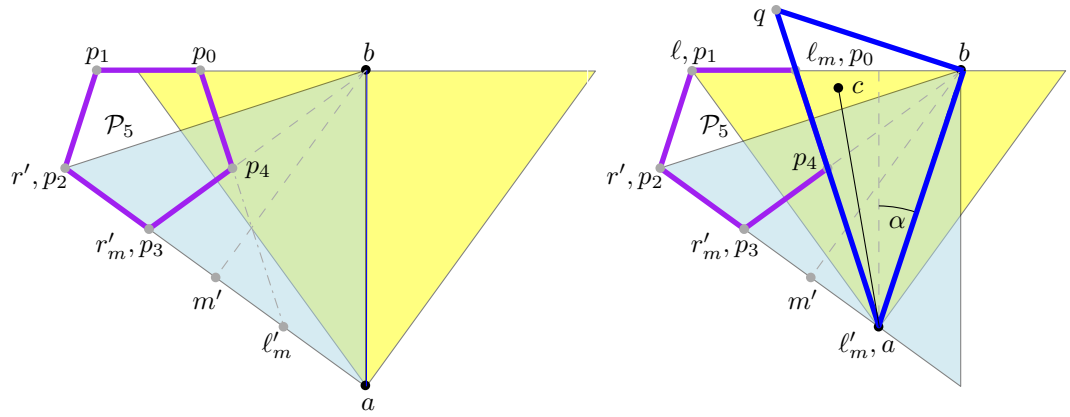

(a) P_5 when $\alpha = 0$.

(b) P_5 when $\alpha = \pi/10$.

Figure 5.9: The two extremes of α with respect to P_5.

Observe that Lemmas 5.4.1, 5.4.2, and 5.4.6 tell us that $|\mathcal{P}\langle a,b\rangle| \leq K|ab|$ for any $K \geq 5.70$ for all possible locations of c except when c is above T_{ba} and in P_5. In the upcoming section, we therefore assume c is above T_{ba} and in P_5 and examine the possible cases for the location of the nearest neighbour of b in C_2^b which we have labeled d.

5.4.1 *Vertex c in P_5*

Lemma 5.4.7. *For any location of c, if d is right of ab, then $|\mathcal{P}\langle a,b\rangle| \leq K|ab|$ for $K \geq 5.70$.*

Proof. Let $(s,t,w,u,v) = (b,a,d,m',\ell')$, thus these points correspond to the triangle T_1. Thus $|ac| + K|cb| \leq K|ab|$ for $K \geq 5.70$ by Lemma 5.3.1. Then our inductive hypothesis and Lemma 5.3.1 imply that there is a path from a to b with length at most

$$|\mathcal{P}\langle a,b\rangle| \leq |ac| + |\mathcal{P}\langle c,b\rangle| \leq |ac| + K|cb| \leq K|ab|.$$

See Fig. 5.10. □

Lemma 5.4.8. *If bd and ac cross, but d is not in P_5, then $|\mathcal{P}\langle a,b\rangle| \leq K|ab|$ for any $K \geq 5.70$.*

Proof. See Fig. 5.11. Since ac and bd cross, d must be outside of T_{ab}. We want to show that d is below br'_m. Assuming this is the case, then $0 \leq \angle ab\ell' \leq \pi/10$, and thus $\angle ab\ell'$ is in the range of $0 \leq \angle vsu \leq \pi/10$. Let points $(s,t,w,u,v) = (b,a,d,r'_m,\ell')$, then these points correspond to the triangle T_2 of Lemma 5.3.2. Thus $|bd| + K|da| \leq K|ab|$ for $K \geq 5.70$.

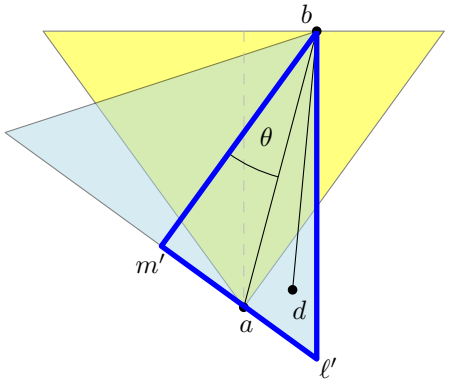

Figure 5.10: Points (b, m', ℓ') correspond to T_1 (in blue) with $t = a$ and $w = d$.

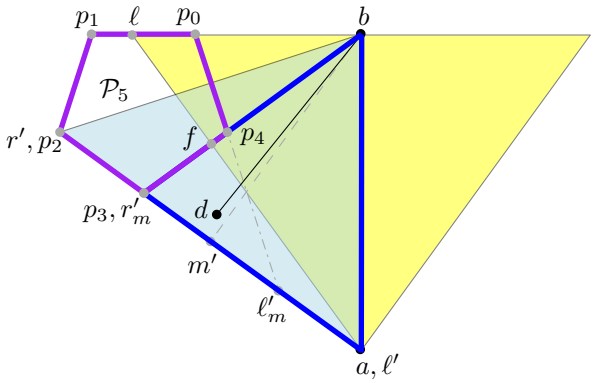

Figure 5.11: We prove p_4 lies in T_{ab}, then apply T_2.

Then our inductive hypothesis and Lemma 5.3.2 imply that there is a path from b to a with length at most

$$|\mathcal{P}\langle a,b\rangle| \leq |bd| + |\mathcal{P}\langle d,a\rangle| \leq |bd| + K|da| \leq K|ab|.$$

We are left with showing that d is below br'_m. Recall that P_5 is fixed with respect to T_{ba}. Since d is outside of T_{ab} and P_5, if p_4p_0 is inside T_{ab}, then d must be below br'_m. Since the slope of p_0p_4 is less than the slope of ℓa, it is sufficient to show that p_4 is inside T_{ab}, or equivalently that p_4 is right of $a\ell$. The rightmost possible position of $a\ell$ is when $\alpha = 0$. Thus if we can prove that p_4 is right of $a\ell$ when $\alpha = 0$, then p_4 is always right of $a\ell$. So we assume $\alpha = 0$. We will show that $a\ell$ intersects p_3p_4, which implies that p_4 is right of $a\ell$. Since $\alpha = 0$, $a = \ell'$. Let f be the intersection of $a\ell$ and br'_m. Note that p_3p_4 is a subsegment of br'_m, and $p_3 = r'_m$, which we will henceforth refer to as p_3. We will show that $|p_3f| < |p_3p_4|$, which implies the lemma. Note $\angle\ell\ell'p_3 = \pi/10$, thus $|p_3f| = |\ell'p_3|\sin(\pi/10)$. When $\alpha = 0$, $|\ell'p_3| = |p_3b|$, and $|p_3p_4| = |p_3p_2| = |\ell'p_3|\sin(\pi/10)/\sin(3\pi/10) > |\ell'p_3|\sin(\pi/10) = |p_3f|$, as required. □

Lemma 5.4.9. *If c is above T_{ba} and in P_5, and d is left of ab, but right of am, then $|\mathcal{P}\langle a,b\rangle| \leq K|ab|$ for $K \geq 5.70$.*

Proof. See Fig.5.12. We will bound the length of the path $|bd| + |\mathcal{P}\langle d,a\rangle|$. By the inductive hypothesis, $|\mathcal{P}\langle d,a\rangle| \leq K|da|$, and we wish to use this to show that $|bd| + K|da| \leq K|ab|$. Let $\Phi = |bd| + K|da| - K|ab|$. To prove the lemma it is sufficient to show that $\Phi \leq 0$ when $K \geq 5.70$. Let d' be the horizontal projection of d onto ab. Let $\Phi_1 = |bd| - K|bd'|$ and $\Phi_2 = K|da| - K|d'a|$, and note that $\Phi = \Phi_1 + \Phi_2$. Thus it is sufficient to show that $\Phi_1 \leq 0$ and $\Phi_2 \leq 0$ for $K \geq 5.70$.

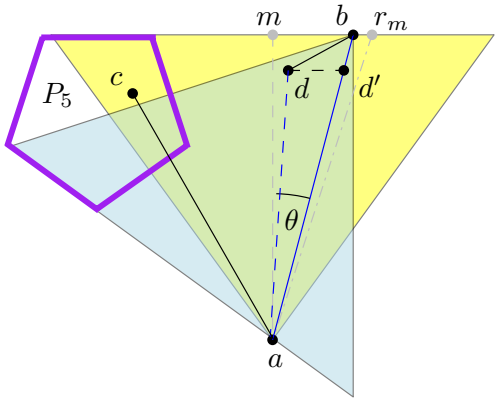

Figure 5.12: c is in $\mathcal{P}_5$ above T_{ba}, d is right of am.

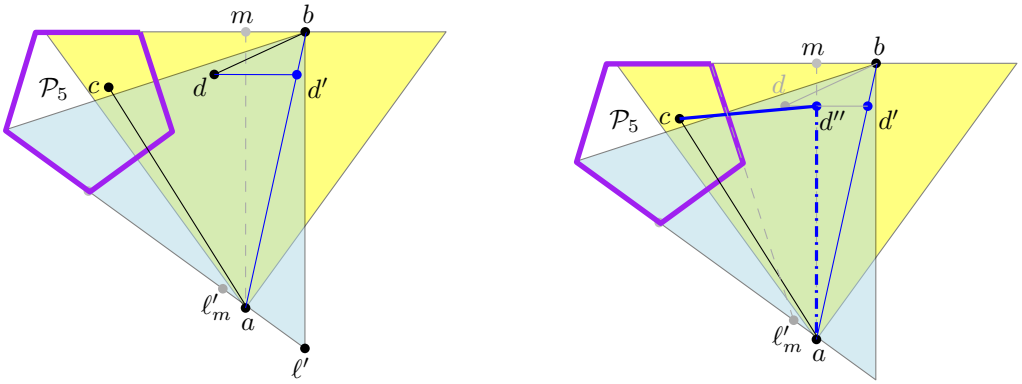

(a) $|db| - K|bd'| \leq 0$. (b) $|ac| + K|cd| - K|ad'| \leq 0$.

Figure 5.13: c is in $\mathcal{P}_5$ above T_{ba}, d is left of am but above c.

To show $\Phi_1 \leq 0$ we require that $K \geq \frac{|bd|}{|bd'|}$. Observe that $d_y(b,d') \leq |bd'|$ and $\angle d'db \geq \pi/10$. Thus $K \geq \frac{|bd|}{d_y(b,d')} \geq \frac{1}{\sin(\pi/10)}$ is sufficient to show that $\Phi_1 \leq 0$. Since $\frac{1}{\sin(\pi/10)} < 3.24$, $K \geq 5.70$ is sufficient. Also observe that $\angle d'da > \pi/2$, since d is right of am, thus $|d'a| > |da|$, and $\Phi_2 \leq 0$ for any value of $K \geq 1$. □

Lemma 5.4.10. *If c is above T_{ba} and in P_5, and d is left of am but above c, then $|\mathcal{P}\langle a,b\rangle| \leq K|ab|$ for $K \geq 5.70$.*

Proof. See Fig. 5.13. We will bound the length of the path $|ac| + |\mathcal{P}\langle c,d\rangle| + |bd|$. By the inductive hypothesis, $|\mathcal{P}\langle c,d\rangle| \leq K|cd|$, and thus we will show that $|ac| + K|cd| + |bd| \leq K|ab|$. Let $\Phi = |ac| + |bd| + K|cd| - K|ab|$. We will split Φ into two parts, and show that each part is less than 0. Let d' be the horizontal projection of d onto ab. Let

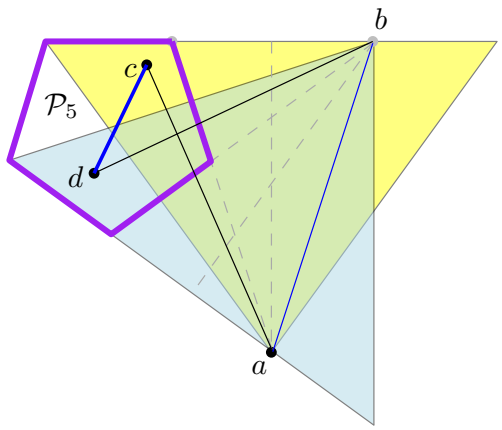

Figure 5.14: ac and bd cross and are in $\mathcal{P}_5$.

$\Phi_1 = |bd| - K|bd'|$, and let $\Phi_2 = |ac| + K|cd| - K|ad'|$. Observe that $\Phi = \Phi_1 + \Phi_2$. We start with Φ_1.

Observe that $d_y(b,d) = d_y(b,d') \leq |bd'|$. Thus let $\Phi_1' = |bd| - K \cdot d_y(b,d)$, and thus if $\Phi_1' \leq 0$, then $\Phi_1 \leq 0$. Let $\theta = \angle d'db$, and observe that $\Phi_1' = |bd|(1 - K\sin\theta)$. Note that $\theta \geq \pi/10$, and thus $K = 5.70$ is sufficient to make $\Phi_1' \leq 0$.

Let d'' be the horizontal projection of d onto am. Since $\angle(ad''d') = \pi/2$, $|ad''| \leq |ad'|$. Since c is above T_{ba}, $\angle cdd'' \geq 9\pi/10$, thus $|cd''| > |cd|$. Let $\Phi_2' = |ac| + K|cd''| - K|ad''|$, and observe that $\Phi_2 \leq \Phi_2'$. Let q be the horizontal projection of d'' onto $a\ell$. Observe $\angle d''ad'' = 0$. Let the points $(s,t,w,u,v) = (a,d'',c,d'',q)$ and thus these points correspond to T_1. Thus $|ac| + K|cd''| \leq K|ad''|$ by Lemma 5.3.1, which implies that $\Phi_2 \leq \Phi_2' \leq 0$. □

Lemma 5.4.11. *If ac and bd cross and both c and d are in P_5, then $|\mathcal{P}\langle a,b\rangle| \leq K|ab|$ for $K \geq 6.16$.*

Proof. See Fig. 5.14. We will bound the length of the path $|ac| + |\mathcal{P}\langle c,d\rangle| + |bd|$. By the inductive hypothesis $|\mathcal{P}\langle c,d\rangle| \leq K|cd|$. Let $\Phi = |ac| + |bd| + K|cd| - K|ab|$. To prove the lemma it is enough to show that $\Phi \leq 0$. Under Transformation 5.4.3, Lemma 5.4.4 implies that Φ is maximized when $\alpha = \pi/10$, so we assume this is the case. Since c, d, and P_5 are fixed, c and d are still inside P_5 after Transformation 5.4.3. Given that c and d are in P_5, the furthest apart c and d can be is if they are both on a diagonal of $\mathcal{P}_5$. The length of one side of $\mathcal{P}_5$ is at most $\frac{\sin(\pi/10)}{\sin(3\pi/10)}|ab|$. That means a diagonal of $\mathcal{P}_5$, and thus $|cd|$, has length $2\sin(3\pi/10)\frac{\sin(\pi/10)}{\sin(3\pi/10)}|ab| = 2\sin(\pi/10)|ab|$. At their longest, $|ac|$ and $|bd|$ each have length $\frac{\sin(3\pi/5)}{\sin(3\pi/10)}|ab|$ by the sine rule. We now assume $\Phi \leq 0$ and solve for K.

$$\begin{aligned}
\Phi &\leq 0 \\
|ac| + K|cd| + |db| - K|ab| &\leq 0 \\
\frac{|ac| + |db|}{|ab| - |cd|} &\leq K \\
\frac{2 \cdot \sin(3\pi/5)}{\sin(3\pi/10) \cdot (1 - 2 \cdot \sin(\pi/10))} &\leq K \\
6.16 &\leq K.
\end{aligned}$$

□

Theorem 5.4.12. *$|\mathcal{P}\langle a, b\rangle| \leq K|ab|$ for $K = 6.16$.*

Proof. Lemmas 5.4.1, 5.4.2, 5.4.6 show a path from a to b with length at most 5.70 for all locations of c except when c is in P_5 above T_{ba}. Lemma 5.4.1 shows the bound when c is right of ab. For c left of ab, Lemma 5.4.2 shows the bound for $c \in T_{ba}$, and Lemma 5.4.6 shows the bound when c is above T_{ba} but right of P_5.

Lemmas 5.4.7, 5.4.9, 5.4.10, and 5.4.8 show a path from a to b with length at most 5.70 when c is in P_5 above T_{ba} but d is not in P_5. Lemma 5.4.7 shows the bound when d is right of ab. Lemma 5.4.9 shows the bound when d is left of ab but right of am. Lemma 5.4.10 shows the bound when d is left of am but still above c, that is, ac and bd don't cross. Lemma 5.4.8 shows the bound when ac and bd cross, but d is not in P_5.

Lemma 5.4.11 shows a path from a to b with length at most 6.16 when both c and d are in P_5, which implies the theorem. □

Of the lemmas cited in the proof of Theorem 5.4.12, only Lemma 5.4.11 requires a value of $K \geq 6.16$. For every other case, $K \geq 5.70$ is sufficient. In the next section we will give a lemma to substitute for Lemma 5.4.11 that gives a bound on the spanning ratio of $K \geq 5.70$.

5.5 DOWN TO $K \geq 5.70$

In this section we show that we can achieve a bound on $|\mathcal{P}\langle a, b\rangle|$ of $K|ab|$ for $K \geq 5.70$ even in the case where ac and bd cross and c and d are in P_5. To demonstrate this requires a careful analysis of the locations of c and d and the tradeoffs between the values of $|ac| + |bd|$ and $K|cd|$. Let $\Phi = |ac| + |bd| + K|cd| - K|ab|$. For the rest of this section, assume we have applied Transformation 5.4.3, and thus $\alpha = \pi/10$ and Φ is maximized. Since P_5, c and d don't move, both c and d are still in P_5. Let c' be the intersection of the line through a and c and the segment p_0p_1, and let d' be the intersection of the line through

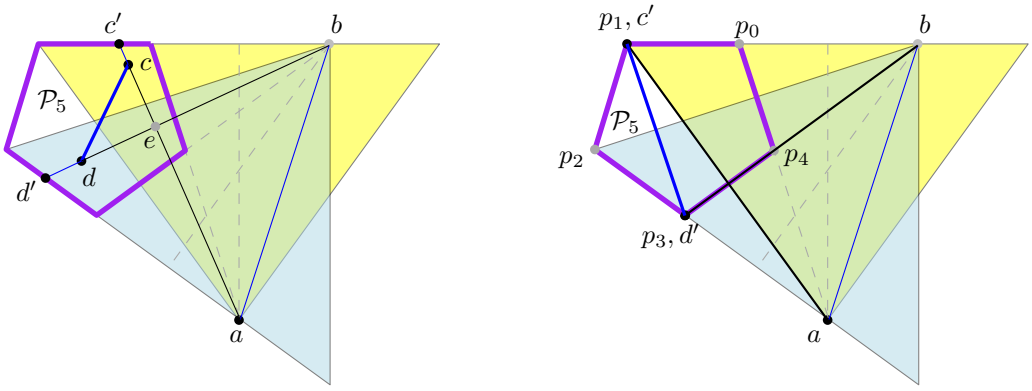

(a) Points c' and d' on $\mathcal{P}_5$.

(b) An example of Φ_2.

Figure 5.15

b and d and the segment p_3p_4. See Fig. 5.15a. Let $\Phi_1 = |ac'| + |bd'| + K|c'd'| - K|ab|$, and let $\Phi_2 = |ap_1| + |bp_3| + K|p_1p_3| - K|ab|$. The following three lemmas are used to prove the main result of this section.

Lemma 5.5.1. *For $K \geq 5.70$, $\Phi \leq \Phi_1$.*

Lemma 5.5.2. *For $K \geq 5.70$, $\Phi_1 \leq \Phi_2$.*

Lemma 5.5.3. *For $K \geq 5.70$, $\Phi_2 \leq 0$.*

Proof of Lemma 5.5.3. See Fig. 5.15b for an example when $c' = p_1$ and $d' = p_3$. Without loss of generality assume that $|ab| = 1$. Then using the sine rule we get $|bp_3| = 1$, $|ap_1| = \frac{\sin(3\pi/5)}{\sin(3\pi/10)}$, and $|p_1p_3| = 2\sin(3\pi/10)\frac{\sin(\pi/10)}{\sin(3\pi/10)} = 2\sin(\pi/10)$. Then

$$\begin{aligned} |ap_1| + |bp_3| + K|p_1p_3| - K|ab| &\leq 0 \\ \frac{|ap_1| + |bp_3|}{|ab| - |p_1p_3|} &\leq K \\ \frac{\frac{\sin(3\pi/5)}{\sin(3\pi/10)} + 1}{1 - 2\sin(\pi/10)} &< 5.696 < K \end{aligned}$$

which is true for $K \geq 5.70$. □

Having proven Lemma 5.5.3 and assuming Lemmas 5.5.1 and 5.5.2 are true, we can prove the main result of this section:

Lemma 5.5.4. *If ac and bd cross and both c and d are in P_5, then $|\mathcal{P}\langle a, b\rangle| \leq K|ab|$ for $K \geq 5.70$.*

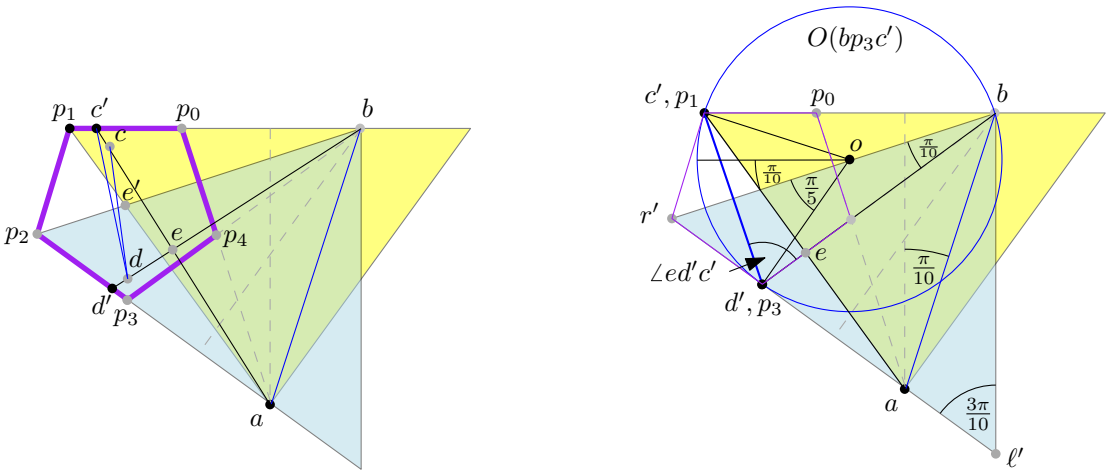

(a) Proof that $|c'd| \geq |cd|$.

(b) Maximum of $\angle ed'c'$.

Figure 5.16

Proof. We will bound the length of the path $|ac| + |\mathcal{P}\langle c, d\rangle| + |bd|$. The inductive hypothesis tells us that $|\mathcal{P}\langle c, d\rangle| \leq K|cd|$, and Lemmas 5.5.1, 5.5.2 and 5.5.3 tell us that $|ac| + |bd| + K|cd| \leq K|ab|$ for $K \geq 5.70$. □

Observe that substituting Lemma 5.5.4 for Lemma 5.4.11 in the proof of Theorem 5.4.12 brings the spanning ratio of the Θ_5-graph down to 5.70. We are left with proving Lemmas 5.5.1 and 5.5.2. We first prove Lemma 5.5.1.

5.5.1 *Lemma 5.5.1*, $\Phi \leq \Phi_1$

In this section we show that $|ac| + |bd| + K|cd| - K|ab| \leq |ac'| + |bd'| + K|c'd'| - K|ab|$. See Fig. 5.16a. Let e be the intersection of ac and bd, and let e' be the intersection of br' and $a\ell$. Observe that $\angle \ell e' r' = 2\pi/5$, and thus we can see that $\angle dec \geq 2\pi/5$. This implies that $\angle dec$ cannot be the smallest angle in $\triangle dec$, since that would require $\angle dec \leq \pi/3$. Thus at least one of $\angle dce$ and $\angle edc$ is the smallest angle in $\triangle dec$. Since we have applied Transformation 5.4.3, and can thus assume that $\alpha = \pi/10$, the cases are symmetric. We can therefore, without loss of generality, assume that $\angle dce$ is the smallest angle in $\triangle dec$.

Proof of Lemma 5.5.1. Since c lies on ac' and d lies on bd', we have $|ac| \leq |ac'|$ and $|bd| \leq |bd'|$, and it is sufficient to show that $|cd| \leq |c'd'|$. We first show that $|cd| \leq |c'd|$. Since $\angle dce$ is the smallest angle in $\triangle dec$, $\angle dce < \pi/3$. That implies that $\angle c'cd > \pi/2$, which implies that $c'd$ is the longest side of triangle $\triangle cc'd$, and thus $|cd| \leq |c'd|$. See Fig.5.16a.

We now show that $|c'd'| \geq |c'd|$. If $\angle c'dd' \geq \pi/2$, then $c'd'$ is the longest side of $\triangle c'dd'$, and $|c'd'| \geq |c'd|$ and we are done. Otherwise assume $\angle c'dd' < \pi/2$.

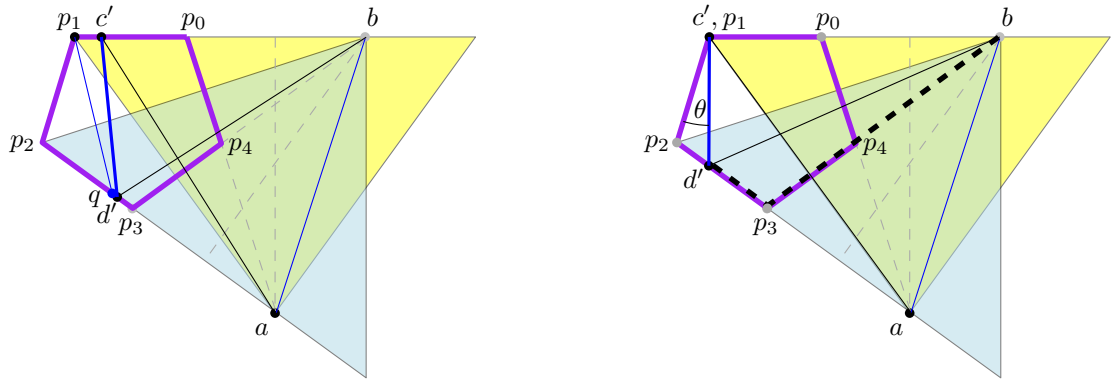

(a) The point q such that $|p_1q| = |c'd'|$ lies between d' and p_2.

(b) We look at the change in $|d'p_3| + K|c'd'|$ with respect to θ.

Figure 5.17

The sine rule tells us that $\frac{|c'd'|}{\sin \angle c'dd'} = \frac{|c'd|}{\sin \angle dd'c'}$. Since $\sin\theta$ is an increasing function for $0 \leq \theta < \pi/2$, showing that $\angle c'dd' \geq \angle dd'c'$ is sufficient to show $|c'd'| \geq |c'd|$, as it would imply both angles are $< \pi/2$. Observe that $\angle c'dd' \geq \angle c'ed'$ and $\angle ed'c' = \angle dd'c'$, thus it is sufficient to prove that $\angle c'ed' \geq \angle ed'c'$.

Observe that $\angle ced = \angle c'ed' \geq 2\pi/5$. We will now find the maximum of $\angle dd'c' = \angle ed'c' \leq 2\pi/5$. Observe that if c' moves left, $\angle ed'c'$ increases, thus assume c' is at p_1. Let $O(bp_3c')$ be the circle through b, p_3, and c' with center o. Observe that o lies on br'. Observe that $\angle r'bd' = \pi/10$, thus $\angle r'op_3 = \pi/5$. Segment or' makes an angle of $\pi/10$ with the horizontal line through o. Thus od' makes an angle of $3\pi/10$ with the horizontal line through o, and thus the line tangent to $O(bp_3c')$ at p_3 is the line supporting $\ell'r'$, since $\ell'r'$ makes an angle of $3\pi/10$ with the vertical line through ℓ'. See Fig. 5.16b. That implies that $[p_2, p_3)$ lies outside of $O(bp_3c')$, which means for every point d', $\angle ed'c' \leq \angle ep_3c' = 2\pi/5$, and thus $\angle c'dd' \geq \angle dd'c'$ as required. □

5.5.2 *Lemma 5.5.2*, $\Phi_1 \leq \Phi_2$

Observe that $|ap_1| + |bp_3| + K|p_1p_3| = |ap_0| + |bp_2| + K|p_0p_2|$ when $\alpha = \pi/10$, as T_{ab} and T_{ba} are the same size and the cases are symmetric. In this section we give proof that $|ac'| + |bd'| + K|c'd'| - K|ab| \leq |ap_1| + |bp_3| + K|p_1p_3| - K|ab| = |ap_0| + |bp_2| + K|p_0p_2| - K|ab|$.

Proof of Lemma 5.5.2. Without loss of generality, we can assume that $|p_1c'| \leq |p_2d'|$. We will show that Φ_1 is maximized when $c' = p_1$ and $d' = p_3$. See Fig. 5.15b. Observe that $|p_1p_2| \leq |c'd'| \leq |p_1p_3|$. Let z be a point on p_2p_3 that moves from p_2 to p_3, and observe that $|p_1z|$ takes on every value from $|p_1p_2|$ to $|p_2p_3|$. Thus there must be a point q on

p_2p_3 such that $|p_1q| = |c'd'|$. See Fig. 5.17a. We claim that $|ap_1| + |bq| \geq |ac'| + |bd'|$, which would imply that $\Phi' \leq |ap_1| + |bq| + K|p_1q| - K|ab|$.

Observe $|ap_1| \geq |ac'|$, since $\angle p_1c'a > \pi/2$, making ap_1 the longest edge in triangle $\triangle ac'p_1$. We claim that q is between d' and p_2, and thus $|bq| \geq |bd'|$ since $\angle bd'q > \pi/2$. We will prove by contradiction, thus assume that q is between d' and p_3. Since $|p_1c'| \leq |p_2d'|$, $\angle qd'c' > \pi/2$, which implies that $|c'q| > |c'd'|$. Also note that $\angle qd'p_1 > \pi/2$, which implies $|p_1q| > |c'q| > |c'd'|$, a contradiction. Thus assuming that $c' = p_1$ and $d' = q$ does not decrease Φ_1.

Now, given that c' is on p_1, we will show that $\Phi_1 \leq |ac'| + |bp_3| + K|c'p_3|$, that is, when d' is on p_3. To do this we define another function $\Phi_1' = |ac'| + |d'p_3| + |p_3b| + K|c'd'| - K|ab|$. See Fig. 5.17b. Since $|bd'| \leq |d'p_3| + |p_3b|$ by the triangle inequality, $\Phi_1 \leq \Phi_1'$, and observe that $\Phi_1 = \Phi_1' = \Phi_2$ when $d' = p_3$. We will show that Φ_1' is maximized when $d' = p_3$, thus implying that Φ_1 is also maximized when $d' = p_3$, and $\Phi_1 \leq \Phi_2$. Let $\theta = \angle p_2p_1d'$. We allow d' to move along p_2p_3 until d' is on p_3, and fix all other points, and observe how Φ_1' changes with θ.

We first rewrite Φ_1' as $\Phi_1' = |ac'| + |p_2p_3| - |p_2d'| + |p_3b| + K|c'd'| - K|ab|$. Using the sine law we get $|p_2d'| = \frac{\sin\theta}{\sin(2\pi/5-\theta)}|p_1p_2|$, and $|c'd'| = \frac{\sin(3\pi/5)}{\sin(2\pi/5-\theta)}|p_1p_2|$. All other terms of Φ_1' have fixed values with respect to θ. Thus

$$\begin{aligned}
\frac{d\Phi_1'}{d\theta} &= \frac{d}{d\theta}\left(K\frac{\sin(3\pi/5)}{\sin(2\pi/5-\theta)}|p_1p_2| - \frac{\sin\theta}{\sin(2\pi/5-\theta)}|p_1p_2|\right) \\
&= \frac{K\cos(2\pi/5-\theta)\sin(3\pi/5) - \cos\theta\sin(2\pi/5-\theta) - \sin\theta\cos(2\pi/5-\theta)}{\sin^2(2\pi/5-\theta)}|p_1p_2| \\
&= \frac{K\cos(2\pi/5-\theta)\sin(3\pi/5) - \sin(2\pi/5)}{\sin^2(2\pi/5-\theta)}|p_1p_2|. \qquad (5.1)
\end{aligned}$$

Observe that $0 \leq \theta \leq 3\pi/10$. The denominator of (5.1) is always positive. The numerator of (5.1) is minimized at $\theta = 0$, which for $K \geq 5.70$ is positive. Thus (5.1) is always positive for $0 \leq \theta \leq 3\pi/10$, thus Φ_1' is increasing in θ, and is maximized when $d' = p_3$, as required. Thus $\Phi_1 \leq \Phi_1' \leq \Phi_2 = |ap_1| + |bp_3| + K|p_1p_3| - K|ab|$ as required. □

5.6 CONCLUSION

Using a few simple geometric observations and arguments, we have lowered the spanning ratio of Θ_5 from 9.96 to 5.70, bringing us closer to the lower bound of 3.798 and thus a tight bound. This work was originally motivated by trying to find a spanning ratio of Θ_5-graph in the constrained setting, that is, we build a Θ_5 graph on a set of points

and edges called constraints, where no edge of Θ_5 can cross a constraint. This was a surprisingly challenging undertaking, and the problem remains open. In addition the question of whether there is an algorithm that can route competitively on the Θ_5-graph remains an open problem.

BIBLIOGRAPHY

[1] Luis Barba, Prosenjit Bose, Jean-Lou De Carufel, André van Renssen, and Sander Verdonschot. On the stretch factor of the theta-4 graph. In Frank Dehne, Roberto Solis-Oba, and Jörg-Rüdiger Sack, editors, *Algorithms and Data Structures - 13th International Symposium, WADS 2013, London, ON, Canada, August 12-14, 2013. Proceedings*, volume 8037 of *Lecture Notes in Computer Science*, pages 109–120. Springer, 2013.

[2] Prosenjit Bose, Jean-Lou De Carufel, Darryl Hill, and Michiel H. M. Smid. On the spanning and routing ratio of theta-four. In Timothy M. Chan, editor, *Proceedings of the Thirtieth Annual ACM-SIAM Symposium on Discrete Algorithms, SODA 2019, San Diego, California, USA, January 6-9, 2019*, pages 2361–2370. SIAM, 2019.

[3] Prosenjit Bose, Jean-Lou De Carufel, Pat Morin, André van Renssen, and Sander Verdonschot. Towards tight bounds on theta-graphs: More is not always better. *Theor. Comput. Sci.*, 616:70–93, 2016.

[4] Prosenjit Bose, Pat Morin, André van Renssen, and Sander Verdonschot. The theta-5-graph is a spanner. *Computational Geometry - Theory and Applications*, 48(2):108–119, 2015.

[5] K. Clarkson. Approximation algorithms for shortest path motion planning. In *Proceedings of the Nineteenth Annual ACM Symposium on Theory of Computing*, STOC '87, pages 56–65, New York, NY, USA, 1987. ACM.

[6] J. Mark Keil. Approximating the complete euclidean graph. In Rolf G. Karlsson and Andrzej Lingas, editors, *SWAT 88, 1st Scandinavian Workshop on Algorithm Theory, Halmstad, Sweden, July 5-8, 1988, Proceedings*, volume 318 of *Lecture Notes in Computer Science*, pages 208–213. Springer, 1988.

[7] J. Mark Keil and Carl A. Gutwin. Classes of graphs which approximate the complete euclidean graph. *Discrete & Computational Geometry*, 7(1):13–28, 1992.

[8] Nawar M. El Molla. *Yao spanners for wireless ad-hoc networks*. PhD thesis, Villanova University, Pennsylvania, USA, 2009.

[9] Jim Ruppert and Raimund Seidel. Approximating the d-dimensional complete euclidean graph. In *Proceedings of the 3rd Canadian Conference on Computational Geometry*, CCCG 1991, 1991.

6

CONCLUSION

We have looked at different geometric graphs in different settings, and improved the analysis of their geometric properties, specifically their spanning and routing ratios. We have also come up with two simple, effective routing algorithms, and analyzed the resulting paths for s. Despite these advancements, many areas of the spanning and routing ratios of geometric graphs remain unexplored. It may interesting to see how ubiquitous the *Greedy/Sweep* algorithm is on other Θ-graphs, or if its routing properties extend to the cousin of the Θ-graph, the *Yao*-graph. Additionally, can the *MinChordArc* algorithm extend to Delaunay graphs in other metrics? The L_2-Delaunay triangulation is the best known plane spanner, yet we still do not have a tight bound on the spanning ratio. Finding that tight bound or improving the current spanning ratio remain tantalizing prospects as well. In addition we have only scratched the surface of the spanning properties of 3-dimensional graphs.